UNIVERSIDADE FEDERAL DE PERNAMBUCO
CENTRO DE BIOCÊNCIAS
PROGRAMA DE PÓS-GRADUAÇÃO EM INOVAÇÃO TERAPÊUTICA

KAYQUE ALMEIDA DOS SANTOS

OBTENÇÃO DE SISTEMAS AMORFOS PARA O INCREMENTO DE SOLUBILIDADE AQUOSA DE NEVIRAPINA

Recife
2024

KAYQUE ALMEIDA DOS SANTOS

OBTENÇÃO DE SISTEMAS AMORFOS PARA O INCREMENTO DE SOLUBILIDADE AQUOSA DE NEVIRAPINA

Tese apresentada ao Programa de Pós-Graduação em Inovação Terapêutica da Universidade Federal de Pernambuco, como requisito parcial para obtenção do título de doutor em Inovação Terapêutica. Área de concentração: Fármacos, Medicamentos e Insumos Essenciais para a Saúde.

Orientador(a): Mônica Felts de La Roca Soares

Recife

2024

.Catalogação de Publicação na Fonte. UFPE - Biblioteca Central

Santos, Kayque Almeida Dos.
   Obtenção de sistemas amorfos para o incremento de solubilidade aquosa de nevirapina / Kayque Almeida Dos Santos. - Recife, 2024.
   139f.: il.

   Tese (Doutorado) - Universidade Federal de Pernambuco, Centro de Biociências, Programa de Pós-Graduação em Inovação Terapêutica, 2024.
   Orientação: Mônica Felts de La Rocs Soares.
   Inclui referências e apêndices.

   1. Co-amorfo; 2. Dispersão sólida ternária; 3. Nevirapina. I. Soares, Mônica Felts de La Rocs. II. Título.

UFPE-Biblioteca Central

KAYQUE ALMEIDA DOS SANTOS

OBTENÇÃO DE SISTEMAS AMORFOS PARA O INCREMENTO DE SOLUBILIDADE AQUOSA DE NEVIRAPINA

Tese apresentada ao Programa de Pós-Graduação em Inovação Terapêutica da Universidade Federal de Pernambuco, como requisito parcial para obtenção do título de doutor em Inovação Terapêutica. Área de concentração: Fármacos, Medicamentos e Insumos Essenciais para a Saúde

.

Aprovado em: 09/08/2024.

BANCA EXAMINADORA

_____
Profª. Drª. Mônica Felts de La Roca Soares (Orientadora)
Universidade Federal de Pernambuco - UFPE

_____
Profª. Drª. Luíse Lopes Chaves (Examinador Interno)
Universidade Federal de Pernambuco - UFPE

_____
Prof. Dr. Lucas José de Alencar (Examinador Interno)
Universidade Federal de Pernambuco - UFPE

_____
Prof. Dr. Dayanne Tomaz Casimiro da Silva (Examinador Externo)
Universidade Federal da Paraíba - UFPB

_____
Prof. Dr. Fábio Henrique Cavalcanti de Oliveira (Examinador Externo)
Universidade de Pernambuco - UPE

Dedico este trabalho a todos os mestres que passaram na minha vida, ajudando a construir essa longa e extensa jornada acadêmica pela qual passei.

AGRADECIMENTOS

Se eu precisasse enumerar todas as pessoas pelas quais eu tenho o sentimento de gratidão, palavras não caberiam nessas páginas. Contudo, eu gostaria de citar alguns personagens importantes nesse capítulo da minha vida e que não seria possível eu deixar de citá-los. Antes de começar a citar os nomes, preciso falar sobre ter chegado até aqui foi uma grande vitória e que eu jamais teria forças para chegar se não fosse por Ele, Autor de toda a vida e que me motiva a andar sempre em frente. Ao me guiar e conduzir, plantou um sonho de amor em mim e me trouxe até aqui. Por isso, minha gratidão eterna à Deus por cada sonho que ele realizou na minha vida.

Minha família sempre deu seu sangue para que eu pudesse crescer na vida. Meus pais vieram de uma família pobre do interior do Maranhão e desde que me entendi por gente, lembro deles conversando sobre meu futuro e o do meu irmão. Isso nos fez sair daquela pequena cidade e nos mudamos para a capital para melhores condições de estudo. Meus pais não tinham muito, mas nunca mediram esforços para que eu e meu irmão tivesse uma boa educação. Lembro, até hoje, de perguntar o que tinha para comer e minha mãe ofereceu uma bolacha de água e sal. Apesar disso, nenhuma mensalidade da escola cara foi atrasada e nenhum livro didático foi deixado de lado. “Vão-se os anéis e ficam os dedos”, minha mãe dizia.

Pelos próximos anos, a situação melhorou, mas os esforços deles nunca foram deixados de lado. A decisão de eu ter vindo a Recife, um outro estado e longe de tudo e todos que eu conhecia pegou a todos de surpresa, mas eles nunca me questionaram. Apenas perguntaram como seria e se prepararam para que eu pudesse vir e me manter nas primeiras semanas. Por seus esforços, amor, carinho e preocupação, quero agradecer à minha família, em especial aos meus pais Sérgio e Vera e a meus irmãos, Kaio e Rita.

Iniciei este doutorado durante a pandemia do COVID-19. Por isso, foi necessário afastamento físico de pessoas tão queridas para mim, mas a tecnologia está aí para nos ajudar e a pandemia foi encerrada nesse meio-termo. Frente à loucura de fazer um doutorado no meio de uma pandemia que tirava milhares de vida, encontrei alegria e felicidade em diversas pessoas que puderam me mostrar a magia da vida e sua importância.

Uma das principais pessoas foi o Solluan Marçal, meu querido Sol. Meu companheiro e namorado que me ouviu em todas as vezes em que eu acreditei que

eu não fosse capaz, que não conseguiria, ou até que eu não fosse bom o suficiente. Ele pôde ouvir meus medos e inseguranças, minhas ansiedades e preocupações. Ao fazer isso, eu não pude apenas desabafar, mas ouvir tantas palavras de amor e carinho que puderam acalmar a tempestade que havia em mim. Com ele, fui formando minha família que traz tanta diversão, felicidade e paz na minha vida através de nossos queridos Kal, Tirêncio e Mia.

Durante essa jornada, uma pessoa foi muito importante para manter minha saúde mental e me lembrar que nem toda tempestade é tão grande quanto parece e que sou capaz de tanto, mesmo que eu me sabote por várias vezes. Este parágrafo gostaria de dedicar ao meu psicólogo, Augusto, a quem sou bastante grato pelo socorro prestado a mim. Não somente pela atenção dada a mim, mas pelos puxões de orelha e me ajudar no caminho da autodescoberta.

Além de todo esse amor, citado acima, me questiono que graça seria a vida se não fossem pelos amigos? A pandemia me afastou de muita gente e acabei me acostumando com a minha solidão, mas com o tempo, pude perceber quem ainda estava comigo, apoiando-me em tantos momentos e trazendo tanta luz na minha vida. Boa parte desse pessoal são meus próprios colegas de pesquisa e que tanto gosto. Na correria do dia a dia, a gente brinca, conversa, fofoca e faz pesquisa. Não necessariamente nessa ordem, mas é tudo feito sim. Dentro do NCQMC, muito pode acontecer e, dentro desse tudo, consegui encontrar muito acolhimento e companheirismo. Dentro de todo esse grande grupo, eu não conseguiria esquecer de alguns nomes tão bons para mim, como o de Amanda Damasceno, Rafaella Moreno, Joandra Leite e Rousy Araújo.

Dentro desse grande grupo, queria lembrar ainda de dois grandes humanos que me fizeram enxergar tudo diferente. Não sei se eu consigo expressar em palavras todo o carinho e amor que tenho por eles dois, mas espero que José Lamartine e Mônica Felts possam entender um pouco disso tudo nestas palavras. Desde o começo, eles fizeram uma grande diferença para mim nesta jornada. Se não fosse por sua compaixão, eu jamais teria feito meu mestrado. Se não fosse por sua paciência, eu jamais teria concluído este doutorado. Neles, encontrei duas figuras importantes e fundamentais nesta jornada, que também foram meus terapeutas e amigos.

Andei fazendo uma lista de tudo que não ensinam na escola. Não ensinam a amar. (...) Não ensinam o que dizer a alguém moribundo. Não ensinam nada que valha a pena saber. Uma amiga está morrendo de AIDS. E como eu me sinto? Vazia. Só isso. Apenas vazia. (Gailman..., 1989).

RESUMO

Inúmeros sistemas de liberação foram desenvolvidos para melhorar a taxa de dissolução de fármacos de baixa solubilidade, como o antirretroviral nevirapina (NVP), um fármaco classe II no Sistema de Classificação Biofarmacêutico. Dentre os sistemas de liberação conhecidos, as dispersões sólidas amorfas (DSAs) se destacam pela vantagem do uso das formas amorfas no incremento de solubilidade ao usar carreadores poliméricos. Contudo, o uso de co-amorfos (CAMs) se torna uma importante alternativa ao uso de polímeros por utilizar moléculas de baixo peso molecular ou um outro fármaco clinicamente relevante para manter o fármaco amorfo e conservar sua vantagem de solubilidade. Neste contexto, parte deste trabalho se conteve em investigar a capacidade de carreadores não poliméricos em estabilizar a forma amorfa de NVP e melhorar a sua dissolução através do planejamento de formação de CAM por modelagem molecular e análises termoanalíticas. Após a escolha dos carreadores conforme suas solubilidades e pontos de interações, uma triagem foi realizada por modelagem computacional e DSC, mostrando evidências de formação de sistemas estáveis amorfos pelas interações dos coformadores com NVP. O preparo das CAMs ocorreu pela técnica *Quench Cooling*, cujas caracterizações indicaram a formação de materiais amorfos através das interações intermoleculares entre os componentes das formulações. A solubilidade de NVP foi investigada, onde se observou a interferência da presença dos coformadores na solubilidade, mas a forma amorfa das CAMs provocou um incremento de solubilidade maior em relação às suas misturas físicas respectivas. A segunda metade do trabalho desenvolveu duas formulações ternárias contendo NVP, lamivudina e um polímero hidrofílico pelo método Quench Cooling, cujas caracterizações físico-químicas apontaram a formação de sistemas amorfos homogêneos formados pelas interações entre NVP e seus carreadores, elevando a solubilidade aquosa do fármaco. Os sistemas amorfos poliméricos e não poliméricos de NVP desenvolvidos neste trabalho foram hábeis em promover o incremento de solubilidade de NVP, o que pode resolver seu problema de solubilidade e gerar alternativas para o tratamento do HIV pediátrico.

Palavras-chave: co-amorfo; dispersão sólida ternária; nevirapina; HIV.

ABSTRACT

Numerous drug delivery systems have been developed to enhance the dissolution rate of poorly soluble drugs, such as the antiretroviral nevirapine (NVP), which belongs to class II in the Biopharmaceutical Classification System. Among the known delivery systems, amorphous solid dispersions (ASDs) stand out due to the advantage of using amorphous forms when employing polymeric carriers to increase solubility. However, the use of co-amorphous (CAM) systems becomes an important alternative to polymers by utilizing low-molecular-weight molecules or another clinically relevant drug to maintain the drug in an amorphous state and preserve its solubility advantage. In this context, part of this work focused on investigating the ability of non-polymeric carriers to stabilize the amorphous form of NVP and improve its dissolution through the design of CAMs using molecular modeling and thermoanalytical analyses. After selecting carriers based on their solubilities and interaction points, a screening process was conducted using computational modeling and DSC, providing evidence of stable amorphous systems formed by interactions between the coformers and NVP. The preparation of CAMs was carried out using the Quench Cooling technique, with characterizations indicating the formation of amorphous materials through intermolecular interactions among the formulation components. NVP solubility was investigated, revealing the influence of coformer presence on solubility, but the amorphous form of CAMs led to a greater increase in solubility compared to their respective physical mixtures. The second half of the work focused on developing two ternary formulations containing NVP, lamivudine, and a hydrophilic polymer using the Quench Cooling method. The physicochemical characterizations indicated the formation of homogeneous amorphous systems resulting from interactions between NVP and its carriers, thereby enhancing the aqueous solubility of the drug. Both polymeric and non-polymeric amorphous systems of NVP developed in this study demonstrated the ability to increase NVP solubility, potentially addressing its solubility challenges and providing alternatives for pediatric HIV treatment

Keywords: co-amorphous; ternary solid dispersion; nevirapine; HIV.

LISTA DE ILUSTRAÇÕES

DISSERTAÇÃO

ARTIGO 3 – DESENVOLVIMENTO DE DISPERSÕES SÓLIDAS TERNÁRIAS FÁRMACO:FÁRMACO:POLÍMERO PARA A TERAPIA DE COMBINAÇÃO ANTIRRETROVIRAL

SUMÁRIO

1 INTRODUÇÃO

Técnicas de busca e seleção de novas moléculas potencialmente ativas tem favorecido na descoberta de inúmeros compostos ativos com baixa solubilidade aquosa nas últimas décadas (IKRAM, 2020). Essa baixa solubilidade impacta diretamente na biodisponibilidade dessas moléculas, quando administrados pela via oral. Para superar esse desafio, inúmeras tecnologias foram desenvolvidas para o incremento de solubilidade aquosa e, consequentemente, uma maior absorção de tais moléculas, como sistemas amorfos, formação de sal, cocristais, ciclodextrinas, nanopartículas e surfactantes.

A manutenção de um estado temporário em que a concentração do fármaco exceda a solubilidade de equilíbrio termodinâmico chamado de supersaturação pode ser uma excelente estratégia para melhorar a absorção desses fármacos de baixa solubilidade aquosa, classificados como classe II e IV no Sistema de Classificação Biofarmacêutico proposto por Amidon et al. (1996). A supersaturação proporciona níveis elevados do fármaco que está disponível para atravessar as membranas biológicas e ser absorvido pelo organismo, superando os problemas de biodisponibilidade (ALMEIDA E SOUSA et al., 2016).

Sistemas amorfos são os principais sistemas supersaturados de liberação de fármacos que geram soluções supersaturadas durante a dissolução. Esses sistemas apresentam fármacos sem qualquer estrutura molecular organizada e com elevada energia livre que os conferem elevada instabilidade química e que faz com que o estado amorfo se recristalize, fazendo-o perder sua vantagem de solubilidade (AUCH et al., 2020). Para isso, é necessária a presença de um segundo componente para carrear o fármaco amorfo e o estabilize em sua forma.

As dispersões sólidas amorfas são sistemas supersaturados onde ocorre a dissolução de um fármaco de baixa solubilidade aquosa em uma matriz polimérica que estabiliza o fármaco em seu estado amorfo, conferindo elevada taxa de dissolução aquosa e estabilidade da sua forma sólida, prevenindo a recristalização e mantendo os níveis elevados da supersaturação (MA; WILLIAMS, 2019). Contudo, é necessária uma enorme quantidade de polímero para conferir essas vantagens, além de que polímeros tendem a absorver umidade, podendo comprometer o sistema disperso ao favorecer o fenômeno da recristalização (DENGALE et al., 2016).

As dispersões co-amorfas se definem como a combinação de um fármaco de baixa solubilidade aquosa com um componente de baixo peso molecular, podendo ser um segundo fármaco, ácido carboxílico, aminoácidos ou pequenos açucares (SAI KRISHNA ANAND et al.,

2018; WU et al., 2019). Tais dispersões são ótimas para terapias multidrogas, onde é possível combinar fármacos de relevância terapêutica, como é o caso dos antirretrovirais nas terapias de combinação para o combate à infecção do vírus da imunodeficiência humana (HIV).

Nevirapina (NVP) é um fármaco antirretroviral que possui uma baixa solubilidade aquosa, classificado pelo Sistema de Classificação Biofarmacêutico como classe II por essa mesma característica. O NVP é um inibidor da transcriptase reversa não análoga a nucleosídeo que interfere no ciclo de replicação viral, sendo indicado no Protocolos Clínicos e Diretrizes Terapêuticas (PCDT) no Brasil para o manejamento do HIV em crianças e adolescentes e em mulheres adultas grávidas para a prevenção da infecção vertical (BRASIL. MINISTÉRIO DA SAÚDE. SECRETARIA DE VIGILÂNCIA EM SAÚDE. DEPARTAMENTO DE VIGILÂNCIA, 2017, 2018).

Devido às suas propriedades físico-químicas, o desenvolvimento de sistemas de liberação que visem o incremento de sua solubilidade aquosa podem ser interessantes para o tratamento do HIV pediátrico, sobretudo quando associado a um outro fármaco antiretroviral já usado na combinação de dose fixa com ele, como é o caso da lamivudina (3TC).

2 OBJETIVOS

2.1 GERAL

Desenvolver sistemas amorfos para liberação do fármaco nevirapina associado a carreadores de baixo peso molecular e poliméricos que possuam a capacidade de promover a estabilidade física do fármaco amorfo e proporcionar o incremento de solubilidade aquosa do fármaco.

2.2 ESPECÍFICOS

- Selecionar os carreadores e a técnica mais adequada para a obtenção dos CAM, levando em consideração a solubilidade, ponto de fusão e estabilidade do fármaco e dos carreadores escolhidos;
- Determinar, experimentalmente, a solubilidade do fármaco cristalino em tampão fosfato pH 6,7 em condições de supersaturação, contendo diferentes carreadores;
- Obter CAMs de nevirapina em associação com diferentes carreadores;
- Verificar as possíveis interações intermoleculares entre o fármaco e os diferentes carreadores através da modelagem molecular;
- Caracterizar o estado sólido dos sistemas co-amorfos através de técnicas físico-químicas de caracterização: difração de raios-X de pó, calorimetria exploratória diferencial, espectroscopia na região do infravermelho e microscopia de luz polarizada.
- Avaliar a solubilidade do fármaco na sua forma isolada cristalina e presente nos sistemas co-amorfos e suas respectivas misturas físicas em meio tampão fosfato pH 6,8 em condição sink.
- Desenvolver e caracterizar dispersões sólidas amorfas (DSAs) ternárias de NVP com 3TC na proporção de dose fixa utilizando polímeros hidrofílicos
- Avaliar a solubilidade de NVP contida nas DSAs em condição sink.

3 REFERENCIAL TEÓRICO

3.1 ESTADO AMORFO DE MATERIAIS FARMACÊUTICOS

Materiais farmacêuticos amorfos são estados termodinamicamente metaestáveis, caracterizados por um desordenamento molecular (Figura 1). A visão termodinâmica de quase-equilíbrio desses materiais faz entender que possuem uma maior solubilidade que sua contraparte cristalina por possuírem uma maior energia livre (LAPUK et al., 2020; PANDI et al., 2020). Materiais amorfos são de natureza vítrea ou também conhecidos como líquidos super-resfriados, podendo ser obtidos através de um rápido resfriamento.

Figura 1 - Arranjo molecular de uma estrutura cristalina (a) e amorfa (b)

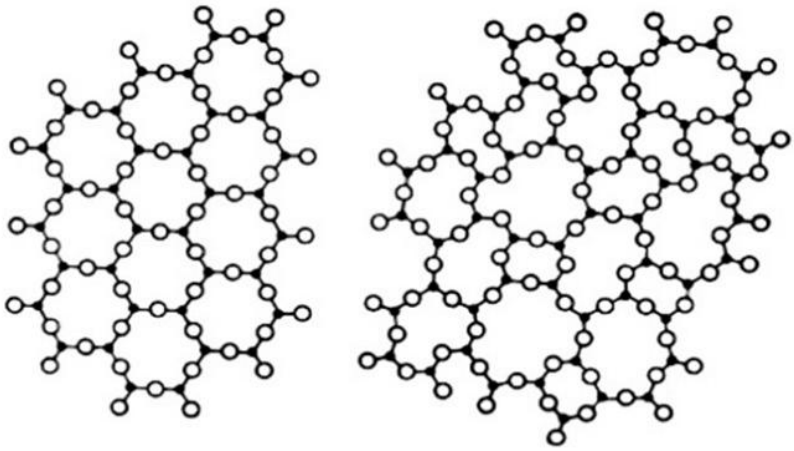

Fonte: Carter & Norton (2007).

Nesse estado, a mobilidade molecular é gradualmente reduzida à medida que o material é resfriado e a viscosidade do material aumenta simultaneamente. Esse evento ocorre em uma temperatura denominada como temperatura de transição vítrea (Tg) e o estado do material é chamado como vítreo (SHEKUNOV, 2020). A transição vítrea é associada com alterações em diversas propriedades termodinâmicas como entalpia, entropia e volume.

Ao mudar a conformação estrutural do estado sólido cristalino para um estado amorfo, as propriedades passam a ter uma maior instabilidade molecular por alcançar um estado metaestável, que lhe confere uma elevada energia livre e uma maior solubilidade aparente (BAGHEL; CATHCART; O'REILLY, 2016). Esse processo de amorfização é feito ao aquecer a molécula cristalina até o seu ponto de fusão (Tf), desordenando seus átomos e resfriando rapidamente para que suas moléculas não se reorganizem para formar uma nova rede cristalina.

Nessa nova fase, o fármaco alcança o estado de líquido super-resfriado até alcançar sua Tg onde entra no estado vítreo (Figura 02).

Figura 2 - Entalpia e volume de diferentes estados de fármacos em função da temperatura; Tg e Tf são, respectivamente, as temperaturas de transição vítrea e de ponto de fusão; o diagrama não está em escala.

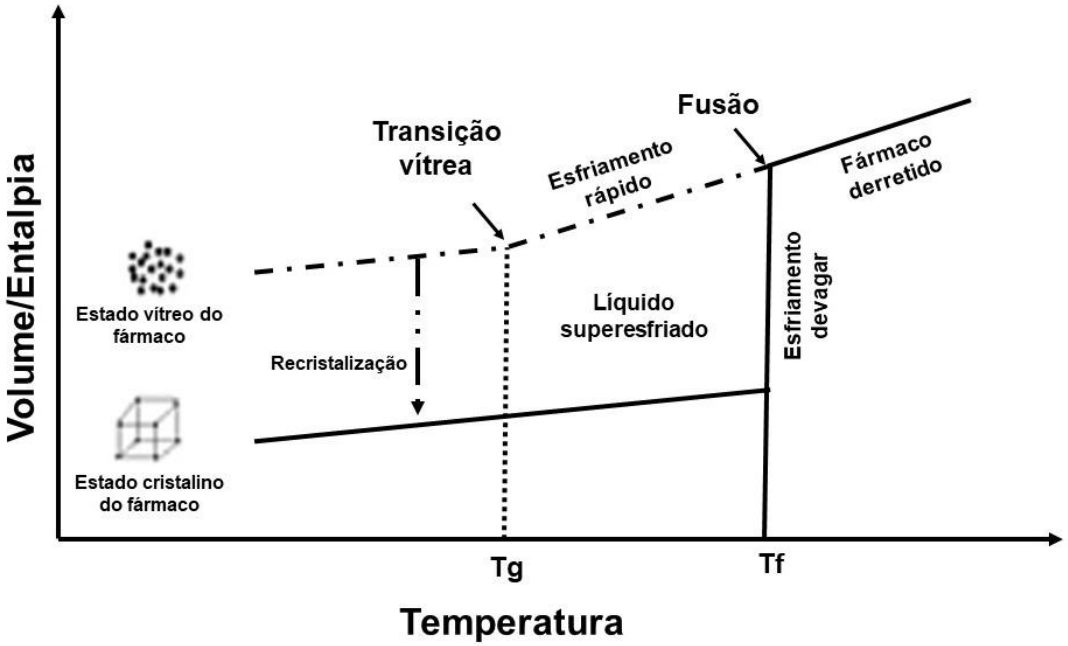

Fonte: Baghel et al. (2016).

3.2 DISPERSÕES SÓLIDAS

3.2.1 Definições

As dispersões sólidas (DS) se definem como a mistura de um fármaco em uma matriz sólida onde essa matriz pode ser uma pequena molécula ou um polímero, formando uma rede dispersa do fármaco amorfo em uma matriz, conforme ilustrado na Figura 3 (HUANG; DAI, 2014). Por possuírem o fármaco amorfo, essa tecnologia pode ser utilizada para o incremento de solubilidade de fármacos de baixa solubilidade, além de prevenirem a recristalização ao proverem uma maior estabilidade física (PANDI et al., 2020; SHI et al., 2022).

Figura 3 - Formação de uma dispersão sólida amorfa através da dispersão ou dissolução do fármaco na matriz polimérica.

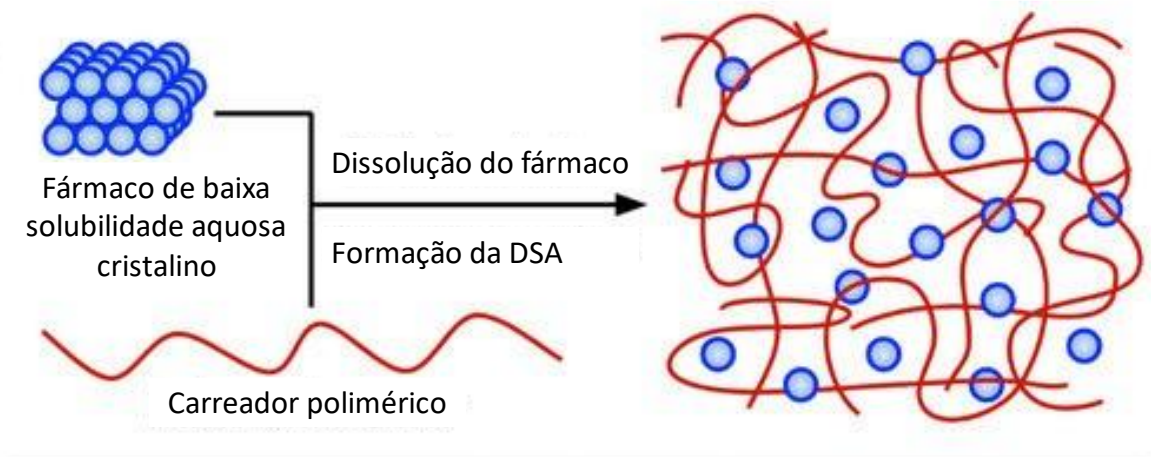

Fonte: Walden et al. (2021).

O arranjo amorfo é caracterizado por possuir uma elevada instabilidade química promovidos pelos excessos de energia, como a entalpia, entropia e energia livre (BAGHEL; CATHCART; O'REILLY, 2016). Essas energias em excesso conduzem os materiais amorfos a possuírem uma tendência ao fenômeno da recristalização e a perderam a vantagem de solubilidade. Para evitar que todo esse processo ocorra, as DS se tornam uma excelente estratégia para estabilizar e manter as moléculas do fármaco amorfas ao combinar o fármaco com um segundo componente que, através de interações intermoleculares e outros fatores físico-químicos, previne a recristalização e preservando a droga amorfa (SANTOS et al., 2022).

Embora as DS possam ter diferentes tipos de matrizes, a polimérica se destaca por promover uma melhor estabilidade ao sistema disperso ao diminuir a mobilidade molecular e elevar a Tg, além de manter a supersaturação do fármaco durante a sua dissolução in vitro. As interações intermoleculares entre o fármaco e o polímero são o principal motivo por essa maior estabilidade ao romper as interações intermoleculares na estrutura cristalina do fármaco, enquanto as forças termodinâmicas e cinéticas são as responsáveis pelo incremento na biodisponibilidade de uma DS (GUO; SHALAEV; SMITH, 2013; VO; PARK; LEE, 2013).

3.2.2 Classificações

Duas formas de classificações das DS são conhecidas, podendo ser de acordo com a fase sólida e estado físico do sistema gerado, ou com o tipo de carreador usado para formar o sistema. As duas classificações podem estar relacionadas, uma vez que um tipo de carreador pode levar a um tipo de fase sólido específico.

3.2.2.1 Fase sólida e estado físico

a) Misturas eutéticas: fases heterogêneas compostas por um carreador cristalino, como a ureia e açúcar, formando um sistema cristalino termodinamicamente estável com o fármaco cuja liberação ocorre de forma lenta (KIM et al., 2011). No processo de obtenção da mistura eutética, os componentes se cristalizam simultaneamente ao serem resfriados em uma composição específica, conhecida como ponto eutético, no qual o sistema se cristaliza em pequenos cristais dos dois componentes utilizados para formar a mistura . A diminuição do tamanho da partícula resultará em uma maior área superficial, o que melhoras as taxas de dissolução e absorção de fármacos de baixa solubilidade aquosa (BINDHANI; MOHAPATRA, 2018; TEKADE; YADAV, 2020; VO; PARK; LEE, 2013). Contudo, as misturas eutéticas formam uma dispersão sólida cristalina, tendo em vista que utilizam carreadores também cristalinos. Isso torna o sistema mais termodinamicamente estável, possuindo taxas de dissolução menores quando comparas às dispersões sólidas amorfas (VASCONCELOS; SARMENTO; COSTA, 2007). Um trabalho conduzido pelo nosso grupo mostrou a formação de uma mistura eutética entre dois fármacos sinérgicos para o combate da doença de chagas, benznidazol e o posaconazol, com taxas de dissolução melhoradas para os dois fármacos (FIGUEIRÊDO et al., 2017);

b) Soluções sólidas: se caracterizam por dois componentes totalmente miscíveis e solúveis, estabilizados através de interações específicas moleculares entre eles. Nesse sistema, os dois componentes estão dispersos de forma molecular, formando uma estrutura amorfa (FIGUEIRÊDO et al., 2017) e o tamanho das partículas do fármaco é reduzido para seu tamanho molecular, aumentando a taxa de dissolução. Essas soluções podem ainda ser do tipo contínuo ou descontinuo dependendo da extensão da miscibilidade entre os componentes (SAREEN; JOSEPH; MATHEW, 2012).

c) Soluções/Suspensões Vítreas Amorfas: A solução é um sistema homogêneo vítreo no qual um soluto/fármaco se dissolve em um carreador amorfo, enquanto a suspensão vítrea se refere a uma mistura na qual partículas precipitadas de fármaco com limitada solubilidade no carreador vítreo ou alto ponto de fusão são suspendidas (BINDHANI; MOHAPATRA, 2018). Ambas possuem fases amorfas supersaturadas, capazes de manter os níveis do fármaco elevadas nos fluidos gastrointestinais, aumentando a taxa de absorção e biodisponibilidade (SAREEN; JOSEPH; MATHEW, 2012). As dispersões mais utilizadas vêm dessa classe, sendo

normalmente conhecidas como dispersões sólidas amorfas (DSAs) por apresentarem uso de polímero amorfos conforme a Figura 4 abaixo.

Figura 4 - Classificação das dispersões sólidas conforme seu estado físico

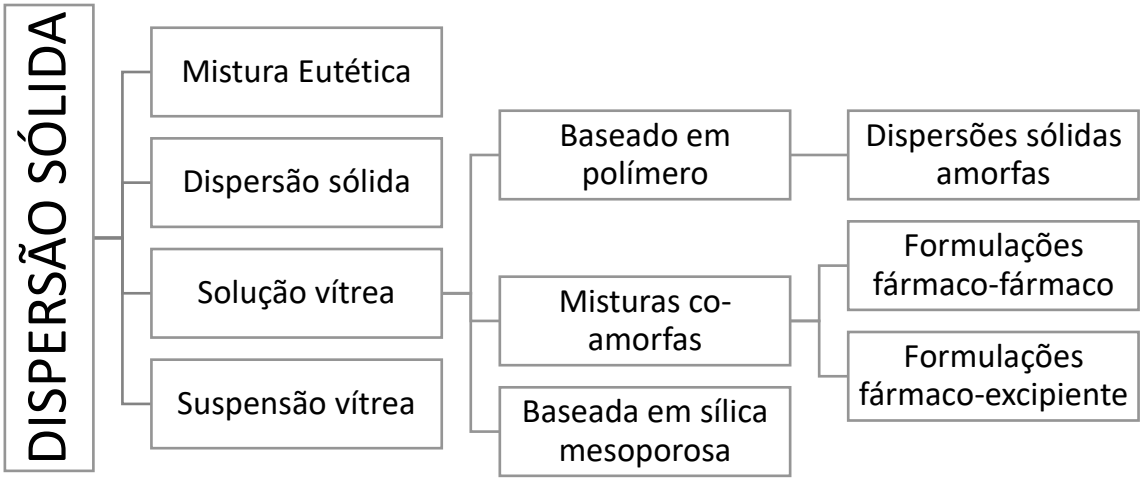

Fonte: O autor (2024)

3.2.2.2 Tipo de carreador

Essa classificação é baseada nos diferentes tipos de carreadores utilizados para formar as dispersões, caracterizando as diferentes gerações de DS. De certa forma, as gerações estão estreitamente ligadas com a classificação anteriormente relatada, uma vez que a utilização de novos excipientes formava novas DS, enquanto iniciavam uma nova geração de sistemas dispersos. As DS foram classificadas em até quatro diferentes gerações (TEKADE; YADAV, 2020).

a) 1ª Geração: preparada usando carreadores cristalinos, como a ureia e açucares. Neste tipo de DS, o sistema cristalino termodinamicamente estável foi formado, na qual a liberação do fármaco ocorrer de forma lenta. Nessa geração, se encontram as misturas eutéticas ou misturas monotéticas (BINDHANI; MOHAPATRA, 2018; TEKADE; YADAV, 2020; VO; PARK; LEE, 2013).

b) 2ª Geração: introduz os carreadores amorfos, como o polivinilpirrolidona (PVP), polietilenoglicol (PEG) e derivados de celulose, além de diversos outros polímeros naturais ou sintéticos. Essa geração foi mais efetiva que a primeira, devido à estabilidade termodinâmica. O maior problema dessa geração é a precipitação do fármaco e a recristalização que afeta a sua liberação in vitro e in vivo (TEKADE; YADAV, 2020).

c) 3ª Geração: consiste no uso de carreadores com atividade de superfície ou propriedades emulsificantes que superam os problemas da precipitação e recristalização característicos da segunda geração. Esse tipo específico de carreador melhora a estabilidade física e química do fármaco ao prevenir a nucleação e aglomeração de cristais, além de melhorar o perfil de dissolução (VASCONCELOS; SARMENTO; COSTA, 2007). Podem ser citados a inulina, Gelucire e poloxamero como representantes dos carreadores utilizados.

d) 4ª Geração: as dispersões de liberação controlada surgem aqui, contendo um fármaco de baixa solubilidade aquosa com um tempo de meia vida curto (VO; PARK; LEE, 2013). Os carreadores utilizados podem ser solúveis ou não em água, como o etil celulose, Eudragit RS, Eudragit RL e hidroxipropilcelulose.

3.2.3 Vantagens

Como as DSAs são as mais populares dentre as classes devido ao uso dos polímeros, seguiremos a revisão sobre o tema ao redor das mesmas. O uso de DSAs na liberação oral de fármacos tem mostrado um aumento na performance in vitro e na biodisponibilidade in vivo em animais (AGRAWAL; DUDHEDIA; ZIMNY, 2016; FULE et al., 2015; FULE; PAITHANKAR; AMIN, 2016; KATE et al., 2016; KNOPP et al., 2018; MITRA et al., 2016; XIA et al., 2016; YU et al., 2013).

O incremento na performance in vitro das DSAs provém das taxas de dissolução aumentadas ao gerar soluções supersaturadas da droga. Isso destaca os sistemas dispersos amorfos frente a outros sistemas utilizados para o incremento de solubilidade, como nanopartículas e ciclodextrinas (SAFFOON et al., 2011; VASCONCELOS et al., 2016). Diversos fatores são descritos como motivos para o incremento de solubilidade, como os seguintes:

I. Tamanho reduzido: o carreador polimérico se dissolve no meio aquoso, liberando o fármaco em pequenas partículas coloidais, o que aumenta a superfície de contato e aumentando a taxa de dissolução de fármacos de baixa solubilidade aquosa (KANG et al., 2004; LEUNER; DRESSMAN, 2000; SHARMA; JOSHI, 2007).

II. Porosidade: as partículas nas DSAs possuem uma elevada porosidade, apressando a liberação do fármaco (KARAVAS et al., 2006; SAREEN; JOSEPH; MATHEW, 2012).

III. Molhabilidade: o fármaco se torna mais molhável em uma dispersão sólida, muito provavelmente devido ao aumento da sua porosidade. Porém, é sugerido ainda que a apresentação das partículas no médio de dissolução como entidades fisicamente separadas pode reduzir a agregação, permitindo uma maior área superficial (POUTON, 2006; SHARMA; JAIN, 2011).

IV. Miscibilidade: descreve o comportamento de fase dos componentes de uma DSA, uma vez que o fármaco está dissolvido em uma determinada matriz polimérica. Se os dois componentes não forem suficientemente miscíveis, ocorrerão uma separação de fases e uma rápida recristalização, criando regiões ricas em fármaco e ricas no segundo componente utilizado. A miscibilidade entre os componentes é formada pelas interações intermoleculares, como as pontes de hidrogênio entre um fármaco e um polímero, mantendo o sistema disperso estável e restringindo a mobilidade molecular.

Por sua vez, o uso de uma matriz polimérica confere outras vantagens ao sistema disperso ao evitar a recristalização dos fármacos. Tal matriz é composta por polímeros, geralmente solúveis em água, que são compostos quimicamente por unidades estruturais repetitivas conhecidas como monômeros, que se conectam entre si para formar uma extensa rede estrutural (BAGHEL; CATHCART; O'REILLY, 2016). Essa rede polimérica aprisiona as moléculas amorfas do fármaco, prevenindo a desvitrificação e preservando a viabilidade do estado amorfo através das seguintes abordagens:

I. Barreira Física: a matriz polimérica mantém separada as moléculas do fármaco, evitando a formação de núcleos cristalinos;

II. Entropia configuracional aumentada: a estrutura grande, complexa e flexível dos polímeros possui uma elevada entropia configuracional por possuírem elevados pesos moleculares e habilidades de existirem em diferentes conformações, diminuindo as chances da nucleação de ocorrer ao diminuir a energia livre da DSA (LAITINEN et al., 2013);

III. Mobilidade molecular diminuída: moléculas poliméricas possuem a capacidade de reduzir a mobilidade molecular de insumos amorfos, sendo essencial para a estabilidade das moléculas amorfas;

IV. Aumento da Tg: esse efeito antiplastificação eleva a energia livre requerida pelo fármaco amorfo para se converter na sua forma cristalina. Isso ocorre devido à Tg dos polímeros

ser mais elevada que a dos fármacos, o que faz elevar a Tg final da dispersão, que ficará entre a dos dois componentes (PENZEL; RIEGER; SCHNEIDER, 1997; WLODARSKI et al., 2015);

V. Aumento das interações fármaco:polímero: diversas interações podem ocorrer entre os dois componentes, sobretudo as mais fracas, como podes de hidrogênio, forças de van der Waals, eletroestáticas, iônicas e hidrofóbicas. Essas interações resultam na diminuição da mobilidade moléculas das moléculas do fármaco na matriz do polímero e provê estabilidade ao sistema (PAUDEL; GEPPI; VAN DEN MOOTER, 2014);

VI. Potencial químico reduzido: a incorporação do fármaco nas cadeias interconectadas poliméricas diminui o potencial químico do fármaco amorfo e o traz mais próximo ao da forma cristalina (CUI, 2007; DONNELLY et al., 2015).

Contudo, o mecanismo do incremento da biodisponibilidade é bem mais complexo. Quando a DSA entra em contato com o meio aquoso, uma dissolução espontânea é formada, onde moléculas do fármaco se torna micelas, suspensões cristalinas ou amorfas e partículas ricas em fármacos, cujo sistema coloidal pode induzir a captação intestinal de fármaco dissolvido (AMIDON et al., 1995; PANDI et al., 2020). A absorção do insumo ativo é um processo com três etapas sendo divididos em dissolução da DSA no meio de dissolução, captação da droga dissolvida e equilíbrio do insumo na solução. Há pelo menos três mecanismos envolvidos na dissolução de uma DSA:

I. Liberação controlada pelo carreador: o meio de dissolução é aprisionado na matriz polimérica e induz a formação de uma camada de gel viscosa por onde a molécula da droga pode se difundir para o meio. Isto é geralmente um processo lento e as concentrações de fármaco são controladas pelo insumo ativo na DSA e o volume do meio de dissolução

II. Liberação controlada pela dissolução: simultaneamente, o fármaco alcança o nível de supersaturação, uma vez que é liberado junto com o polímero no meio e isso acelera o processo de dissolução. A concentração de supersaturação é controlada pela quantidade total do fármaco na DSA e pelo volume do meio de dissolução.

III. Liberação controlada pelo fármaco: o polímero e o fármaco se dissolvem no meio de dissolução, mas o fármaco amorfo da dispersão se dissolve em uma taxa controlada. Neste mecanismo, há uma chance do fármaco se recristalizar durante a dissolução e isso pode ocorrer se a forma amorfa não for estável o suficiente.

Figura 5 - Conceito básico da captação de fármaco das DSA. Do estado sólido das DSAs contendo polímero, micelas, cristais e mistura complexa do fármaco em solução e partículas coloidais surge, dos quais a absorção do fármaco através da membrana intestinal é aumentada e seguida por três conceitos para a dissolução.

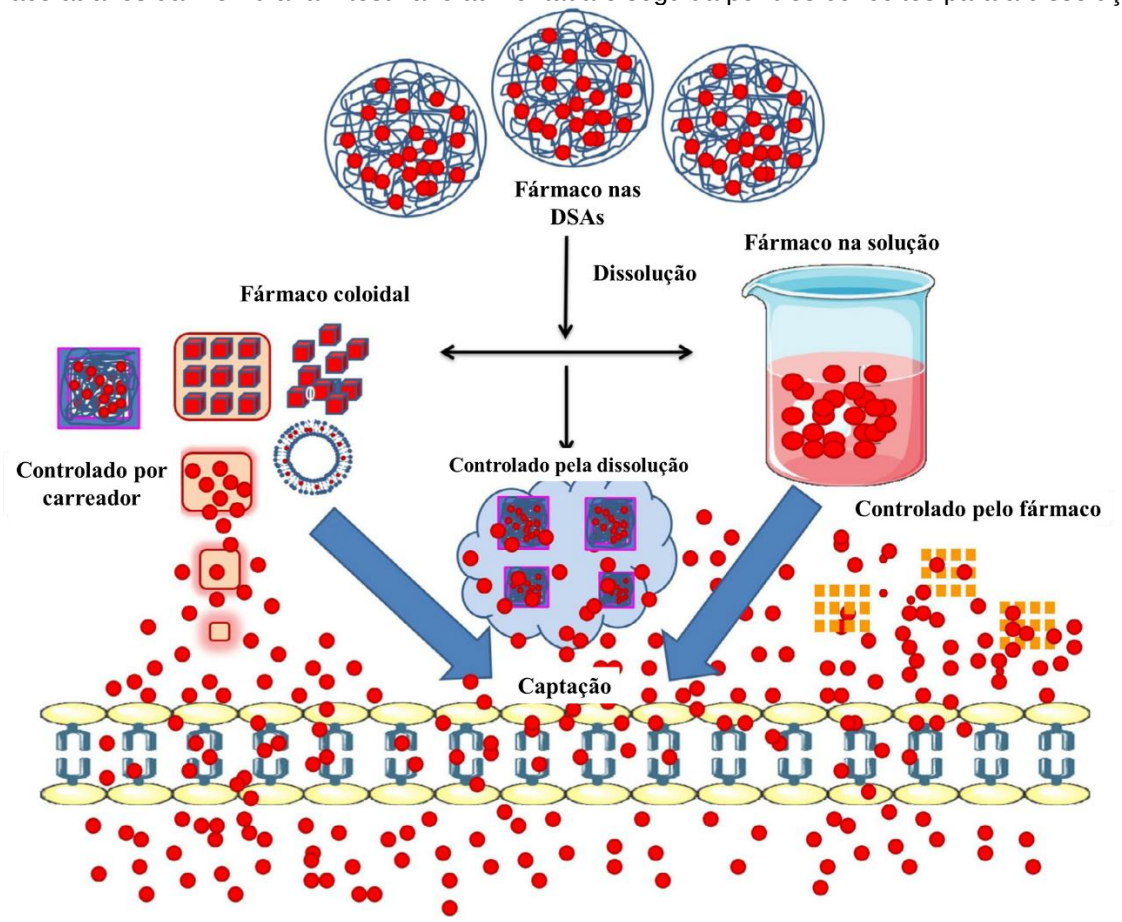

Fonte: Pandi, et al. (2020)

Os três mecanismos estão representados na Figura 5 e, independente do mecanismo de liberação, o sucesso da DSA na liberação para o incremento de solubilidade dependerá da habilidade do polímero em manter a supersaturação do fármaco tempo suficiente sem ocorrer precipitação de partículas para que a absorção seja mais facilitada (BAGHEL; CATHCART; O'REILLY, 2016).

3.2.4 Estabilidade de dispersões sólidas

A cristalinidade de um fármaco em uma DS deve ser zero quando recém preparada, porque um pequeno número de cristais pode induzir à cristalização do fármaco durante o armazenamento, onde a cristalinidade ainda precisa ser investigada para assegurar a

estabilidade física simplesmente pela capacidade que esse fenômeno tem de levar à perda na taxa de dissolução e uma biodisponibilidade reduzida (GUO; SHALAEV; SMITH, 2013).

Portanto, a estabilidade física de uma DS dependerá do grau de interação molecular entre o fármaco e seu carreado, onde os seguintes fatores devem ser considerados para alcançar uma ótima estabilidade física:

I. as fases intrínsecas do estado sólido e estabilidade da DS

II. as propriedades físico-químicas do carreador, que inclui peso molecular, cristalinidade, ponto de fusão ou temperatura de transição-vítrea, hidrofilicidade, higroscopicidade, capacidade de formar pontes de hidrogênio, presença de grupamentos funcionais ácidos ou básicos para interações iônicas e impurezas

III. a carga de fármaco (ou a razão de peso do fármaco para o carreador) na DS. Geralmente, uma maior estabilidade física pode ser alcançada com cargas de fármaco mais baixas (SANTOS et al., 2022).

IV. métodos de fabricação. As transições de fase sólida durante os processos de fabricação, como a cristalização da fase amorfa, podem ter um efeito significativo na performance de uma DS e formas de dosagem subsequente (ZHANG et al., 2004).

A água pode ter ainda um significativo efeito na estabilidade física e química de materiais amorfos. Tais materiais são geralmente mais higroscópicos que os estados cristalinos por poderem absorver água e distribuído por todo o material, no que resulta em uma maior absorção de água, enquanto os materiais cristalinos absorvem umidade na sua superfície (OHTAKE; SHALAEV, 2013; RUMONDOR et al., 2011).

O efeito plastificante das moléculas de água pode diminuir significativamente a Tg da maioria dos fármacos amorfos, mesmo com pequenos teores de umidade, afetando ainda a força, temperatura de transição de viscosidade e aumenta a mobilidade molecular que eventualmente leva para instabilidade química e física (LI et al., 2020).

A miscibilidade entre os componentes pode ficar comprometida em ambientes com elevada umidade, formando fases separadas ricas em fármaco e do segundo componente, sendo inevitável a recristalização através de duas rotas: a partir da fase única da DS plastificada ou da fase amorfa rica em fármaco plastificado (RUMONDOR et al., 2009).

A temperatura entra como um importante fator de estabilidade, uma vez que esse tipo de material possui energia livre maior que sua forma cristalina quando está abaixo do ponto de fusão, podendo desencadear o fenômeno da recristalização. Contudo, as DS podem sofrer de outro problema de estabilidade física, que é caracterizada pela separação de fases amorfa-amorfa (SFAA) que ocorre quando há uma transição da fase vítrea para a líquida em temperaturas acima da Tg (LAPUK et al., 2019). Esse problema também influencia na vantagem de solubilidade e é definido por domínios distintos e amorfos de cada um dos componentes da mistura, favorecendo a cristalização ao diminuir as interações entre os componentes e o efeito inibitório do polímero (BHUJBAL et al., 2021; RUMONDOR; JACKSON; TAYLOR, 2010).

Figura 6 - (A) Estabilização termodinâmica das interações sem ligação de fármaco:polímero promove a dispersão do fármaco por toda a matriz de transporte do polímero. (B) A mobilidade molecular pode levar ao aumento da interação e agregação fármaco:fármaco. (C) Pequenos pontos de agregação e nucleação podem crescer para cristais de fármaco maiores, levando a uma solubilidade reduzida.

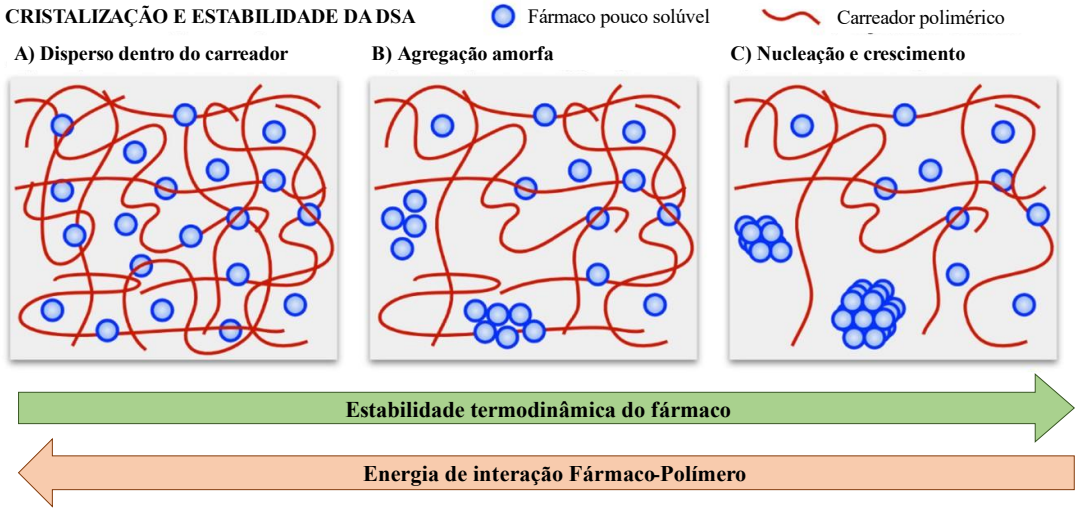

Fonte: Walden et al. (2021).

A facilidade que a cristalização do fármaco do seu estado amorfo depende da força motriz para esse fenômeno, sendo governada pela diferença de energia livre que existe entre os dois estados e as interações moleculares (LIU et al., 2020b; MOSESON et al., 2020). A presença de grupos funcionais que são doadores ou receptores de hidrogênio resultam em interações intermoleculares fármaco:polímero energeticamente favoráveis que, juntas com uma elevada entropia, resultam em pequeno potencial químico do fármaco em uma sistema disperso fármaco:polímero miscível que o fármaco puramente amorfo, levando para uma redução na força motriz termodinâmica para a conversão do fármaco para sua forma cristalina (MARSAC; SHAMBLIN; TAYLOR, 2006; MATSUMOTO; ZOGRAFI, 1999; TAYLOR; ZOGRAFI, 1997).

A redução da mobilidade das moléculas do fármaco é necessária para atrasar a separação de fases e prevenir a cristalização, principalmente pela condição supersaturada promovida pela DS. Assim, faz-se primordial a presença de uma matriz com uma Tg mais alta que a do fármaco, uma vez que o sistema disperso teria uma Tg entre a dos componentes, aumentando a barreira cinética para a cristalização (ASO; YOSHIOKA, 2006; HANCOCK; ZOGRAFI, 1994; VAN DEN MOOTER et al., 2001). Portanto, a mobilidade molecular de um sólido amorfo se torna desprezível 50°C abaixo de sua Tg sendo crucial a escolha de um segundo componente com uma alta Tg, como polímeros hidrofílicos, e que tenha uma boa miscibilidade com o fármaco para formar uma DS termodinamicamente estável (BHUJBAL et al., 2021; KAPOURANI et al., 2020; MONSCHKE; KAYSER; WAGNER, 2020)

3.3 CO-AMORFOS

As dispersões sólidas co-amorfas (CAM) têm se mostrado como uma alternativa para as DSA poliméricas ao demonstrarem melhorias na solubilidade e estabilidade dos fármacos amorfos. Introduzidas primeiramente por Chieng e colaboradores em 2009 em um trabalho que consistia em material amorfo de uma mistura de hidrocloreto de Ranitidina e indometacina, esse tipo de dispersão se baseia na combinação de dois ou mais componentes de baixo peso molecular em uma fase única homogênea e amorfa e tem sido utilizada para estabilizar as formas amorfas de fármacos de baixa solubilidade (CHIENG et al., 2009; KARAGIANNI; KACHRIMANIS; NIKOLAKAKIS, 2018; LÖBMANN et al., 2014).

CAMs são classificados como um subtipo de solução vítrea, assim como as soluções baseadas em polímero ou sílica mesoporosa, tendo o uso de componentes de baixo peso molecular como principal diferenciador entre os três tipos de soluções (DENGALE et al., 2016). Chieng et al. cunhou o termo em 2009 ao propor que a quantidade o excipiente estabilizador pode ser reduzido drasticamente devido ao seu baixo peso molecular.

CAMs possuem diversas vantagens sobre as DSAs, uma vez que o fármaco está incorporado na matriz polimérica e há problemas relacionados a esse tipo de dispersão, como a baixa miscibilidade entre fármacos e polímeros, o que faz precisar de grandes quantidades de polímero e de razões polímero-fármaco maiores, aumentando as dosagens (LU; ZOGRAFI, 1998; SANTOS et al., 2022; SERAJUDDLN, 1999; VASCONCELOS; SARMENTO; COSTA, 2007). Além disso, polímero possuem uma natureza higroscópica, o que os torna mais sensíveis ao calor e humidade, fazendo com que a matriz tenha uma ação plastificante e reduzindo a Tg do sistema,

aumentando a mobilidade molecular, no que pode provocar a separação de fase e recristalização (VASCONCELOS et al., 2016). Esses fatores prejudicam a formulação de DSAs poliméricas, justificando o fato de haver poucas no mercado ainda (DENGALE et al., 2016).

Pode haver dois tipos de CAM a depender do tipo de excipiente estabilizante: as combinações fármaco:fármaco e as misturas fármaco-excipiente (Figura 7). No primeiro, dois fármacos farmacologicamente relevantes para terapias multidrogas são combinando, sendo que ambos se estabilizam na forma amorfa. Assim, ambos os fármacos funcionam como ativos e excipientes ao mesmo tempo. No segundo tipo, excipientes de baixo peso molecular, como aminoácidos, ácidos carboxílicos, ureia e pequenos carboidratos, são usados para preparar blendas fármaco-excipiente estáveis de rápida dissolução (KORHONEN; PAJULA; LAITINEN, 2016; SHI; MOINUDDIN; CAI, 2019).

Figura 7 - Classificação de misturas amorfas baseadas nos coformadores. Insumo farmacêutico ativo (IFA).

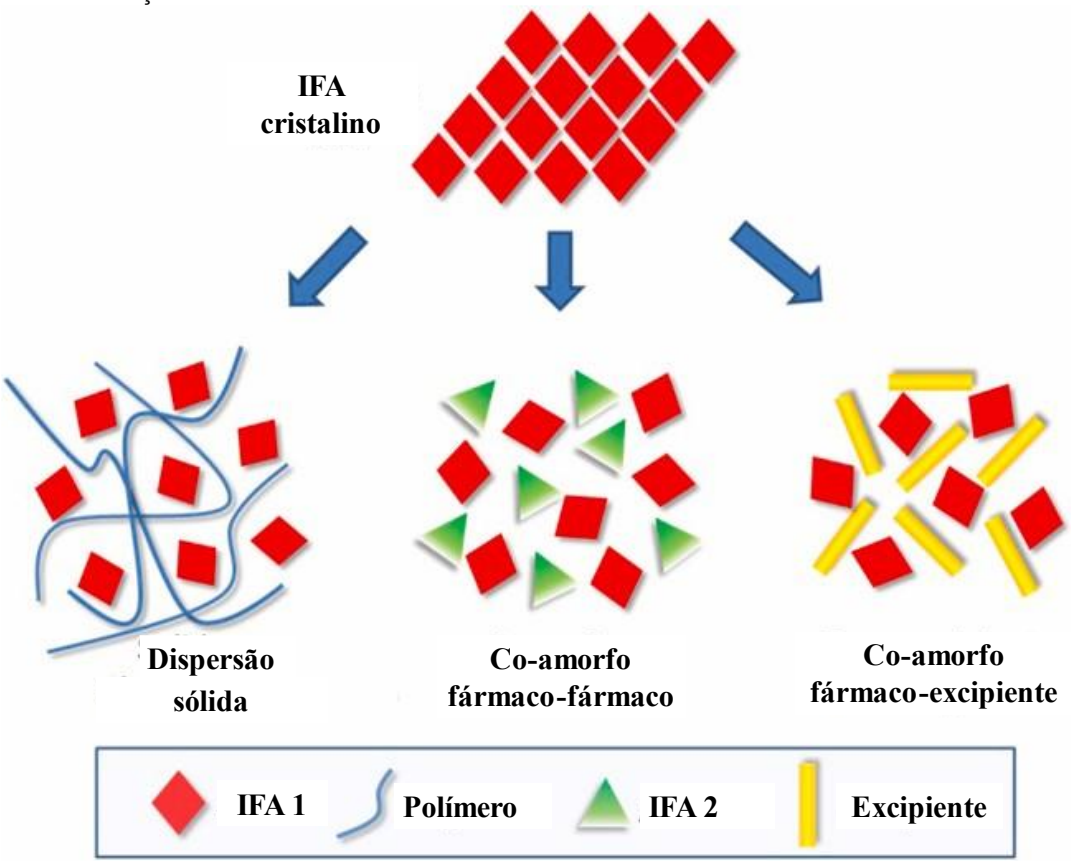

Fonte: Shi, Moinuddi, Cai (2018)

CAMs podem ser descritos por três atributos críticos de qualidade, conhecidos como co-formabilidade, estabilidade física e performance de dissolução. A co-formabilidade se refere à

possibilidade de formação de um CAM consistindo em um fármaco e um coformador escolhido a uma razão definida dos dois para um método de preparação definido. A estabilidade física é necessária para a preservação da forma amorfa instável do fármaco e a performance é de extrema importância para verificar o incremento de solubilidade do fármaco no estado amorfo em comparação a sua forma cristalina (Figura 8). Para isso, o CAM precisa obter e manter a supersaturação, resultando em uma maior biodisponibilidade in vivo (LIU et al., 2021).

Figura 8 - Os três atributos críticos de qualidade (ACQ) dos sistemas de liberação co-amorfo: (1) co-formabilidade; (2) estabilidade física; e (3) performance de dissolução. Os tijolos azuis representam uma molécula de fármaco e o verde, vermelho e amarelos indicam diferentes coformadores.

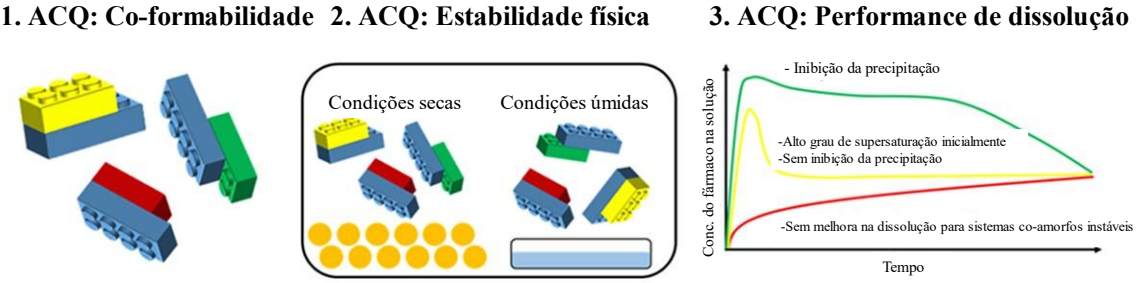

Fonte: Liu et al. (2021)

3.3.1 Vantagens dos CAMs

Dispersões CAM provem uma alta solubilidade ao fármaco devido à alta energia do estado amorfo e por não nenhuma energia ser necessária para o rearranjo da estrutura cristalina durante a dissolução (KARAGIANNI; KACHRIMANIS; NIKOLAKAKIS, 2018). Ademais, eles podem exibir alta estabilidade e dissolução melhoradas em comparação às suas contrapartes cristalinas e formas amorfas individuais (LENZ et al., 2015; LÖBMANN et al., 2011a).

Um significativo aumento da Cmax (1,3 a 30 vezes) e área sob a curva (ASC) (1 a 5 vezes), assim como a diminuição da Tmax tem sido registrado por muitos sistemas CAM, não somente por testes in vitro como em in vivo também (DENGALE et al., 2015; JENSEN et al., 2016a; SHAYANFAR et al., 2013; SURESH; CHAITANYA MANNAVA; NANGIA, 2014). Interações moleculares entre os componentes justificam a estabilidade da forma amorfa e, por consequência, o incremento de solubilidade (LAITINEN et al., 2013).

3.3.2 Mecanismos de estabilização física

Diversos mecanismos podem ser responsáveis para uma boa estabilidade física de misturas CAM, tais como a formação de sais, interações intermoleculares (pontes de hidrogênio,

forças iônicas, interações π-π, forças de van Der Waals), misturas íntimas e efeito antiplastificante.

I. Coformadores

Coformadores são componentes de baixo peso molecular que estabilizam fisicamente a forma amorfa do fármaco através de interações a nível molecular com o fármaco ou por mistura molecular, podendo ser um outro fármaco terapeuticamente relevante ou ainda aminoácidos, ácidos orgânicos, ureia, açucares ou nicotinamida (LIU et al., 2021; SHI; MOINUDDIN; CAI, 2019).

Apesar de farmacologicamente úteis, CAMs de fármaco:fármaco são difíceis de combinar para formar uma solução vítrea na dose requerida. Por isso, é interessante combinações de fármacos com outras moléculas inertes capazes de formar pontes de hidrogênio (KARAGIANNI; KACHRIMANIS; NIKOLAKAKIS, 2018).

II. Miscibilidade amorfa e Tg

Para o CAM se formar como uma fase única amorfa, é necessário que os componentes possuam uma miscibilidade completa dos componentes no estado amorfo, o que pode ser determinada pelo diagrama de fases quando se trata de componentes termoestáveis no estado fundido e, ao resfriar essas fases únicas fundidas, pode-se obter uma fase única co-amorfa (DENGALE et al., 2016; LÖBMANN et al., 2011b; SHIMADA et al., 2013). Contudo, a cálculos podem ser realizados para prever a miscibilidade entre os componentes, como os parâmetros de solubilidade Hansen e o de interações Flory Huggins. Ambos foram utilizados por diversos trabalhos com CAM para prever a possibilidade de formação de uma mistura amorfa (ALHALAWEH; ALZGHOUL; KAIALY, 2014; KITAK et al., 2015; KORHONEN; PAJULA; LAITINEN, 2016).

Um bom indicador para a formação de uma fase única CAM homogênea é a observação de uma só Tg, sendo que componentes imiscíveis ou parcialmente miscíveis resultariam em misturas amorfas de duas fases, produzindo duas diferentes Tgs (VAN DROOGE et al., 2006). Comparado aos excipientes poliméricos, os coformadores empregados para o desenvolvimento de uma CAM geralmente possuem uma baixa Tg, tornando limitada a possibilidade de um efeito antiplastificação. Contudo, esse princípio tem sido relatado em diversos casos de formulações de

CAM, como é o caso da formulação de carbamazepina e indometacina (LÖBMANN et al., 2013; LÖBMANN; GROHGANZ; et al., 2013).

III. Interações intermoleculares

Nos componentes amorfos individuais, as moléculas são geralmente organizadas em uma ordem molecular de curto alcance, que se reflete em interações moleculares entre moléculas semelhantes, como na formação de homodímeros. Tais moléculas são geralmente encontradas de forma semelhante no estado cristalino e, portanto, a recristalização na forma amorfa pura ocorre a uma taxa bastante elevada. Contudo, nos materiais CAM, essa ordem molecular de curto alcance favorece as interações intermoleculares entre as moléculas diferentes, que são os dois componentes diferentes na blenda, formando os heterodímeros relatados em outros estudos (LÖBMANN et al., 2011b; TANTISHAIYAKUL; SUKNUNTHA; VAO-SOONGNERN, 2010).

Portanto, para que uma recristalização ocorra, é necessário que as ligações intermoleculares do heterodímeros sejam quebradas, para que as moléculas se rearranjem em homodímeros, organizando a estrutura cristalina de longo alcance. Contudo, todo esse processo leva um longo tempo, o que torna a probabilidade de uma recristalização menor e prolonga a estabilidade física dos sistemas CAM (LAITINEN et al., 2013; SANDHU et al., 2014). Além disso, interações iônicas ou outras mais fortes tem ocorrido em sistemas CAM, não somente em misturas binárias, como em terciárias também (DENGALE et al., 2016).

A proporção molar dos componentes nos sistemas CAMs binários pode afetar significativamente a estabilidade física, uma vez que razões estequiométricas do fármaco e coformador são preferenciais para manter a estabilidade física, uma vez que excesso de componentes pode levar à cristalização (ALLESØ et al., 2009; LÖBMANN et al., 2013b; UEDA et al., 2016).

CAMs binárias preparadas em razões 1:1 tem demonstrado uma maior estabilidade que as de 2:1 ou 1:2, por terem muitas interações intermoleculares específicas pela formação dos heterodímeros pelas pontes de hidrogênio ou interações iônicas (KARAGIANNI; KACHRIMANIS; NIKOLAKAKIS, 2018). Porém a composição eutética depende das interações intermoleculares e essa razão pode não ser a melhor, como é o caso de um sistema CAM de naproxeno e indometacina, que mostrou uma maior estabilidade física na razão molar de 3:2 (BEYER et al., 2016).

IV. Mistura íntima

É relatado que moléculas similares numa blenda homogênea CAM se separam fisicamente como resultado de uma mistura íntima entre os componentes de uma mistura, levando a uma estabilidade física melhorada, como é o caso de uma mistura binária de sinvastatina e glipizida que possuíram estabilidade física melhorada em relação aos mesmos fármacos amorfos isolados que não possuíam interações intermoleculares entre si (LÖBMANN et al., 2012).

A probabilidade da ocorrência de uma recristalização é maior quando ocorre a mistura dos componentes é desfeita e ocorre uma separação de fases, o que é muito difícil de ocorrer para a maioria dos sistemas CAMs devido às interações moleculares presentes, além da mistura dos componentes ocorrer a um nível molecular, fortalecendo as interações formadas (LÖBMANN et al., 2013c, 2013a).

3.3.3 Performance in vitro

Por possuírem uma elevada energia interna, fármacos amorfos possuem uma maior solubilidade e taxa de dissolução em relação às suas contrapartes cristalina. Esse fato ganha ainda mais destaque quando é analisado o sistema CAM que tem demonstrado uma dissolução melhorada em relação até à forma amorfa individual (DENGALE et al., 2014; LÖBMANN et al., 2011b; QIAN et al., 2015).

É comum que em sistemas amorfos, o incremento da taxa de dissolução seja atribuído a um salto de concentração para níveis elevados. Esse salto é a maior energia amorfa do insumo ativo que facilita a dissolução e a supersaturação de fármacos quando se dissolve junto com outros componentes. Tal supersaturação pode ser afetada por diversos fatores, como a natureza exata do meio de dissolução, a diferença de energia livre entre as fases amorfa e cristalina e as taxas de liberação dos componentes. Após o salto, há uma diminuição progressiva de concentração denominada como “paraquedas”. Esse processo ocorre pela presença do coformador que, ao impedir uma rápida e imediata nucleação, atrasa a recristalização, mantendo a supersaturação por um tempo mais prolongado (SHI; MOINUDDIN; CAI, 2019; SUN; LEE, 2013b).

Contudo, nem sempre isso é regra. Foi demonstrado que alguns sistemas CAMs perdem rapidamente a supersaturação, apesar de exibirem taxas de dissolução melhor que suas contrapartes cristalinas e amorfa isolada. Isso pode ter ocorrido devido ao aumento da área superficial das partículas, diminuição do tamanho das mesmas e solubilidade melhorada do

fármaco, como ocorreu com um sistema CAM de cetoconazol-ácido succínico (FUNG; BĒRZIŅŠ; SURYANARAYANAN, 2018).

Alguns CAMs têm mostrado dissolução sincronizada dos componentes individuais devido ao seu arranjo molecular de curto alcance, isto é, a formação de heterodímeros através das pontes de hidrogênio (ALLESØ et al., 2009). Tal sincronismo é relacionado com as fortes interações intermoleculares entre os componentes, sendo a presença do coformador o principal motivo pelo incremento de solubilidade e da taxa de dissolução do CAM, uma vez que a solubilidade do coformador e a força da interação entre os componentes são quem determina a taxa de dissolução do fármaco de baixa solubilidade, como demonstrado por Löbmann et al. (2013).

Além desses fatores, a solubilidade do coformador também influencia na taxa de dissolução do fármaco, sendo o uso de um coformador solúvel preferível para a dissolução de fármacos de baixa solubilidade aquosa (LÖBMANN et al., 2013a; SHI; MOINUDDIN; CAI, 2019). Contudo, a manutenção da supersaturação ainda é de extrema importância, sobretudo para a absorção do fármaco, e isso pode ser prejudicado caso a solubilidade do coformador seja tão alta, que ele se dissolva rapidamente e não estabilize o fármaco amorfo o suficiente para ser absorvido (SUN; LEE, 2013a).

3.4 NEVIRAPINA

3.4.1 Química

Nevirapina (NVP) ou, segundo IUPAC, 1-ciclopropil-5,11-dihidro-4-metil-6H-dipirido[3,2-b:2’,3’-e][1,4] diazepin-6-ona é o princípio ativo do medicamento comercial Viramune®, representado na fórmula estrutural na Figura 9. Ela possui como fórmula molecular C15H14N4O, com um peso molecular de 266,3 g/mol, sendo reportado 3 impurezas e um ponto de fusão de 247 a 249°C e LogP de 2,5 e altamente solúvel em pH<3 (SANGANWAR et al., 2010).

Esse fármaco se apresenta como um pó branco, ligeiramente solúvel em diclorometano e metanol e praticamente insolúvel em água (USP, 2014), sendo uma base orgânica fraca cujo ácido conjugado possui um pKa=2,8 (LOKAMATHA; KUMAR; RAO, 2011; PEREIRA et al., 2007). NVP é classificado como pertencente à classe II do SCB, devido à sua baixa solubilidade aquosa e alta permeabilidade nas membranas plasmáticas (LINDENBERG; KOPP; DRESSMAN, 2004).

Figura 9 - Estrutura molecular da Nevirapina

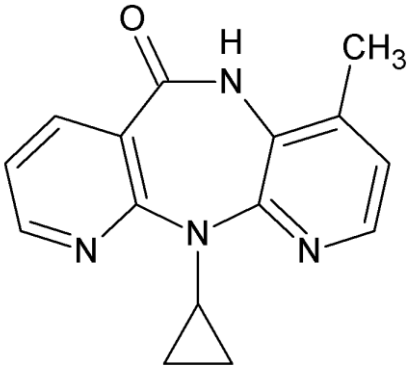

Fonte: O autor (2024)

3.4.2 Farmacodinâmica

O NVP é um fármaco da classe das dipiridodiazepinonas pertencente à classe dos inibidores de transcriptase reversa não análogos a nucleosídeos (ITRNN). A transcriptase reversa é uma enzima que participa do ciclo de replicação viral do HIV, sendo responsável pela conversão do material genético virulento de RNA para DNA. Sua inibição específica e não competitiva pelo NVP impede a continuação do ciclo de vida do HIV (FINDLAY, 2007; HANNONGBUA; PRASITHICHOKEKUL; PUNGPO, 2001).

3.4.2.1 Efeitos Adversos

A NVP é o fármaco com maior potencial para causar uma hepatite clínica dentre a sua classe de medicamentos, levando a ocorrência de reações cutâneas severas e até erupções com risco de vida em 2% dos pacientes tratados clinicamente (FINDLAY, 2007). Foram descritas anormalidades psiquiátricas, tais como casos de delírio e psicose em pacientes que receberam a administração de NVP entre 10 e 14 dias, sendo que responderam bem à retirada da droga (WISE; MISTRY; REID, 2002).

Outros estudos mostraram que 33 de 70 pacientes soropositivos que receberam NVP desenvolveram aumento nas atividades da aminotransferase, em que altas concentrações de NVP e infecção do vírus da Hepatite C foram previsores independentes de toxicidade hepática. Naqueles com hepatite C crônica, as concentrações de NVP acima de 6 µg/ml foram associados com um risco de 92% de toxicidade hepática (GONZALEZ DE REQUENA et al., 2002)

3.4.3 Farmacocinética

A NVP é administrada por via oral com picos de níveis sorológicos 4 horas após uma dose única de 200 mg, sendo que comida não afeta na extensão da absorção (CHEMICAL, 2013). Ela apresenta uma biodisponibilidade relativa seguindo a ordem a seguir: jejuno>íleo>cólon ascendente> cólon descendente. Isso se dá porque, embora ele seja absorvido por todo o trato gastrointestinal, sua taxa de absorção diminui a partir do jejuno (MACHA et al., 2009).

Possui um volume de distribuição de 1,21 l/Kg, com ligação plasmática de 60%, e metabolização hepática via hidroxilação e glicuronidação. Sua eliminação se dá principalmente pelos rins, com menos de 5% indo como fármaco não alterado e pequenas porções são também excretadas nas fezes (FINDLAY, 2007).

3.4.4 Terapêutica

A NVP foi o primeiro fármaco antirretroviral da classe dos ITRNN a ser aprovado pelo Food and Drug Administration (FDA), com o nome comercial de Viramune®, nome também comercializado no Brasil em forma de comprimido simples de 200 mg ou na forma de suspensão de 10mg/ml (DE CLERCQ, 2009).

Devido a sua ação, a NVP é indicada para a prevenção de mãe para filho do HIV-1 em mulheres grávidas que não estão fazendo uso de TARV durante o trabalho de parto. Ela também é utilizada em combinação com outros antirretrovirais, como a lamivudina (3TC) para o tratamento da infecção do HIV tanto em crianças, quanto em adultos, embora para estes últimos seu uso tem ficado ultrapassado nos últimos anos (BARDSLEY-ELLIOT; PERRY, 2000; FINDLAY, 2007).

No Brasil, ela é utilizada junto da Zidovudina (AZT) por 4 semana em 3 doses por via oral em recém-nascidos expostos ao vírus e com AZT e 3TC durante os 14 dias até 3 anos de vida da criança. Ela ainda é utilizada em crianças de 14 dias a 8 anos com uma dose de 200 mg/m2 1x/dia por 14 dias, depois 200mg/m2 12/12 horas. Acima de 8 anos é usado na dose de 120-150mg/m2 (dose máxima 200mg 12/12 horas) e em adolescentes com dosagem de 200 mg por dia e após os 14 dias iniciais, 200mg 12/12 horas (BRASIL. MINISTÉRIO DA SAÚDE. SECRETARIA DE VIGILÂNCIA EM SAÚDE. DEPARTAMENTO DE VIGILÂNCIA, 2018).

3.4.5 Sistemas de Liberação para o incremento de solubilidade aquosa de nevirapina

Durante os anos, outros estudos foram feitos na tentativa de melhorar a solubilidade aquosa de NVP. Ahire, Rane e Pawar (2010) tentaram melhorar a solubilidade de NVP pela técnica da dispersão sólida usando o polímero polivinilpirrolidona K30 (PVP K30) como carreador.

A dispersão foi feita pelas técnicas de evaporação de solvente e amassamento e os autores perceberam a presença do fármaco amorfo, além do incremento de solubilidade do fármaco na dispersão em comparação com ele na mistura física e isolado (AHIRE et al., 2010).

A produção simultânea e co-mistura de micropartículas de NVP com lactose e celulose microcristalina pelo método antisolvente supercrítico foi realizado para um incremento de dissolução. As micropartículas do fármaco foram preparadas e depositadas simultaneamente na superfície dos excipientes para reduzir a agregação das partículas fármaco:fármaco. As misturas obtidas foram caracterizadas e, embora não tenham alterado a cristalinidade ou propriedades físico-químicas da NVP, tiveram uma taxa de dissolução mais rápida em relação às micropartículas do fármaco isolado ou na mistura física com os excipientes (SANGANWAR et al., 2010).

Outro estudo também pretendia alcançar uma dissolução mais rápida de NVP utilizando dispersões sólidas e agentes hidrotrópicos, como a ureia, lactose, ácido cítrico e manitol em diferentes proporções. Inicialmente, foi determinado a solubilidade do fármaco individualmente na presença dos quatro excipientes e, após descobrir que a maior solubilidade foi o da solução de ácido cítrico 40%, foi feito combinações de 2 e 3 agentes hidrotrópicos em diferentes razões para determinar a solubilidade, sem, entretanto, ultrapassar a concentração de 40% dos agentes na mistura. Foi concluído que a técnica dissolve os fármacos na forma molecular e eleva a solubilidade da NVP, tendo um potencial para outros fármacos (MADAN et al., 2017).

Um outro tipo de dispersão sólida de NVP foi desenvolvida para o incremento de solubilidade e do perfil in vivo ao utilizar a vitamina E TGPS, um surfactante não iônico, como carreador usando a técnica da evaporação do solvente e a formulação otimizada foi convertida em comprimidos de rápida dissolução. O estudo indicou que há uma relação linear entre a solubilidade do fármaco e a concentração do carreador e os comprimidos se tornaram uma forma de farmacêutica imediata ao possuir uma liberação do fármaco rápida (SINGH et al., 2019).

Mais recentemente, nosso grupo desenvolveu dispersões sólidas de NVP para avaliar o impacto da quantidade de fármaco na dissolução e difusão por membranas. Para isso, desenvolvemos três DSAs com carregamentos de NVP diferentes e percebemos que quanto menor a quantidade de fármaco, mais interações existiam entre ele e o polímero, o que estabilizava mais o sistema amorfo disperso, além de manter a supersaturação por um tempo mais prolongado e que isso afetava na permeação do fármaco (SANTOS et al., 2022).

4 ARTIGO 1 – NEW HORIZONS IN ANTIRETROVIRAL DRUG DELIVERY SYSTEMS FOR HIV MANAGEMENT

5 ARTIGO 2 – COMBINED USE OF COMPUTATIONAL AND THERMAL TECHNIQUES TO OBTAIN NEVIRAPINE CO-AMORPHOUS

6 ARTIGO 3 – DESENVOLVIMENTO DE DISPERSÕES SÓLIDAS TERNÁRIAS fármaco:fármaco:polímero para a terapia de combinação antirretroviral

INTRODUÇÃO

O HIV ainda é uma grande questão de saúde pública, atingindo cerca de 39 milhões de pessoas no mundo, com 1,3 milhões de novos infectados apenas em 2022. A terapia atual consiste na combinação de fármacos para alcançar uma vida de maior qualidade e manter a carga viral indetectável (KAKAD; KSHIRSAGAR, 2020). O uso combinado de fármacos é a terapia atual para o combate ao HIV, conhecido como terapia antiretroviral altamente ativa (HAART) onde dois ou mais fármacos são utilizados na mesma forma farmacêutica. O uso de HAART melhora a adesão do paciente ao tratamento, reduzindo a "carga de comprimidos diário" (BERG, 2020; KIRTANE; LANGER; TRAVERSO, 2016).

Entretanto, a baixa solubilidade aquosa dos fármacos pode comprometer a biodisponibilidade oral, inclusive os utilizados na terapia HAART. Isso ocorre porque até 90% das novas entidades químicas em desenvolvimento são pouco solúveis e pertencem à Classe II ou IV do Sistema de Classificação Biofarmacêutica (SCB) (AMIDON et al., 1995; SOSNIK; AUGUSTINE, 2015). Fármacos com solubilidade aquosa limitada frequentemente enfrentam obstáculos em seu processo de dissolução, como a existência de uma estrutura cristalina robusta, sustentada por fortes interações intermoleculares, que impede a desagregação de sua forma sólida, característico de moléculas com ponto de fusão alto (ACHARYA et al., 2018; SAVJANI, K. T.; GAJJAR; SAVJANI, J. K., 2012).

Nestas circunstâncias, será desejável desenvolver estratégias que melhorem simultaneamente a solubilidade aquosa e, consequentemente, a biodisponibilidade dos fármacos de baixa solubilidade aquosa (SHAH, N. et al., 2013). Ao considerar estratégias de melhoria da solubilidade em terapias de combinação, o potencial para interações intermoleculares entre drogas para aumentar a solubilidade pode ser explorado, podendo formar um sal droga-droga, co-cristal ou co-amorfo entre si.

Em cocristais e sais, existe uma proporção molar definida das duas moléculas, onde a proporção molar 1:1 é a mais convencional pela igualdade de interações intermoleculares formadas. Isso ocorre até mesmo para sistemas co-amorfos, que são flexíveis em sua composição, mas possuem maior estabilidade físico-química em alguma estequiometria pré-definida (ADEOYE et al., 2020; JENSEN et al., 2016; WU, W. et al., 2018). Contudo, fazer uso de

proporções definidas entre dois fármacos não é a realidade da HAART, que requer sistemas de liberação que não exigem estequiometria molecular específica.

O uso da dispersão sólida amorfa (DSA) é uma estratégia popular de estabilização física ao combinar dispersar molecularmente um ou mais fármacos em um veículo polimérico hidrofílico, pode superar as limitações relacionadas à baixa solubilidade aquosa (BAGHEL; CATHCART; O'REILLY, 2016; BHUJBAL et al., 2021). Contudo, o sucesso no desenvolvimento dessas dispersões depende da escolha correta de um veículo que não apenas melhore a dissolução do fármaco, mas também atue prevenindo sua precipitação ou recristalização, mantendo a estabilidade tanto em estado sólido quanto em solução (ARUNACHALAM et al., 2010; BINDHANI; MOHAPATRA, 2018; SCHITTNY; HUWYLER; PUCHKOV, 2020; SZAFRANIEC-SZCZĘSNY et al., 2021).

Portanto, o objetivo geral desta parte do trabalho foi projetar uma formulação alternativa aos CAMs para o aumento da dissolução de nevirapina (NVP), um antiretroviral usado no tratamento do HIV pediátrico de classe II no SCB utilizado em combinação com o antiretroviral lamivudina (3TC). Visto que clinicamente a proporção molar entre os dois fármacos é de 1,8:1 (NVP:3TC), NVP está em excesso e corre risco de sofrer recristalização. Logo, é necessário o acréscimo de polímero para interagir com as moléculas de fármaco, sobretudo as que estão em excesso e estabilizá-la no estado amorfo.

As fortes interações droga-polímero podem reduzir dramaticamente a mobilidade molecular das DSAs, levando a uma pronunciada inibição da cristalização. As interações, quando retidas em solução, resultaram em supersaturação sustentada do medicamento. Assim, levantamos a hipótese de que as interações droga-droga e droga-polímero, ao reduzir a mobilidade molecular, estabilizarão fisicamente NVP nas DSAs ternárias e aumentarão a dissolução da droga.

METODOLOGIA

Materiais

Nevirapina foi adquirido de Farmanguinhos (Rio de Janeiro, Brasil). Lamivudina foi doado pelo Laboratório Farmacêutico de Pernambuco (LAFEPE). Soluplus e PVP VA-64 foram obtidos pela BASF®. A água ultrapura foi obtida através de sistema MilliQ® (Milipore, Bedford, EUA). Todos os demais reagentes e solventes foram de grau analítico ou de grau para CLAE, tendo

sido comprados e usados assim que recebidos. Os principais materiais usados estão ilustrados na Figura 1.

Figura 1 - Estrutura molecular dos compostos utilizados para formação dos sistemas *co-amorfos*

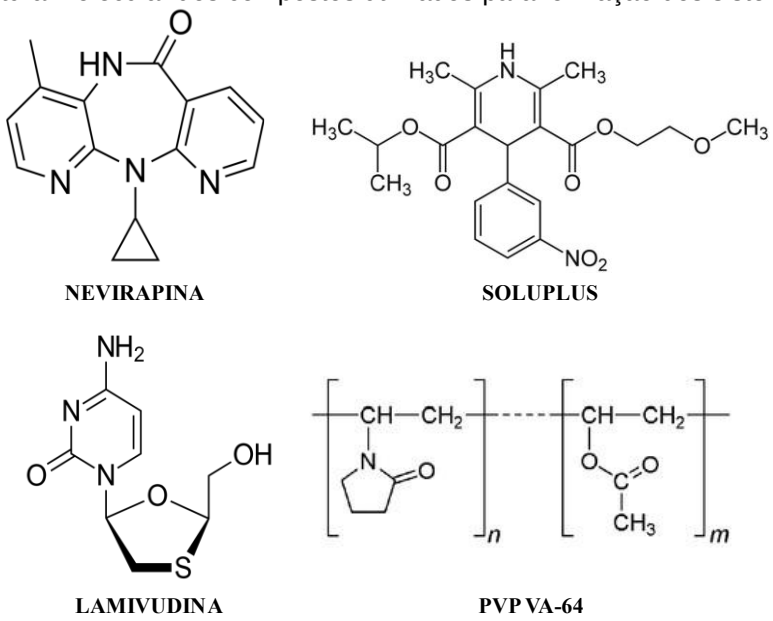

Fonte: O autor (2024)

Preparo de DSAs Ternárias pelo método *Quench-Cooling*

As DSAs ternárias foram preparadas por meio da fusão das misturas físicas (MFs) de NVP, 3TC e polímero. A equivalência molar para a proporção terapêutica entre NVP:3TC é de 1,8:1 respectivamente (BRASIL. MINISTÉRIO DA SAÚDE. SECRETARIA DE VIGILÂNCIA EM SAÚDE. DEPARTAMENTO DE VIGILÂNCIA, 2018). Com essa informação, quantidades específicas dos fármacos foram pesadas obedecendo a proporção terapêutica em que os dois são usados para o tratamento do HIV. Após a pesagem dos fármacos e polímeros, misturas ternárias com *drug loading* de 20% em relação à quantidade total de fármaco foram preparadas e misturadas em um grau para promover o contato íntimo entre as partículas formando as MFs, conforme relatado na literatura (LI et al., 2022; PACULT et al., 2019).

O pó triturado foi colocado em um cadinho de alumínio e aquecido a 260 °C em chapa de aquecimento. Após a completa fusão da amostra (1-2 minutos), o recipiente foi rapidamente transportado para um banho de gelo onde sofreu um resfriamento rápido. Em seguida, a amostra sólida foi retirada e armazenada em dessecador contendo sílica em gel, para prevenção de umidade, até sua moagem em grau e pistilo. As partículas foram padronizadas para um tamanho menor que 150 µm.

Caracterizações do estado sólido

Todas as caracterizações foram realizadas com NVP, 3TC, Soluplus e PVP VA-64 isoladamente e com MFs e DSAs obtidas experimentalmente.

Espectroscopia de Infravermelho com transformada de Fourier (FTIR)

Os espectros de infravermelho na região média com transformada de Fourier de foram obtidos utilizando o equipamento PerkinElmer® (modelo 400) com dispositivo de reflexão total atenuada (ATR) com cristal de seleneto de zinco.

As amostras analisadas foram transferidas diretamente para o compartimento do dispositivo de ATR, com o auxílio de uma espátula, tendo uma análise de "branco" efetuada entre cada ensaio, com a célula higienizada por acetona. O resultado foi obtido no modo de transmitância pela média de 16 varreduras por espectro, obtidas de 4000 a 650 cm^{-1} na resolução de 4 cm^{-1}.

Calorimetria Exploratória Diferencial (DSC)

As curvas DSC foram obtidas em calorímetro de varredura Shimadzu®, modelo DSC-50, interligado ao software Shimadzu® TA-60WS com atmosfera de nitrogênio (50 ml/min) na faixa de temperatura de 25–300 °C. O ensaio foi feito ao pôr as amostras na porta amostra de alumínio hermeticamente fechados com massa equivalente a 3,0 mg (± 0.1 mg) de NVP. Foi utilizado índio metálico com pureza de 99,9% para calibrar a escala de temperatura e a resposta de entalpia.

Difração de Raios-X (DRX)

Análises de difração de raios-X foram realizadas em um difratrômetro Siemens X-Ray Diffratometer D-500, equipado com um ânodo de cobre. O intervalo de ângulo 2θ de 5-70° com uma velocidade de digitalização de 0,02° 2θ/s. preparados em suportes de vidro com uma fina camada de material do pó sem solvente.

Método de Quantificação por cromatografia líquida de alta eficiência de NVP

O equipamento de cromatografia líquida de alta eficiência (CLAE) usado é composto pelo sistema de série 10AVP da Shimadzu, consistindo em uma bomba quaternária LC-10AVP, um detector ultravioleta SPP-M10AVP. A aquisição de dados foi realizada pelo software LC Solutions

(versão 1,25). A separação cromatográfica ocorreu em uma coluna C8 Shim-Pack (150 x 4,6 mm; 5 µm), a uma temperatura de 25 °C e volume de injeção de 10 µm.

A separação foi alcançada no modo gradiente de baixa pressão tendo como fase móvel A, o tampão acetato de amônio 25mM pH 3,9, e metanol como fase móvel B. O perfil gradiente (%v/v) consistiu em um aumento linear da fase B de 25% para 75% até 7 minutos enquanto o A diminuía linearmente de 75% para 25% no mesmo tempo. A concentração se invertia novamente entre 7 e 8 minutos e se manteve isocrático até o fim da análise, em 15 minutos. A curva de calibração demonstrou boa linearidade (R>0,99) no intervalo de concentração relevante e uma análise preliminar realizada com soluções a 10 µg/mL mostrou que 3TC, Soluplus e PVP-VA64 não interferem com o tempo de retenção de NVP (~10 min).

Preparo de tampão/fase móvel

Um tampão de 1000 ml de 25mM acetato de amônio foi preparado ao pesar uma quantidade do pó de acetato de amônio, o qual foi dissolvido em uma quantidade de água ultrapura e transferido para uma vidraria volumétrica. O pH foi ajustado com ácido acético para 3,9 e, ainda em agitação contínua, o volume foi completado com o solvente para o volume pretendido. Em seguida, o tampão foi filtrado com um filtro de membrana de 0,45 µm e desgaseificado.

Dissolução em condição SINK

Os estudos cinéticos foram avaliados em condição *sink* em um Dissolutor Vankel VK-7040. Quantidades de amostra da NVP isolada, misturas físicas e sistemas amorfos foram pesados para um peso equivalente de 25 mg de NVP e colocados em 250 mL em tampão fosfato pH 6,8, mantido em temperatura de 37,5 °C e com agitação de pás a 75 rpm. Amostras foram coletadas em tempos pré-determinados, submetidas a centrifugação e o sobrenadante foi quantificado por metodologia CLAE previamente descrita 5.2.4.

A eficiência de dissolução também foi utilizada para comparar os perfis de dissolução gerados e foi calculada a partir das curvas da concentração de NVP dissolvida (%) pelo tempo (min) após obter a área sob a curva e a área total do gráfico para os tempos de 120 min e 360 min.

Análises estatísticas

Análises de variância (ANOVA) de uma via e testes de comparações múltiplas de Tukey foram realizados a fim de verificar a significância estatística ($p < 0,05$, com um intervalo de confiança de 95%) das comparações entre as amostras de NVP e as MFs e DSAs.

RESULTADOS E DISCUSSÕES

Caracterizações do estado sólido

Espectroscopia de Infravermelho com Transformada de Fourier (FTIR)

A espectroscopia de infravermelho foi utilizada para investigar as interações entre os polímeros e fármaco nas DSAs e MFs obtidas, sendo que as interações realizadas por meio da ligação de hidrogênio primordiais para o estabelecimento de sistemas dispersos amorfos (SUN et al., 2012), provocando mudanças na posição ou na forma das bandas no espectro infravermelho dos grupos envolvidos nas interações.

As análises de FTIR dos fármacos, polímeros e suas MFs e DSAs estão reveladas na Figura 2.

O espectro de NVP revelam as bandas características do fármaco cristalino, com um estiramento do grupo -NH da amida em 3186 cm^{-1}, estiramento -CH do ciclopropil em 3124 cm^{-1}, estiramento -CH em 3062 cm^{-1}, estiramento -C=O da amida em 1642 cm^{-1} e vibração tesoura -CH3 em 1582 cm^{-1}. 3TC cristalina revelou suas bandas largas de estiramento dos grupos -OH e -NH2 entre 3504 cm^{-1} e 3325 cm^{-1} respectivamente, a amina primária em 3199 cm^{-1}, grupo aromático -CH em 3076 cm^{-1}, ligação -C=O em 1631 cm^{-1}, deformação -NH em 1606 cm^{-1} e o estiramento -CO em 1058 cm^{-1}.

As análises de indicam um deslocamento da banda 1642 cm^{-1} do grupo amida de NVP para 1639 cm^{-1} na DS com Soluplus, onde também sofreu alargamento. Essa banda se sobrepõe ao pico 1582 cm^{-1} de NVP. Um grande alargamento das bandas 3186 cm^{-1} e 3062 cm^{-1} de NVP foi identificado na DS com Soluplus, onde alargamentos das bandas entre 3504 e 3325 de 3TC também foram identificados e sobreposição das bandas 1631 e 1606 na DS com Soluplus. Para as dispersões contendo PVP VA-64, foram detectados deslocamentos e alargamentos da banda 1642 cm^{-1} para 1648 cm^{-1}, além de outros alargamentos das bandas 1585 cm^{-1} e de 3323 cm^{-1} a 2825 cm^{-1} de NVP.

Figura 2 - Espectros de FTIR de NVP e 3TC, das MFs e DSAs contendo PVP-VA64 (A) e Soluplus (B)

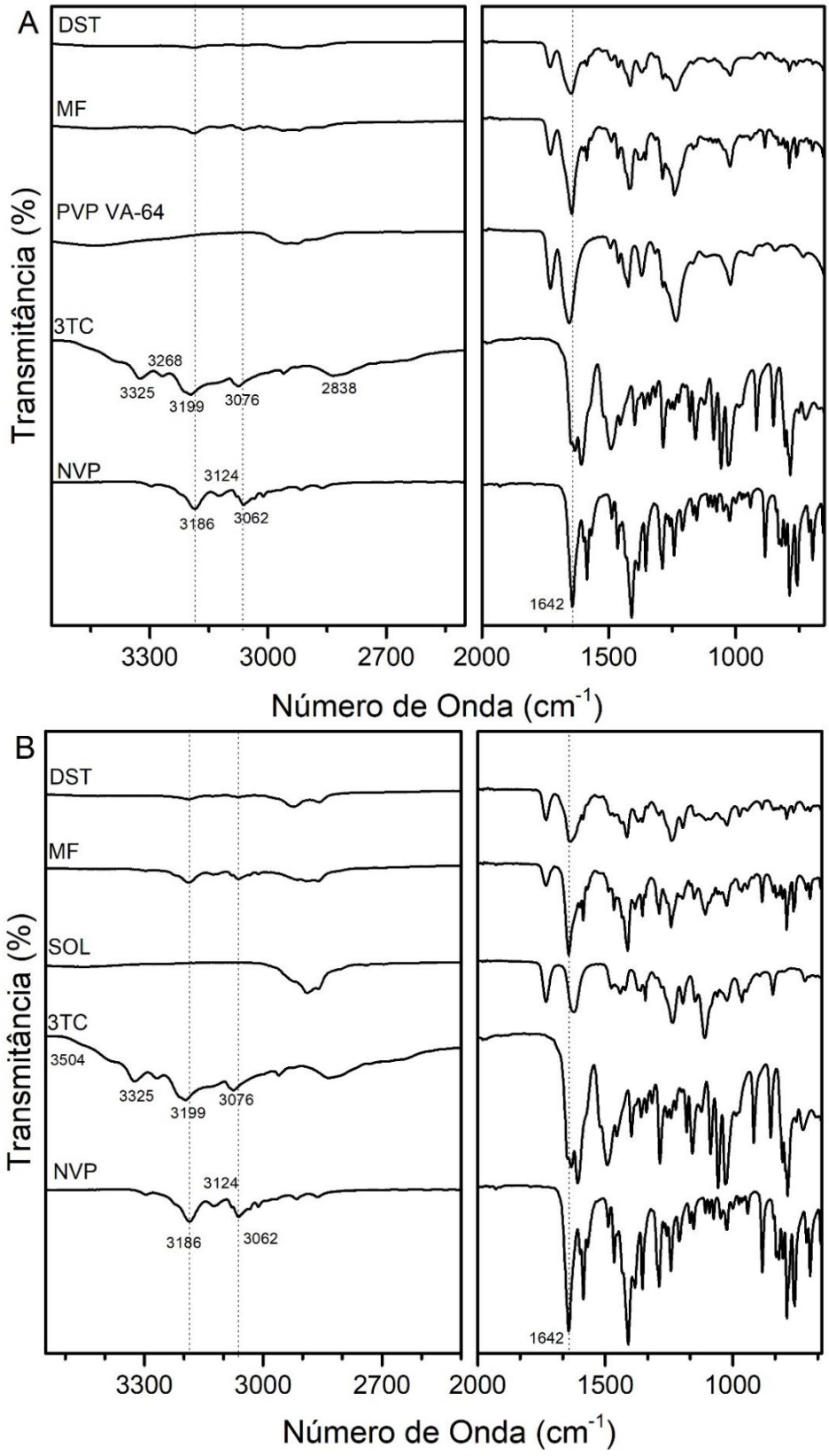

Fonte: O autor (2024)

Alargamentos de bandas é típico de materiais amorfos devido à falta de uma ligação específica de ordem de longo-alcance, levando o material amorfo a numerosos arranjos ligeiramente diferentes com moléculas vizinhas, alterando a frequência vibracional (D'ANGELO et al., 2018). Como a presença das interações intermoleculares são percebidas através dos espectros de infravermelho sobretudo em mudanças nos espectros relacionados às regiões pertencentes a grupos aceptores ou doadores de hidrogênio, pode-se entender que houve interações entre os materiais, o que sugere a formação de um sistema estável amorfo de NVP graças à presença de 3TC e do polímero.

Calorimetria Exploratória Diferencial (DSC)

Para verificar a natureza cristalina de NVP nas amostras e se os componentes usados eram miscíveis entre si, análises de DSC foram realizadas nos componentes isolados, MFs e suas DSAs respectivas (Figura 3). A NVP cristalina apresenta uma temperatura de fusão em 244 °C e 3TC em 175 °C.

Figura 3 - Curvas de DSC de NVP e 3TC, das MFs e DSAs contendo PVP-VA64 e Soluplus

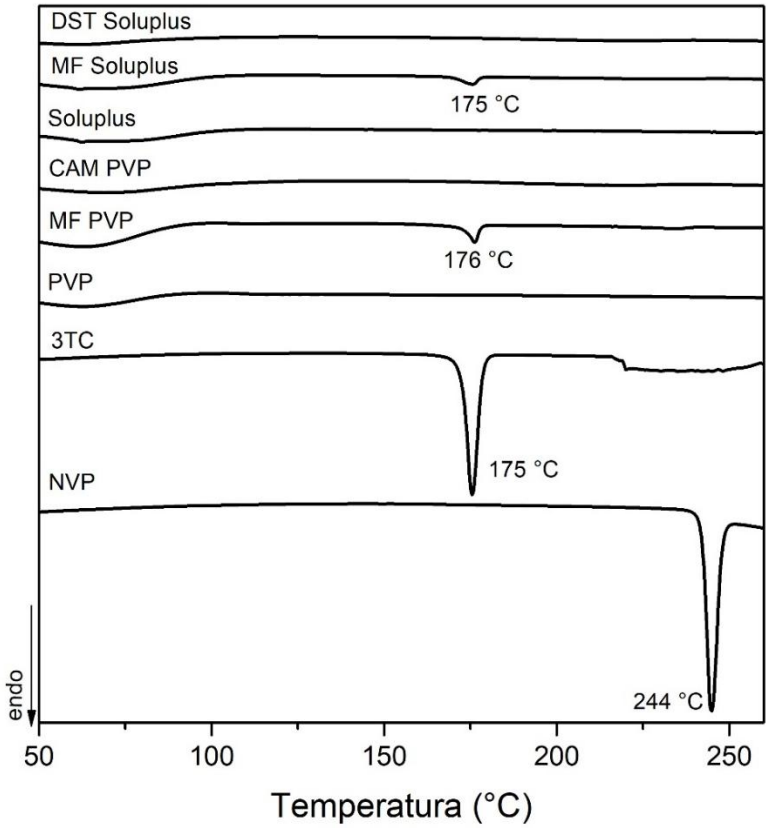

Fonte: O autor (2024)

Devido à natureza amorfa dos polímeros, eles não apresentam picos endotérmicos de fusão, mas um evento que indica a temperatura na qual as cadeias poliméricas se tornam mais flexíveis quando abaixo dela, a transição vítrea (Tg). A Tg do PVP VA-64 foi evidenciada em 108°C, conforme descrito em literatura (CHAN et al., 2015). Contudo a Tg do Soluplus em 72 °C (LIU et al., 2013), não foi identificado, devido a sobreposição de uma banda larga de desidratação na região, uma vez que o polímero é hidrofílico e possui alta tendência de absorção de umidade.

As duas misturas físicas apresentaram um pico endotérmico cada em 175°C que corresponde à temperatura de fusão do 3TC, indicando a presença de material cristalino do fármaco nas duas MFs, enquanto nenhum evento relacionado à NVP foi detectado nas MFs. Na DAS poliméricas não foi identificado eventos térmicos relevantes, além de uma grande banda endotérmica referente à desidratação do material até 100°C que pode estar sobrepondo as Tgs dos sistemas amorfos.

A presença cristalina de 3TC pode indicar que a simples trituração e mistura intima com os demais componentes não foi o suficiente para miscibilizar os três componentes completamente, principalmente sendo esse fármaco o componente de menor quantidade nas formulações, fato esse que não ocorreu nas DSAs geradas, onde não há evidências de qualquer material cristalino. Apesar disso, a não observação de Tg, tão comum em materiais amorfos, pode estar relacionada às bandas de desidratação vistas nos dois polímeros, pela sobreposição de bandas, o que não exclui a possibilidade do material ser homogêneo. Diante do que foi exposto, foi possível presumir a formação de sistemas homogêneos amorfos, corroborando com os resultados de infravermelho nos quais interações intermoleculares ocorrem entre os componentes na presença de 80% de polímero na formulação.

Difração de Raios-X (DRX)

Amorficidade de uma dispersão sólida é de extrema importância para garantir a performance final da DAS. Por isso, DRX foi empregado para checar a cristalinidade de todas as amostras preparadas. A natureza cristalina dos fármacos é representada pelos difratogramas na Figura 4, onde os picos de difração característicos cristalinos são revelados com intensidade variável. A sobreposição do padrão de difração cristalino dos dois fármacos foi identificada nas MFs obtidas, com difratogramas similares, indicando que a trituração adotada para gerar as MFs não alterou o estado sólido dos componentes, que mantiveram suas características cristalinas.

Figura 4 - Difratogramas de raios-X de NVP e 3TC, das MFs e DSAs contendo PVP-VA64) e Soluplus

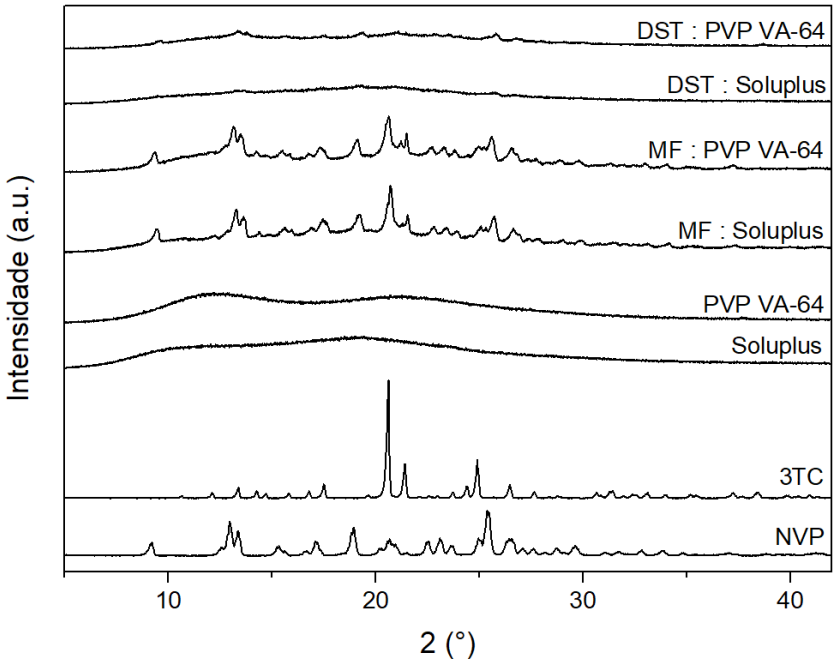

Fonte: O autor (2024)

Os polímeros mostraram grandes halos de difração que correspondem às suas naturezas amorfas, assim como halos de difração também foram vistos nas DSAs obtidas, confirmando que as interações formadas entre os componentes foram hábeis em manter o fármaco amorfo pela técnica de fusão na proporção utilizada de fármaco:polímero, corroborando com os demais ensaios discutidos previamente.

Dissolução

Os perfis de liberação de NVP nas diferentes formulações estão representadas na Figura 5, com as eficiências de dissolução (ED%) calculados tabelados na tabela 1. Como esperado, a baixa solubilidade aquosa de NVP levou a uma baixa taxa de dissolução do fármaco em sua forma pura, chegando a uma concentração final de 64% de NVP, apresentando uma ED% de 28,2% e 46,3% para os tempos de 120 e 360 minutos de ensaio. Apesar da maior velocidade de dissolução promovida pela presença dos polímeros, a MF preparada a base de Soluplus terminou o ensaio com 63% de NVP, com uma eficiência de dissolução (ED%) de 55,7% e 66,5% para os tempos de 120 e 360 minutos respectivamente, enquanto a MF feita com PVP VA-64 terminou com 76%, alcançando uma ED% de 38,5% e 40,7% para os mesmos tempos, ambos com diferença estatística em relação à NVP pura.

Figura 5 - Perfis de dissolução de NVP e 3TC, das MFs e DSAs contendo PVP-VA64 e Soluplus

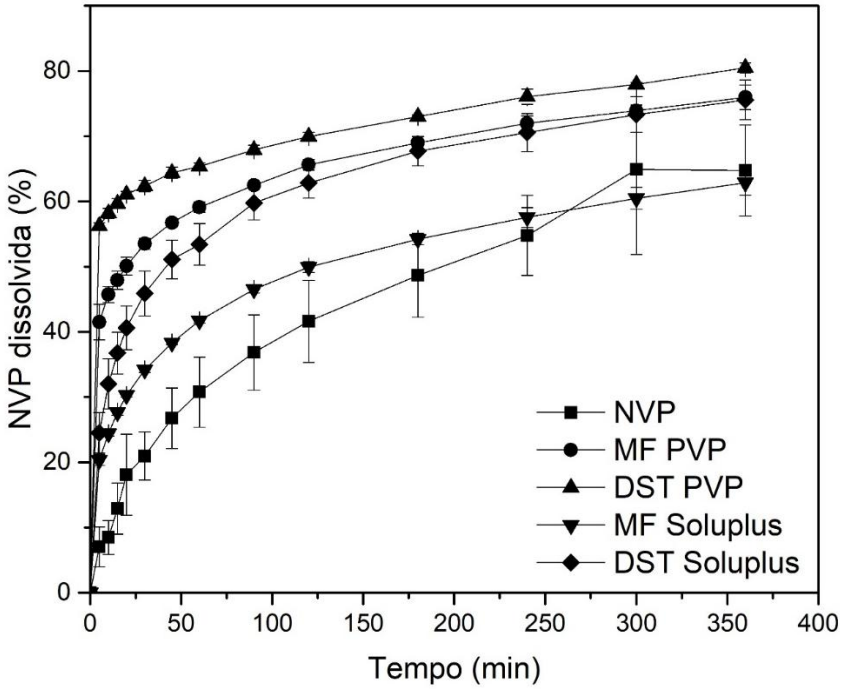

As dispersões sólidas de PVP VA-64 chegaram a 80% de liberação de NVP, gerando ED% de 62,4% e 71,2% para 120 e 360 minutos respectivamente, com resultados mais promissores em relação à dispersão contendo Soluplus, que alcançou 76% de NVP dissolvida, com ED% de 50,0% e 63,4% para os mesmos tempos. Apesar dessa diferença, ambos entregaram taxas maiores de dissolução em relação à NVP pura, atingindo concentrações maiores que 75% de NVP no meio.

Tabela 1 - Eficiência de dissolução calculado dos perfis de dissolução gerados pela nevirapina e de suas MFs e DSAs com os polímeros PVP VA-64 e Soluplus em 120 e 360 minutos.

Amostras		**Eficiência de Dissolução (%)**	
		120 MIN	*360 MIN*
NVP		28,2 ± 4,7	46,3 ± 6,6
PVP VA-64	*MF*	55,7^{*a} ± 0,5	66,5^{*a} ± 0,5
	DSA	62,4^{*a,b} ± 0,6	71,2^{*a} ± 0,3
Soluplus	*MF*	38,5^{*a} ± 0,3	40,7 ± 2,4
	DSA	50,0^{*a,c} ± 1,0	63,4^{*a,c} ± 2,4

Média ± DP, n = 3;
*Estatisticamente diferente p<0.05 vs. ^{a}NVP, ^{b}MF PVP VA-64 e ^{c}MF Soluplus

Fonte: O autor (2024)

O copolímero de PVP VA é amplamente utilizado na tecnologia farmacêutica e pode atuar como aglutinante seco em compressão direta, como agente formador de filme ou como agente solubilizante. Porém, no ASD, é utilizado como estabilizador de forma amorfa, potencializando a liberação do fármaco, além aumentar a solubilidade e biodisponibilidade (JADHAV et al., 2020). O incremento de solubilidade promovido pelo PVP VA-64 foi descrito também em outros trabalhos, como o Szafraniec-Szczęsny et al. (2021), no qual desenvolveram dispersões sólidas de Ezetimiba, um fármaco classe II no BCS. Eles perceberam que a partir de 66% do polímero na formulação, o sistema se torna independente do teor de PVP VA-64, alcançando liberações por volta de 80%, assim como as DSAs deste trabalho, devido à determinação de molhabilidade do sistema trabalhado, onde ocorre uma reorganização molecular do fármaco, influenciando as interações dos componentes ente si e com a água, permitindo sua entrada no material, a "molhando" mais fácil e dissolvendo melhor, permitindo alcançar altas taxas de dissolução (SZAFRANIEC-SZCZĘSNY et al., 2021).

Soluplus é um copolímero de enxerto anfifílico, sendo capaz de aumentar muito a molhabilidade do fármaco disperso em DSA e inibir a precipitação ou cristalização durante a dissolução, formando ligações de hidrogênio com o fármaco (LIU et al., 2020a). Essas ligações são formadas por diferentes regiões do Soluplus que interagem com moléculas do fármaco, resultando em micelas, com um aumento linear na solubilidade do fármaco à medida que se eleva a concentração do Soluplus (DARWICH et al., 2023). Dessa forma, o incremento de solubilidade promovido pelo Soluplus pode ser percebido inclusive na MF, uma vez que a trituração responsável pelo preparo pode ter causado um contato entre os fármacos e polímero o suficiente para provocar esse efeito, uma vez que resultados prévios indicaram uma miscibilidade entre NVP com 3TC e Soluplus, além de interações intermoleculares ocorrendo na MF. Porém, o incremento de solubilidade promovido pela DSA contendo Soluplus foi maior que sua MF, com diferença estatística entre elas, devido ao estado amorfo causado pelo preparo da dispersão, garantindo uma boa performance de dissolução para NVP.

CONCLUSÃO

Este estudo oferece perspectivas valiosas sobre a aplicação de polímeros como Soluplus e PVP VA-64 na formulação de DSAs e MFs ternárias contendo NVP e 3TC. Através de análises de FTIR, DSC, DRX, e ensaios de dissolução, foi possível observar o papel crucial das interações

intermoleculares, especialmente a formação de ligações de hidrogênio, na estabilização da forma amorfa dos fármacos e na melhoria da solubilidade e dissolução de NVP.

As análises de FTIR evidenciaram mudanças significativas nos espectros vibracionais devido às interações fármaco-fármaco-polímero, apontando para a formação de estruturas amorfos estáveis. Isso foi corroborado pelos dados de DSC e DRX, que indicaram a ausência de estruturas cristalinas nas DSAs, diferentemente das MFs, e confirmaram a formação de sistemas homogêneos amorfos. Esses resultados sugerem uma eficaz miscibilidade entre os polímeros e os fármacos, atribuível às interações intermoleculares que limitam a recristalização dos fármacos.

Os ensaios de dissolução revelaram uma melhoria significativa na liberação de NVP a partir das DSAs, quando comparadas às suas formas cristalinas e às MFs. Isso indica que a amorficidade induzida pelos polímeros, juntamente com a melhoria da molhabilidade e a prevenção da recristalização durante a dissolução, contribuiu para a eficiência de dissolução aumentada. O papel do PVP VA-64 como estabilizador da forma amorfa e seu impacto na solubilidade e biodisponibilidade foram claramente demonstrados, alinhando-se com a literatura existente. Da mesma forma, o Soluplus provou ser eficaz na melhoria da molhabilidade e na inibição da cristalização do fármaco.

Portanto, este trabalho destaca a utilização de tecnologias que permitam a melhoria da solubilidade dos fármacos pode desempenhar um papel importante na HAART. A escolha de Soluplus e PVP VA-64 como auxiliares na formação de sistemas amorfos se mostrou uma estratégia promissora para superar desafios de solubilidade e melhorar a biodisponibilidade de fármacos, abrindo caminho para futuras investigações e aplicações no campo farmacêutico.

REFERÊNCIAS

1. Kakad SP, Kshirsagar SJ. Neuro-AIDS: Current Status and Challenges to Antiretroviral Drug Therapy (ART) for Its Treatment. Curr Drug ther. 2020;15:469–81.

2. Berg A. Insights of Antiretrovirals: A New Drug Delivery Systems. J Antivir Antiretrovir [Internet]. 2020 [cited 2023 May 15];0:1–1. Available from: https://www.longdom.org/open-access/insights-of-antiretrovirals-a-new-drug-delivery-systems-60809.html

3. Kirtane AR, Langer R, Traverso G. Progress in Formulation-Based Approaches for Antiretrovirals. J Pharm Sci [Internet]. 2016;105:3471–82. Available from: http://dx.doi.org/10.1016/j.xphs.2016.09.015

4. Amidon GL;, Lennernäs H, Shah VP;, R. CJ. A Theoretical Basis for a Biopharmaceutic Drug Classification: The Correlation of in Vitro Drug Product Dissolution and in Vivo Bioavailability. Pharm Res. 1995;12:413–20.

5. Sosnik A, Augustine R. Challenges in oral drug delivery of antiretrovirals and the innovative strategies to overcome them. Adv Drug Deliv Rev. 2015;103:105–20.

6. Savjani KT, Gajjar AK, Savjani JK. Drug Solubility: Importance and Enhancement Techniques. ISRN Pharm [Internet]. 2012;2012:1–10. Available from: https://www.hindawi.com/archive/2012/195727/

7. Acharya PC, Fernandes C, Suares D, Shetty S, Tekade RK. Solubility and Solubilization Approaches in Pharmaceutical Product Development. Dosage Form Design Considerations: Volume I. Elsevier; 2018. p. 513–47.

8. Shah N, Iver R, Mail H, Choi D, Tian H, Diodane R. Improved Human Bioavailabilty of Vemurafenib, a practically Insoluble Drug, using an amorphous polymer-stabilised solid dispersion prepared by a solvent-controlled coprecipitation process. J Pharm Sci. 2013;102:967–81.

9. Jensen KT, Larsen FH, Löbmann K, Rades T, Grohganz H. Influence of variation in molar ratio on co-amorphous drug-amino acid systems. Eur J Pharm Biopharm. 2016;107:32–9.

10. Adeoye O, Conceição J, Serra PA, Bento da Silva A, Duarte N, Guedes RC, et al. Cyclodextrin solubilization and complexation of antiretroviral drug lopinavir: In silico prediction; Effects of derivatization, molar ratio and preparation method. Carbohydr Polym. 2020;227:115287.

11. Wu W, Ueda H, Löbmann K, Rades T, Grohganz H. Organic acids as co-formers for co-amorphous systems – Influence of variation in molar ratio on the physicochemical properties of the co-amorphous systems. European Journal of Pharmaceutics and Biopharmaceutics. 2018;131:25–32.

12. Baghel S, Cathcart H, O'Reilly NJ. Polymeric Amorphous Solid Dispersions: A Review of Amorphization, Crystallization, Stabilization, Solid-State Characterization, and Aqueous Solubilization of Biopharmaceutical Classification System Class II Drugs. J Pharm Sci. 2016;105:2527–44.

13. Bhujbal S V., Mitra B, Jain U, Gong Y, Agrawal A, Karki S, et al. Pharmaceutical amorphous solid dispersion: A review of manufacturing strategies. Acta Pharm Sin B. 2021;11:2505–36.

14. Szafraniec-Szczęsny J, Antosik-Rogóż A, Kurek M, Gawlak K, Górska A, Peralta S, et al. How Does the Addition of Kollidon®VA64 Inhibit the Recrystallization and Improve Ezetimibe Dissolution from Amorphous Solid Dispersions? Pharmaceutics. 2021;13:147.

15. Arunachalam A, Ashutoshkumar S, Karthikeyan M, Konam K, Prasad PH, Sethuraman S. Solid Dispersions: A Review. Current Pharmaceutic Research. 2010;1:82–90.

16. Bindhani S, Mohapatra S. RECENT APPROACHES OF SOLID DISPERSION: A NEW CONCEPT TOWARD ORAL BIOAVAILABILITY . Asian Journal of Pharmaceutical and Clinical

Research [Internet]. 2018 [cited 2023 Feb 2];11:72–8. Available from: https://innovareacademics.in/journals/index.php/ajpcr/article/view/23161

17. Schittny A, Huwyler J, Puchkov M. Mechanisms of increased bioavailability through amorphous solid dispersions: a review. Drug Deliv [Internet]. 2020 [cited 2022 Jun 13];27:110–27. Available from: https://doi.org/10.1080/10717544.2019.1704940

18. Brasil. Ministério da Saúde. Secretaria de Vigilância em Saúde. Departamento de Vigilância P e C das IST do H e das HVirais. Protocolo Clínico e Diretrizes Terapêuticas para Manejo da Infecção pelo HIV em Crianças e Adolescentes. Brasília: Secretaria de Vigilância em Saúde, Programa Nacional de DST e AIDS, Brasília; 2018. p. 218.

19. Pacult J, Rams-Baron M, Chmiel K, Jurkiewicz K, Antosik A, Szafraniec J, et al. How can we improve the physical stability of co-amorphous system containing flutamide and bicalutamide? The case of ternary amorphous solid dispersions. European Journal of Pharmaceutical Sciences. 2019;136.

20. Li J, Duggirala NK, Kumar NSK, Su Y, Suryanarayanan R. Design of Ternary Amorphous Solid Dispersions for Enhanced Dissolution of Drug Combinations. Mol Pharm. 2022;19:2950–61.

21. Sun Y, Zhu L, Wu T, Cai T, Gunn EM, Yu L. Stability of Amorphous Pharmaceutical Solids: Crystal Growth Mechanisms and Effect of Polymer Additives. AAPS J. 2012;14:380–8.

22. D'Angelo A, Edgar B, Hurt AP, Antonijević MD. Physico-chemical characterisation of three-component co-amorphous systems generated by a melt-quench method. J Therm Anal Calorim. 2018;134:381–90.

23. Chan S-Y, Chung Y-Y, Cheah X-Z, Tan EY-L, Quah J. The characterization and dissolution performances of spray dried solid dispersion of ketoprofen in hydrophilic carriers. Asian J Pharm Sci. 2015;10:372–85.

24. Liu J, Cao F, Zhang C, Ping Q. Use of polymer combinations in the preparation of solid dispersions of a thermally unstable drug by hot-melt extrusion. Acta Pharm Sin B [Internet]. 2013;3:263–72. Available from: http://linkinghub.elsevier.com/retrieve/pii/S2211383513000646

25. Jadhav P, Gokarna V, Deshpande V, Vavia P. Bioavailability Enhancement of Olmesartan Medoxomil Using Hot-Melt Extrusion: In-Silico, In-Vitro, and In-Vivo Evaluation. AAPS PharmSciTech. 2020;21:254.

26. Liu P, Zhou J, Chang J, Liu X, Xue H, Wang R, et al. Soluplus-Mediated Diosgenin Amorphous Solid Dispersion with High Solubility and High Stability: Development, Characterization and Oral Bioavailability. Drug Des Devel Ther. 2020;Volume 14:2959–75.

27. Darwich M, Mohylyuk V, Kolter K, Bodmeier R, Dashevskiy A. Enhancement of itraconazole solubility and release by hot-melt extrusion with Soluplus®. J Drug Deliv Sci Technol. 2023;81:104280.

5 CONSIDERAÇÕES FINAIS

A combinação de métodos de triagem, estudos computacionais, térmicos e de solubilidade desempenhou um papel fundamental no desenvolvimento de sistemas co-amorfos envolvendo NVP, mostrando-se uma estratégia eficaz para prever e estabilizar a formação de interações intermoleculares favoráveis e miscibilidade entre componentes. A aplicação de metodologias computacionais, em particular, permitiu a previsão da formação de complexos de hidrogênio entre NVP, 3TC e CAc, indicando geração de ligações de hidrogênio entre os componentes. A obtenção de co-amorfos de NVP com 3TC e CAc, seguindo as previsões das interações de hidrogênio, corroborou a utilidade dessas técnicas computacionais e experimentais na fabricação de sistemas amorfos com melhor solubilidade e dissolução. Além disso, a formação destes sistemas amorfos foi comprovada por microscopia e análise por DRX, mostrando a miscibilidade entre os componentes e sugerindo a formação de interações de hidrogênio que estabilizam a forma amorfa do NVP, levando a uma taxa de dissolução superior à da droga isolada. Esta melhoria na dissolução é de significativa importância para a terapia antirretroviral combinada, visando combater o HIV de maneira mais eficaz.

Este estudo também destacou a importância dos polímeros, como Soluplus e PVP VA-64, na formação de sistemas de dispersão sólida amorfos (DSA) e misturas físicas ternárias (MFs) contendo NVP e 3TC. As análises de FTIR, DSC, DRX e ensaios de dissolução enfatizaram o papel crucial das interações intermoleculares, particularmente a formação de ligações de hidrogênio, na estabilização das formas amorfas dos fármacos e na consequente melhoria da solubilidade e da taxa de dissolução do NVP. Os polímeros demonstraram eficácia na indução e estabilização da amorficidade dos fármacos, resultando em uma significativa melhoria na dissolução do NVP em comparação com suas formas cristalinas e as MFs. A eficácia do PVP VA-64 como estabilizador da forma amorfa e seu impacto positivo na solubilidade e biodisponibilidade dos fármacos foram claramente evidenciados, assim como a capacidade do Soluplus em melhorar a molhabilidade e inibir a cristalização do fármaco.

Adicionalmente, a abordagem multidisciplinar empregada neste estudo, combinando ciência computacional com técnicas farmacêuticas avançadas, serve como um modelo para futuras pesquisas na área de desenvolvimento de fármacos. Isso não apenas estabelece um precedente para a inovação técnica, mas também sublinha a importância da colaboração interdisciplinar na resolução de desafios complexos de saúde pública. Por isso, este trabalho

apresenta inovações na terapia antirretroviral combinada, abordando duas das principais barreiras enfrentadas no tratamento do HIV: a solubilidade e a biodisponibilidade dos fármacos antirretrovirais. Os resultados deste trabalho sublinham a sinergia entre estudos computacionais e experimentais no desenvolvimento de sistemas co-amorfos e destacam o papel vital dos polímeros na estabilização de formas amorfas, na melhoria da solubilidade e na biodisponibilidade de fármacos antirretrovirais.

Essas descobertas abrem novos caminhos para a otimização da terapia antirretroviral, mediante a superação de desafios relacionados à solubilidade dos fármacos, pavimentando o caminho para futuras investigações e aplicações de sistemas amorfos supersaturados no campo farmacêutico. Isso fornece uma base sólida para o desenvolvimento de novas formulações que podem transformar o panorama do tratamento do HIV, contribuindo para uma melhor gestão da resistência ao HIV e melhorando a qualidade de vida dos pacientes, com o desenvolvimento de formulações mais eficazes e menos tóxicas, o que pode resultar em regimes terapêuticos mais toleráveis e aderentes para os pacientes. Isso é particularmente crucial no contexto do HIV, onde a resistência aos medicamentos e os efeitos colaterais podem comprometer seriamente a eficácia do tratamento.

Em resumo, este trabalho não apenas avança no conhecimento científico sobre a formação de sistemas amorfos e sua estabilização por meio de polímeros, mas também apresenta implicações práticas significativas para a melhoria da terapia antirretroviral. Ao focar em superar os desafios de solubilidade e biodisponibilidade, este estudo fornece uma base sólida para o desenvolvimento de novas formulações que podem transformar o panorama do tratamento do HIV, tornando-o mais eficaz, acessível e amigável ao paciente. A natureza e a importância prática deste trabalho destacam seu potencial para contribuir significativamente para o combate ao HIV/AIDS, reafirmando o papel crucial da inovação farmacêutica na melhoria dos resultados de saúde para populações em todo o mundo.

REFERÊNCIAS

AGRAWAL, A. M.; DUDHEDIA, M. S.; ZIMNY, E. Hot Melt Extrusion: Development of an Amorphous Solid Dispersion for an Insoluble Drug from Mini-scale to Clinical Scale. **AAPS PharmSciTech**, 1 fev. 2016. v. 17, n. 1, p. 133–147. Disponível em: <https://pubmed.ncbi.nlm.nih.gov/26729533/>. Acesso em: 2 fev. 2023.

AHIRE, B. R. *et al.* Solubility Enhancement of Poorly Water Soluble Drug by Solid Dispersion Techniques. **International Journal of PharmTech Research**, 2010. v. 2, n. 3, p. 2007–2015.

ALHALAWEH, A.; ALZGHOUL, A.; KAIALY, W. Data mining of solubility parameters for computational prediction of drug–excipient miscibility. **Drug Development and Industrial Pharmacy**, 2014. v. 40, n. 7, p. 904–909. Disponível em: <https://www.tandfonline.com/doi/abs/10.3109/03639045.2013.789906>. Acesso em: 12 abr. 2023.

ALLESØ, M. *et al.* Enhanced dissolution rate and synchronized release of drugs in binary systems through formulation: Amorphous naproxen–cimetidine mixtures prepared by mechanical activation. **Journal of Controlled Release**, 21 maio. 2009. v. 136, n. 1, p. 45–53. . Acesso em: 12 abr. 2023.

ALMEIDA E SOUSA, L. *et al.* Supersaturation Potential of Salt, Co-Crystal, and Amorphous Forms of a Model Weak Base. **Crystal Growth and Design**, 3 fev. 2016. v. 16, n. 2, p. 737–748. . Acesso em: 18 ago. 2019.

AMIDON, G. L. ; *et al.* A Theoretical Basis for a Biopharmaceutic Drug Classification: The Correlation of in Vitro Drug Product Dissolution and in Vivo Bioavailability. **Pharmaceutical Research**, 1995. v. 12, n. 3, p. 413–420.

ASO, Y.; YOSHIOKA, S. Molecular mobility of nifedipine-PVP and phenobarbital-PVP solid dispersions as measured by 13C-NMR spin-lattice relaxation time. **Journal of pharmaceutical sciences**, 2006. v. 95, n. 2, p. 318–325. Disponível em: <https://pubmed.ncbi.nlm.nih.gov/16372315/>. Acesso em: 5 abr. 2023.

AUCH, C. *et al.* Impact of amorphization and GI physiology on supersaturation and precipitation of poorly soluble weakly basic drugs using a small-scale in vitro transfer model. **International Journal of Pharmaceutics**, 25 jan. 2020. v. 574, p. 118917. . Acesso em: 29 set. 2020.

BAGHEL, S.; CATHCART, H.; O'REILLY, N. J. Polymeric Amorphous Solid Dispersions: A Review of Amorphization, Crystallization, Stabilization, Solid-State Characterization, and Aqueous Solubilization of Biopharmaceutical Classification System Class II Drugs. **Journal of Pharmaceutical Sciences**, 2016. v. 105, n. 9, p. 2527–2544.

BARDSLEY-ELLIOT, A.; PERRY, C. M. Nevirapine: A review of its use in the prevention and treatment of Paediatric HIV infection. **Pediatric Drugs**, 2000. v. 2, p. 373–407.

BEYER, A. *et al.* Influence of the cooling rate and the blend ratio on the physical stability of co-amorphous naproxen/indomethacin. **European journal of pharmaceutics and biopharmaceutics : official journal of Arbeitsgemeinschaft fur Pharmazeutische Verfahrenstechnik e.V**, 1 dez. 2016. v. 109, p. 140–148. Disponível em: <https://pubmed.ncbi.nlm.nih.gov/27746228/>. Acesso em: 12 abr. 2023.

BHUGRA, C.; PIKAL, M. J. Role of thermodynamic, molecular, and kinetic factors in crystallization from the amorphous state. **Journal of Pharmaceutical Sciences2**, 2008. v. 97, p. 1329–1349.

BHUJBAL, S. V. *et al.* Pharmaceutical amorphous solid dispersion: A review of manufacturing strategies. **Acta Pharmaceutica Sinica B**, 1 ago. 2021. v. 11, n. 8, p. 2505–2536. . Acesso em: 12 out. 2022.

BINDHANI, S.; MOHAPATRA, S. RECENT APPROACHES OF SOLID DISPERSION: A NEW CONCEPT TOWARD ORAL BIOAVAILABILITY . **Asian Journal of Pharmaceutical and Clinical Research**, 1 fev. 2018. v. 11, n. 2, p. 72–78. Disponível em: <https://innovareacademics.in/journals/index.php/ajpcr/article/view/23161>. Acesso em: 2 fev. 2023.

BRASIL. MINISTÉRIO DA SAÚDE. SECRETARIA DE VIGILÂNCIA EM SAÚDE. DEPARTAMENTO DE VIGILÂNCIA, P. E C. Das I. S. T. Do H. E Das H. Virais. **Protocolo clínico e diretrizes terapêuticas para manejo da infecção pelo HIV em adultos.** (Ministério da Saúde, Org.). **Protocolo Clínico e Diretrizes Terapêuticas para o Manejo da Infecção pelo HIV em adultos**. Secretaria de Vigilância em Saúde, Programa Nacional de DST e AIDS, Brasília.

_____. **Protocolo Clínico e Diretrizes Terapêuticas para Manejo da Infecção pelo HIV em Crianças e Adolescentes**. Secretaria de Vigilância em Saúde, Programa Nacional de DST e AIDS, Brasília.

CHEMICAL, C. **Product Information - Nevirapine**.

CHIENG, N. *et al.* Physical characterization and stability of amorphous indomethacin and ranitidine hydrochloride binary systems prepared by mechanical activation. **European journal of pharmaceutics and biopharmaceutics : official journal of Arbeitsgemeinschaft fur Pharmazeutische Verfahrenstechnik e.V**, jan. 2009. v. 71, n. 1, p. 47–54. Disponível em: <https://pubmed.ncbi.nlm.nih.gov/18644443/>. Acesso em: 10 abr. 2023.

CLERCQ, E. DE. Anti-HIV drugs: 25 compounds approved within 25 years after the discovery of HIV. **International Journal of Antimicrobial Agents**, 2009. v. 33, n. 4, p. 307–320.

CUI, Y. A material science perspective of pharmaceutical solids. **International journal of pharmaceutics**, 18 jul. 2007. v. 339, n. 1–2, p. 3–18. Disponível em: <https://pubmed.ncbi.nlm.nih.gov/17537600/>. Acesso em: 9 abr. 2023.

DENGALE, Swapnil J. *et al.* Preparation and characterization of co-amorphous Ritonavir-Indomethacin systems by solvent evaporation technique: Improved dissolution behavior and

physical stability without evidence of intermolecular interactions. **European Journal of Pharmaceutical Sciences**, 1 out. 2014. v. 62, p. 57–64. . Acesso em: 9 mar. 2021.

_____ *et al.* Fabrication, solid state characterization and bioavailability assessment of stable binary amorphous phases of Ritonavir with Quercetin. **European journal of pharmaceutics and biopharmaceutics : official journal of Arbeitsgemeinschaft fur Pharmazeutische Verfahrenstechnik e.V**, 2015. v. 89, p. 329–338. Disponível em: <https://pubmed.ncbi.nlm.nih.gov/25542681/>. Acesso em: 10 abr. 2023.

DENGALE, Swapnil Jayant *et al.* Recent advances in co-amorphous drug formulations. **Advanced Drug Delivery Reviews**, 1 maio. 2016. v. 100, p. 116–125. Disponível em: <https://www.sciencedirect.com/science/article/pii/S0169409X1530003X?via%3Dihub>. Acesso em: 4 jul. 2019.

DONNELLY, C. *et al.* Probing the Effects of Experimental Conditions on the Character of Drug-Polymer Phase Diagrams Constructed Using Flory-Huggins Theory. **Pharmaceutical Research**, 30 jan. 2015. v. 32, n. 1, p. 167–179. Disponível em: <http://link.springer.com/10.1007/s11095-014-1453-9>. Acesso em: 4 jul. 2019.

DROOGE, D. J. VAN *et al.* Characterization of the molecular distribution of drugs in glassy solid dispersions at the nano-meter scale, using differential scanning calorimetry and gravimetric water vapour sorption techniques. **International journal of pharmaceutics**, 9 mar. 2006. v. 310, n. 1–2, p. 220–229. Disponível em: <https://pubmed.ncbi.nlm.nih.gov/16427226/>. Acesso em: 10 abr. 2023.

FIGUEIRÊDO, C. B. M. *et al.* Enhancement of dissolution rate through eutectic mixture and solid solution of posaconazole and benznidazole. **International Journal of Pharmaceutics**, 15 jun. 2017. v. 525, n. 1, p. 32–42. . Acesso em: 19 out. 2020.

FINDLAY, V. J. Nevirapine. **xPharm: The Comprehensive Pharmacology Reference**. [S.l.]: Elsevier, 2007, p. 1–4.

FULE, R. *et al.* Development of hot melt co-formulated antimalarial solid dispersion system in fixed dose form (ARLUMELT): Evaluating amorphous state and in vivo performance. **International Journal of Pharmaceutics**, 30 dez. 2015. v. 496, n. 1, p. 137–156. . Acesso em: 2 fev. 2023.

_____; PAITHANKAR, V.; AMIN, P. Hot melt extrusion based solid solution approach: Exploring polymer comparison, physicochemical characterization and in-vivo evaluation. **International journal of pharmaceutics**, 29 fev. 2016. v. 499, n. 1–2, p. 280–294. Disponível em: <https://pubmed.ncbi.nlm.nih.gov/26746801/>. Acesso em: 2 fev. 2023.

FUNG, M.; BĒRZIŅŠ, K.; SURYANARAYANAN, R. Physical Stability and Dissolution Behavior of Ketoconazole-Organic Acid Coamorphous Systems. **Molecular Pharmaceutics**, 7 maio. 2018. v. 15, n. 5, p. 1862–1869. Disponível em: <https://pubs.acs.org/doi/abs/10.1021/acs.molpharmaceut.8b00035>. Acesso em: 16 abr. 2023.

GONZALEZ DE REQUENA, D. *et al.* Liver toxicity caused by nevirapine. **AIDS**, 2002. v. 16, n. 2, p. 290–291.

GUO, Y.; SHALAEV, E.; SMITH, S. Physical stability of pharmaceutical formulations: Solid-state characterization of amorphous dispersions. **Trends in Analytical Chemistry**, 2013. v. 49, p. 137–144. Disponível em: <http://dx.doi.org/10.1016/j.trac.2013.06.002>.

GUTZOW, I. S.; SCHMELZER, J. W. P. States of Aggregation, Thermodynamic Phases, Phase Transformations, and the Vitreous State. **The Vitreous State**. [S.l.]: Springer Berlin Heidelberg, 2013, p. 7–67.

HANCOCK, B. C.; PARKS, M. What is the true solubility advantage for amorphous pharmaceuticals? **Pharmaceutical research**, 2000. v. 17, n. 4, p. 397–404. Disponível em: <https://pubmed.ncbi.nlm.nih.gov/10870982/>. Acesso em: 23 mar. 2023.

_____; ZOGRAFI, G. The relationship between the glass transition temperature and the water content of amorphous pharmaceutical solids. **Pharmaceutical research**, 1994. v. 11, n. 4, p. 471–477. Disponível em: <https://pubmed.ncbi.nlm.nih.gov/8058600/>. Acesso em: 5 abr. 2023.

HANNONGBUA, S.; PRASITHICHOKEKUL, S.; PUNGPO, P. Conformational analysis of nevirapina, a non-nucleoside HIV-1 reverse transcriptase inhibitor, based on quantum mechanical calculations. **Journal of Computer-Aided Molecular Design**, 2001. v. 15, n. 11, p. 997–1004.

HUANG, Y.; DAI, W.-G. Fundamental aspects of solid dispersion technology for poorly soluble drugs. **Acta Pharmaceutica Sinica B**, 2014. v. 4, n. 1, p. 18–25.

IKRAM, K. K. Solid Dispersion: Solubility Enhancement Technique of Poorly Water Soluble Drug. **Journal of Drug Delivery and Therapeutics**, 14 mar. 2020. v. 10, n. 1, p. 173–177. . Acesso em: 13 fev. 2023.

JANSSENS, S.; MOOTER, Guy VAN DEN. Review: physical chemistry of solid dispersions. **Journal of Pharmacy and Pharmacology**, 1 dez. 2009. v. 61, n. 12, p. 1571–1586. Disponível em: <http://doi.wiley.com/10.1211/jpp/61.12.0001>. Acesso em: 22 jun. 2019.

JENSEN, K. T. *et al.* Preparation and characterization of spray-dried co-amorphous drug-amino acid salts. **Journal of Pharmacy and Pharmacology**, 1 maio. 2016. v. 68, n. 5, p. 615–624. . Acesso em: 18 ago. 2019.

KANG, B. K. *et al.* Development of self-microemulsifying drug delivery systems (SMEDDS) for oral bioavailability enhancement of simvastatin in beagle dogs. **International Journal of Pharmaceutics**, 15 abr. 2004. v. 274, n. 1–2, p. 65–73. . Acesso em: 13 fev. 2023.

KAPOURANI, A. *et al.* Crystallization tendency of APIs possessing different thermal and glass related properties in amorphous solid dispersions. **International Journal of Pharmaceutics**, 15 abr. 2020. v. 579, p. 119149. . Acesso em: 6 abr. 2023.

KARAGIANNI, A.; KACHRIMANIS, K.; NIKOLAKAKIS, I. Co-Amorphous Solid Dispersions for Solubility and Absorption Improvement of Drugs: Composition, Preparation, Characterization and Formulations for Oral Delivery. **Pharmaceutics**, 2018. v. 10, n. 98, p. 1–26.

KARAVAS, E. *et al.* Effect of hydrogen bonding interactions on the release mechanism of felodipine from nanodispersions with polyvinylpyrrolidone. **European Journal of Pharmaceutics and Biopharmaceutics**, 1 jun. 2006. v. 63, n. 2, p. 103–114. . Acesso em: 13 fev. 2023.

KATE, L. *et al.* Bioavailability enhancement of atovaquone using hot melt extrusion technology. **European Journal of Pharmaceutical Sciences**, 30 abr. 2016. v. 86, p. 103–114. . Acesso em: 2 fev. 2023.

KIM, K. T. *et al.* Solid Dispersions as a Drug Delivery System. **Journal of Pharmaceutical Investigation**, 2011. v. 41, n. 3, p. 125. . Acesso em: 2 fev. 2023.

KITAK, T. *et al.* Determination of Solubility Parameters of Ibuprofen and Ibuprofen Lysinate. **Molecules (Basel, Switzerland)**, 3 dez. 2015. v. 20, n. 12, p. 21549–21568. Disponível em: <https://pubmed.ncbi.nlm.nih.gov/26633347/>. Acesso em: 12 abr. 2023.

KNOPP, M. M. *et al.* Effect of amorphous phase separation and crystallization on the in vitro and in vivo performance of an amorphous solid dispersion. **European Journal of Pharmaceutics and Biopharmaceutics**, 1 set. 2018. v. 130, p. 290–295. Disponível em: <https://www.sciencedirect.com/science/article/pii/S0939641118306945?via%3Dihub>. Acesso em: 4 jul. 2019.

KORHONEN, O.; PAJULA, K.; LAITINEN, R. Rational excipient selection for co-amorphous formulations. **Expert Opinion on Drug Delivery**, 2016. v. 14, n. 4, p. 551–569.

LAITINEN, R. *et al.* Emerging trends in the stabilization of amorphous drugs. **International journal of pharmaceutics**, 2013. v. 453, n. 1, p. 65–79. Disponível em: <https://pubmed.ncbi.nlm.nih.gov/22569230/>. Acesso em: 9 abr. 2023.

LAPUK, S. E. *et al.* Kinetic stability of amorphous solid dispersions with high content of the drug: A fast scanning calorimetry investigation. **International Journal of Pharmaceutics**, 1 maio. 2019. v. 562, p. 113–123. . Acesso em: 6 abr. 2023.

_____ *et al.* Kinetic stability of amorphous dipyridamole: A fast scanning calorimetry investigation. **International Journal of Pharmaceutics**, 25 jan. 2020. v. 574, p. 118890. . Acesso em: 27 mar. 2023.

LENZ, E. *et al.* Solid-state properties and dissolution behaviour of tablets containing co-amorphous indomethacin-arginine. **European Journal of Pharmaceutics and Biopharmaceutics**, 25 jul. 2015. v. 96, p. 44–52. . Acesso em: 18 ago. 2019.

LEUNER, C.; DRESSMAN, J. Improving drug solubility for oral delivery using solid dispersions. **European Journal of Pharmaceutics and Biopharmaceutics**, 3 jul. 2000. v. 50, n. 1, p. 47–60.

Disponível em: <https://www.sciencedirect.com/science/article/abs/pii/S093964110000076X>. Acesso em: 15 jul. 2019.

LI, J. *et al.* Effect of Moisture Sorption on Free Volume and Relaxation of Spray Dried Dispersions: Relation to Drug Recrystallization. **Journal of Pharmaceutical Sciences**, 1 fev. 2020. v. 109, n. 2, p. 1050–1058. . Acesso em: 6 abr. 2023.

LINDENBERG, M.; KOPP, S.; DRESSMAN, J. B. Classification of orally administered drugs on the World Health Organization Model list of Essential Medicines according to the biopharmaceutics classification system. **European Journal of Pharmaceutics and Biopharmaceutics**, set. 2004. v. 58, n. 2, p. 265–278. . Acesso em: 4 ago. 2022.

LIU, J. *et al.* Co-amorphous drug formulations in numbers: Recent advances in co-amorphous drug formulations with focus on co-formability, molar ratio, preparation methods, physical stability, in vitro and in vivo performance, and new formulation strategies. **Pharmaceutics**, 2021. v. 13, n. 3.

LIU, S. *et al.* Investigation of Drug-Polymer Miscibility, Molecular Interaction, and Their Effects on the Physical Stabilities and Dissolution Behaviors of Norfloxacin Amorphous Solid Dispersions. **Crystal Growth and Design**, 6 maio. 2020. v. 20, n. 5, p. 2952–2964. Disponível em: <https://pubs.acs.org/doi/abs/10.1021/acs.cgd.9b01571>. Acesso em: 6 abr. 2023.

LÖBMANN, K. *et al.* Coamorphous drug systems: Enhanced physical stability and dissolution rate of indomethacin and naproxen. **Molecular Pharmaceutics**, 3 out. 2011a. v. 8, n. 5, p. 1919–1928. . Acesso em: 18 ago. 2019.

_____ *et al.* Coamorphous drug systems: enhanced physical stability and dissolution rate of indomethacin and naproxen. **Molecular pharmaceutics**, 3 out. 2011b. v. 8, n. 5, p. 1919–1928. . Acesso em: 10 abr. 2023.

_____ *et al.* Co-amorphous simvastatin and glipizide combinations show improved physical stability without evidence of intermolecular interactions. **European Journal of Pharmaceutics and Biopharmaceutics**, maio. 2012. v. 81, n. 1, p. 159–169. . Acesso em: 18 ago. 2019.

_____; LAITINEN, R.; STRACHAN, C.; *et al.* Amino acids as co-amorphous stabilizers for poorly water-soluble drugs - Part 2: Molecular interactions. **European Journal of Pharmaceutics and Biopharmaceutics**, 2013. v. 85, n. 3 PART B, p. 882–888. . Acesso em: 18 ago. 2019.

_____; _____; GROHGANZ, H.; *et al.* A theoretical and spectroscopic study of co-amorphous naproxen and indomethacin. **International journal of pharmaceutics**, 2013. v. 453, n. 1, p. 80–87. Disponível em: <https://pubmed.ncbi.nlm.nih.gov/22613066/>. Acesso em: 12 abr. 2023.

_____; GROHGANZ, H.; *et al.* Amino acids as co-amorphous stabilizers for poorly water soluble drugs - Part 1: Preparation, stability and dissolution enhancement. **European Journal of Pharmaceutics and Biopharmaceutics**, 2013. v. 85, n. 3 PART B, p. 873–881. . Acesso em: 18 ago. 2019.

_____ *et al.* Stabilized Amorphous Solid Dispersions with Small Molecule Excipients. 2014. p. 613–636. Disponível em: <https://link.springer.com/chapter/10.1007/978-1-4939-1598-9_21>. Acesso em: 10 abr. 2023.

LOKAMATHA, K. M.; KUMAR, S. M. S.; RAO, N. R. Enhancement of solubility and dissolution rate of nevirapine by solid dispersion technique using dextran: preparation and in vitro evaluation. **International Journal of Pharmaceutical Research & Development**, 2011. v. 2, p. 1–8.

LU, Q.; ZOGRAFI, G. Phase behavior of binary and ternary amorphous mixtures containing indomethacin, citric acid, and PVP. **Pharmaceutical Research**, 1998. v. 15, n. 8, p. 1202–1206. Disponível em: <https://link.springer.com/article/10.1023/A:1011983606606>. Acesso em: 10 abr. 2023.

MA, X.; WILLIAMS, R. O. Characterization of amorphous solid dispersions: An update. **Journal of Drug Delivery Science and Technology**, 2019. v. 50, n. January, p. 113–124.

MACHA, S. *et al.* Assessment of Nevirapine Bioavailability from Targeted Sites in the Human Gastrointestinal Tract. **Journal of Clinical Pharmacology**, 2009. v. 49, n. 12, p. 1417–1425.

MADAN, J. *et al.* Improving the solubility of nevirapine using A hydrotropy and mixed hydrotropy based solid dispersion approach. **Polymers in medicine**, 1 dez. 2017. v. 47, n. 2, p. 83–90. Disponível em: <https://pubmed.ncbi.nlm.nih.gov/30009585/>. Acesso em: 21 abr. 2023.

MARSAC, P. J.; SHAMBLIN, S. L.; TAYLOR, L. S. Theoretical and practical approaches for prediction of drug-polymer miscibility and solubility. **Pharmaceutical research**, out. 2006. v. 23, n. 10, p. 2417–2426. Disponível em: <https://pubmed.ncbi.nlm.nih.gov/16933098/>. Acesso em: 5 abr. 2023.

MATSUMOTO, T.; ZOGRAFI, G. Physical properties of solid molecular dispersions of indomethacin with poly(vinylpyrrolidone) and poly(vinylpyrrolidone-co-vinyl-acetate) in relation to indomethacin crystallization. **Pharmaceutical Research**, 1999. v. 16, n. 11, p. 1722–1728. . Acesso em: 5 abr. 2023.

MITRA, A. *et al.* Impact of polymer type on bioperformance and physical stability of hot melt extruded formulations of a poorly water soluble drug. **International journal of pharmaceutics**, 30 maio. 2016. v. 505, n. 1–2, p. 107–114. Disponível em: <https://pubmed.ncbi.nlm.nih.gov/27012984/>. Acesso em: 2 fev. 2023.

MONSCHKE, M.; KAYSER, K.; WAGNER, K. G. Processing of Polyvinyl Acetate Phthalate in Hot-Melt Extrusion—Preparation of Amorphous Solid Dispersions. **Pharmaceutics 2020, Vol. 12, Page 337**, 9 abr. 2020. v. 12, n. 4, p. 337. Disponível em: <https://www.mdpi.com/1999-4923/12/4/337/htm>. Acesso em: 6 abr. 2023.

MOOTER, G. VAN DEN *et al.* Physical stabilisation of amorphous ketoconazole in solid dispersions with polyvinylpyrrolidone K25. **European journal of pharmaceutical sciences : official journal of the European Federation for Pharmaceutical Sciences**, 1 jan. 2001. v. 12,

n. 3, p. 261–269. Disponível em: <https://pubmed.ncbi.nlm.nih.gov/11113645/>. Acesso em: 5 abr. 2023.

MOSESON, D. E. *et al.* Amorphous solid dispersions containing residual crystallinity: Influence of seed properties and polymer adsorption on dissolution performance. **European Journal of Pharmaceutical Sciences**, 15 abr. 2020. v. 146, p. 105276. . Acesso em: 18 jan. 2021.

OHTAKE, S.; SHALAEV, E. Effect of Water on the Chemical Stability of Amorphous Pharmaceuticals: I. Small Molecules. **Journal of Pharmaceutical Sciences**, 1 abr. 2013. v. 102, n. 4, p. 1139–1154. . Acesso em: 4 abr. 2023.

PANDI, P. *et al.* **Amorphous solid dispersions: An update for preparation, characterization, mechanism on bioavailability, stability, regulatory considerations and marketed products**. **International Journal of Pharmaceutics**. Elsevier B.V. . Acesso em: 29 set. 2020.

PARKS, G. S.; SNYDER, L. J.; CATTOIR, F. R. Studies on Glass. XI. Some Thermodynamic Relations of Glassy and Alpha-Crystalline Glucose. **The Journal of Chemical Physics**, 3 nov. 2004. v. 2, n. 9, p. 595. Disponível em: <https://aip.scitation.org/doi/abs/10.1063/1.1749540>. Acesso em: 23 mar. 2023.

PAUDEL, A.; GEPPI, M.; MOOTER, Guy VAN DEN. Structural and Dynamic Properties of Amorphous Solid Dispersions: The Role of Solid-State Nuclear Magnetic Resonance Spectroscopy and Relaxometry. **Journal of Pharmaceutical Sciences**, 2014. v. 103, n. 9, p. 2635–2662. Disponível em: <http://dx.doi.org/10.1002/jps.23966>.

PENZEL, E.; RIEGER, J.; SCHNEIDER, H. The glass transition temperature of random copolymers: 1. Experimental data and the Gordon-Taylor equation. **Polymer**, 1997. v. 38, p. 325–327.

PEREIRA, B. G. *et al.* Pseudopolymorphs and intrinsic dissolution of nevirapine. **Crystal Growth and Design**, out. 2007. v. 7, n. 10, p. 2016–2023.

POUTON, C. W. Formulation of poorly water-soluble drugs for oral administration: Physicochemical and physiological issues and the lipid formulation classification system. **European Journal of Pharmaceutical Sciences**, 1 nov. 2006. v. 29, n. 3–4, p. 278–287. . Acesso em: 13 fev. 2023.

QIAN, S. *et al.* Coamorphous lurasidone hydrochloride-saccharin with charge-assisted hydrogen bonding interaction shows improved physical stability and enhanced dissolution with ph-independent solubility behavior. **Crystal Growth and Design**, 3 jun. 2015. v. 15, n. 6, p. 2920–2928. Disponível em: <https://pubs.acs.org/doi/abs/10.1021/acs.cgd.5b00349>. Acesso em: 12 abr. 2023.

RUMONDOR, A. C. F. *et al.* Phase Behavior of Poly(vinylpyrrolidone) Containing Amorphous Solid Dispersions in the Presence of Moisture. **Molecular Pharmaceutics**, 5 out. 2009. v. 6, n. 5, p. 1492–1505. Disponível em: <https://pubs.acs.org/doi/10.1021/mp900050c>. Acesso em: 2 dez. 2019.

RUMONDOR, A. C. F. *et al.* Understanding the Tendency of Amorphous Solid Dispersions to Undergo Amorphous–Amorphous Phase Separation in the Presence of Absorbed Moisture. **AAPS PharmSciTech**, dez. 2011. v. 12, n. 4, p. 1209. Disponível em: </pmc/articles/PMC3225547/>. Acesso em: 6 abr. 2023.

_____; JACKSON, M. J.; TAYLOR, L. S. Effects of moisture on the growth rate of felodipine crystals in the presence and absence of polymers. **Crystal Growth and Design**, 3 fev. 2010. v. 10, n. 2, p. 747–753. Disponível em: <https://pubs.acs.org/doi/abs/10.1021/cg901157w>. Acesso em: 23 mar. 2023.

SAFFOON, N. *et al.* Enhancement of Oral Bioavailability and Solid Dispersion: A Review. **Journal of Applied Pharmaceutical Science**, 2011. v. 1, n. 7, p. 13–20.

SAI KRISHNA ANAND, V. *et al.* The relevance of co-amorphous formulations to develop supersaturated dosage forms: In-vitro, and ex-vivo investigation of Ritonavir-Lopinavir co-amorphous materials. **European Journal of Pharmaceutical Sciences**, 2018. v. 123, p. 124–134.

SANDHU, H. *et al.* Overview of Amorphous Solid Dispersion Technologies. *Em*: SHAH, N; *et al.* (Org.). **Amorphous Solid Dispersions**. New York: Springer, 2014, p. 91–122.

SANGANWAR, G. P. *et al.* Simultaneous production and co-mixing of microparticles of nevirapine with excipients by supercritical antisolvent method for dissolution enhancement. **European Journal of Pharmaceutical Sciences**, 2010. v. 39, n. 1–3, p. 164–174.

SANTOS, K. A. Dos *et al.* The drug loading impact on dissolution and diffusion: a case-study with amorphous solid dispersions of nevirapine. **Research, Society and Development**, 23 out. 2022. v. 11, n. 14, p. e168111436117–e168111436117. . Acesso em: 28 out. 2022.

SAREEN, S.; JOSEPH, L.; MATHEW, G. Improvement in solubility of poor water-soluble drugs by solid dispersion. **International Journal of Pharmaceutical Investigation**, 2012. v. 2, n. 1, p. 12–17. Disponível em: <http://www.jpionline.org/text.asp?2012/2/1/12/96921>.

SCHITTNY, A.; HUWYLER, J.; PUCHKOV, M. Mechanisms of increased bioavailability through amorphous solid dispersions: a review. **Drug Delivery**, 1 jan. 2020. v. 27, n. 1, p. 110–127. Disponível em: <https://doi.org/10.1080/10717544.2019.1704940>. Acesso em: 13 jun. 2022.

SERAJUDDLN, A. T. M. Solid dispersion of poorly water-soluble drugs: early promises, subsequent problems, and recent breakthroughs. **Journal of pharmaceutical sciences**, 1999. v. 88, n. 10, p. 1058–1066. Disponível em: <https://pubmed.ncbi.nlm.nih.gov/10514356/>. Acesso em: 10 abr. 2023.

SHARMA, A.; JAIN, C. P. Solid dispersion: A promising technique to enhance solubility of poorly water soluble drug. **International Journal of Drug Delivery**, 10 maio. 2011. v. 3, n. 2, p. 149–170. Disponível em: <http://www.arjournals.org/index.php/ijdd/article/view/211>. Acesso em: 25 jun. 2019.

SHARMA, D. K.; JOSHI, S. B. SOLUBILITY ENHANCEMENT STRATEGIES FOR POORLY WATER-SOLUBLE DRUGS IN SOLID DISPERSIONS: A REVIEW. **Asian Journal of Pharmaceutics (AJP)**, 2007. v. 1, n. 1. Disponível em: <https://www.asiapharmaceutics.info/index.php/ajp/article/view/734>. Acesso em: 13 fev. 2023.

SHAYANFAR, A. *et al.* Coamorphous atorvastatin calcium to improve its physicochemical and pharmacokinetic properties. **Journal of pharmacy & pharmaceutical sciences : a publication of the Canadian Society for Pharmaceutical Sciences, Societe canadienne des sciences pharmaceutiques**, 2013. v. 16, n. 4, p. 577–587. Disponível em: <https://pubmed.ncbi.nlm.nih.gov/24210065/>. Acesso em: 10 abr. 2023.

SHEKUNOV, B. Kinetics of Crystallization and Glass Transition in Amorphous Materials. **Crystal Growth and Design**, 2 jan. 2020. v. 20, n. 1, p. 95–106. Disponível em: <https://pubs.acs.org/doi/abs/10.1021/acs.cgd.9b00651>. Acesso em: 27 mar. 2023.

SHI, Q. *et al.* Amorphous Solid Dispersions: Role of the Polymer and Its Importance in Physical Stability and In Vitro Performance. **Pharmaceutics**, 1 ago. 2022. v. 14, n. 8.

_____; MOINUDDIN, S. M.; CAI, T. Advances in coamorphous drug delivery systems. **Acta Pharmaceutica Sinica B**, 2019. v. 9, n. 1, p. 19–35.

SHIMADA, Y. *et al.* Features of heat-induced amorphous complex between indomethacin and lidocaine. **Colloids and surfaces. B, Biointerfaces**, 1 fev. 2013. v. 102, p. 590–596. Disponível em: <https://pubmed.ncbi.nlm.nih.gov/23104030/>. Acesso em: 10 abr. 2023.

SINGH, G. *et al.* Development and characterization of nevirapine loaded amorphous solid dispersions for solubility enhancement. **Asian Journal of Pharmaceutical and Clinical Research**, 7 ago. 2019. v. 12, p. 176–182. . Acesso em: 21 abr. 2023.

SUN, D. D.; LEE, P. I. Evolution of supersaturation of amorphous pharmaceuticals: The effect of rate of supersaturation generation. **Molecular Pharmaceutics**, 2013a. v. 10, n. 11, p. 4330–4346.

_____; _____. Evolution of Supersaturation of Amorphous Pharmaceuticals: The Effect of Rate of Supersaturation Generation. **Molecular Pharmaceutics**, 4 nov. 2013b. v. 10, n. 11, p. 4330–4346. Disponível em: <http://pubs.acs.org/doi/10.1021/mp400439q>. Acesso em: 8 jul. 2019.

SURESH, K.; CHAITANYA MANNAVA, M. K. C.; NANGIA, A. A novel curcumin–artemisinin coamorphous solid: physical properties and pharmacokinetic profile. **RSC Advances**, 5 nov. 2014. v. 4, n. 102, p. 58357–58361. Disponível em: <https://pubs.rsc.org/en/content/articlehtml/2014/ra/c4ra11935e>. Acesso em: 10 abr. 2023.

TANTISHAIYAKUL, V.; SUKNUNTHA, K.; VAO-SOONGNERN, V. Characterization of Cimetidine–Piroxicam Coprecipitate Interaction Using Experimental Studies and Molecular Dynamic Simulations. **AAPS PharmSciTech**, jun. 2010. v. 11, n. 2, p. 952. Disponível em: </pmc/articles/PMC2902308/>. Acesso em: 10 abr. 2023.

TAYLOR, L. S.; ZHANG, G. G. Z. Physical chemistry of supersaturated solutions and implications for oral absorption. **Advanced Drug Delivery Reviews**, 1 jun. 2016. v. 101, p. 122–142. . Acesso em: 27 mar. 2023.

_____; ZOGRAFI, G. Spectroscopic characterization of interactions between PVP and indomethacin in amorphous molecular dispersions. **Pharmaceutical research**, 1997. v. 14, n. 12, p. 1691–1698. Disponível em: <https://pubmed.ncbi.nlm.nih.gov/9453055/>. Acesso em: 5 abr. 2023.

TEKADE, A. R.; YADAV, J. N. A Review on Solid Dispersion and Carriers Used Therein for Solubility Enhancement of Poorly Water Soluble Drugs. **Advanced Pharmaceutical Bulletin**, 2020. v. 10, n. 3, p. 359. Disponível em: </pmc/articles/PMC7335980/>. Acesso em: 2 fev. 2023.

UEDA, H. *et al.* A Strategy for Co-former Selection to Design Stable Co-amorphous Formations Based on Physicochemical Properties of Non-steroidal Inflammatory Drugs. **Pharmaceutical Research**, 1 abr. 2016. v. 33, n. 4, p. 1018–1029. . Acesso em: 8 mar. 2020.

USP. **United States Pharmacopeia**. 37. ed. Rockville: The United States Pharmacopeial Conventional, 2014.

VASCONCELOS, T. *et al.* Amorphous solid dispersions: Rational selection of a manufacturing process. **Advanced Drug Delivery Reviews**, 2016. v. 100, p. 85–101.

_____; SARMENTO, B.; COSTA, P. Solid dispersions as strategy to improve oral bioavailability of poor water soluble drugs. **Drug Discovery Today**, 1 dez. 2007. v. 12, n. 23–24, p. 1068–1075. . Acesso em: 13 fev. 2023.

VO, C. L. N.; PARK, C.; LEE, B. J. Current trends and future perspectives of solid dispersions containing poorly water-soluble drugs. **European Journal of Pharmaceutics and Biopharmaceutics**, 2013. v. 85, n. 3 PART B, p. 799–813. Disponível em: <http://dx.doi.org/10.1016/j.ejpb.2013.09.007>.

WISE, M. E.; MISTRY, K.; REID, S. Drug points: neuropsychiatric complications of nevirapine treatment. **British Medical Journal**, 2002. v. 324, n. 7342, p. 879.

WLODARSKI, K. *et al.* Physical stability of solid dispersions with respect to thermodynamic solubility of tadalafil in PVP-VA. **European Journal of Pharmaceutical Sciences**, 2015. v. 96, p. 237–246.

WU, W. *et al.* Transformations between Co-Amorphous and Co-Crystal Systems and Their Influence on the Formation and Physical Stability of Co-Amorphous Systems. **Molecular Pharmaceutics**, 2019. v. 16, n. 3, p. 1294–1304.

XIA, D. *et al.* Supersaturated polymeric micelles for oral cyclosporine A delivery: The role of Soluplus–sodium dodecyl sulfate complex. **Colloids and Surfaces B: Biointerfaces**, 1 maio. 2016. v. 141, p. 301–310. . Acesso em: 2 fev. 2023.

YU, H. *et al.* Supersaturated polymeric micelles for oral cyclosporine A delivery. **European journal of pharmaceutics and biopharmaceutics : official journal of Arbeitsgemeinschaft fur Pharmazeutische Verfahrenstechnik e.V**, 2013. v. 85, n. 3 Pt B, p. 1325–1336. Disponível em: <https://pubmed.ncbi.nlm.nih.gov/23954511/>. Acesso em: 2 fev. 2023.

ZHANG, G. G. Z. *et al.* Phase transformation considerations during process development and manufacture of solid oral dosage forms. **Advanced Drug Delivery Reviews**, 23 fev. 2004. v. 56, n. 3, p. 371–390. . Acesso em: 30 mar. 2023.

APÊNDICE A – New Horizons in Antiretroviral Drug Delivery Systems for HIV Management

Title: New Horizons in Antiretroviral Drug Delivery Systems for HIV Management

Kayque Almeida dos Santos [a,b*], Lívia Maria Coelho de Carvalho Moreira [a,c] ,José Lamartine Soares-Sobrinho [a,c] and Mônica Felts de La Roca Soares [a,c]

[a] *Center for Quality Control of Medicines and Related Products, Federal University of Pernambuco, Recife, PE, Brazil;*
[b] *Program of Scientific Innovation, Federal University of Pernambuco, Recife, PE, Brazil,*
[c] *Program of Pharmaceutical Sciences, Federal University of Pernambuco, Recife, PE, Brazil.*
[*] *Correspondence: kayquealmeida@yahoo.com.br or kayque.almeida@ufpe.br*

ARTICLE HISTORY

Received:
Revised:
Accepted:

DOI:

Abstract:

Introduction: Human Immunodeficiency Virus (HIV) infection is still a major global problem, whose drug treatment consists of prophylactic prevention and antiretroviral combination therapy for better pharmacological efficacy and control of circulating virus. However, there are still pharmacological problems that need to be overcome, such as low aqueous solubility of drugs, toxicity, and low patient adherence. Drug delivery technologies can be used to overcome these barriers.

Objective: This review summarized the latest drug delivery systems for HIV treatment. Initially, an overview of the current therapy was presented along with the problems it presents. Then, the latest drug delivery systems used to overcome the challenges imposed in conventional HIV therapy were discussed.

Conclusion: This review examines innovative approaches for HIV treatment, where various drug delivery systems have shown significant advantages such as high drug encapsulation, improved solubility, and enhanced bioavailability both *in vitro* and *in vivo*. Strategies like cyclodextrins, solid dispersions, microneedles, and nanoparticles are explored to address challenges in drug solubility, bioavailability, and administration routes. Despite progress, obstacles like limited clinical trials and industrial scalability hinder widespread adoption of these formulations, emphasizing the need for further research and collaboration to optimize and ensure accessibility of innovative HIV therapies, mainly in regions where access to HIV treatment are scarce and remain a challenge.

Keywords: HIV, antiretroviral treatment, drug delivery systems, controlled drug release, pharmaceutical technology, biopharmaceutical classification system.

1. INTRODUCTION

The human immunodeficiency virus (HIV), a contagious lentivirus and member of the *Retroviridae* family that affects the body's immune system, was initially reported in the early 1980s. Its transmission occurs through exposure to blood or other contaminated body fluids, such as breast milk and semen, with sexual intercourse being the main source of infection and, as the infection spreads, its progression leads to a chronic immunosuppressive condition known as acquired immunodeficiency syndrome (AIDS) [1–3].

The oldest HIV infection was found in 1959 in Congo, indicating that the global HIV epidemic may have originated in Central Africa through transmission between multiple cross-species of simian immunodeficiency viruses (SIVs), affecting African primates [4]. Some of these genetic transfers may have resulted in a virus that spread to humans in a limited way, until a transmission involving SIVs in chimpanzees in southeastern Cameroon may have originated a specific group of HIV-1, the main responsible for the AIDS pandemic [4,5].

HIV attacks immune cells, such as T_{CD4}^{+} cells, monocytes, macrophages, and dendritic cells, characterizing an infection divided into four stages: primary infection or seroconversion, clinically asymptomatic stage, symptomatic infection, and AIDS [4]. As the T_{CD4}^{+} cell count decreases, the infection progresses to more advanced stages, characterizing a profound immune suppression that characterizes AIDS, where the T_{CD4}^{+} cell count is below 200 cells/µl, increasing the number of opportunistic infections and cancers [6].

It is estimated that 39.0 million people are living with the virus, with 1.3 million of them infected only in 2022 [7,8]. Despite prevention and treatment efforts, 24% of people living with HIV do not have access to treatment, which may have contributed to the death of 630,000 people from AIDS-related illnesses in 2022, totaling 40.4 million people who have died from the same diseases since the beginning of the epidemic [8]. However, there has been a 68% reduction in AIDS-related deaths since the peak in 2004 and a 52% reduction since 2010, with the greatest reduction occurring among women and girls (57%) [8,9].

In the absence of a cure, the goal of HIV treatment is to suppress viral replication as much as possible and to keep the viral plasma level below the detection level with the highly active antiretroviral therapy (HAART) regimen, especially in key populations, where the median prevalence is higher, such as transgender people (10.3%), gay men and other men who have sex with men (7.7%), people who inject drugs (5.0%) and sex workers (2.5%) [8]. The therapy is considered a success when, in addition to suppressing viral replication without resistance, it has few costs to the patient, low toxicity, few long-lasting adverse effects, lower risk of pharmacological interaction, and positive impact on quality of life [10].

Since the introduction of HAART, a drop of up to 80% in mortality in industrialized nations has been recorded [11]. However, significant limitations persist, especially in underdeveloped countries, where infection rates are higher, in addition to problems derived from it, since antiretroviral therapy is of chronic use and many challenges related to it still need to be overcome, such as solubility problems, toxicity and poor adherence [12]. Therefore, the use of delivery strategies is required to improve antiretroviral therapy and overcome such limitations.

Drug delivery systems (DDSs) can be used for existing drugs on the market to help them reach their site of action, ranging from nanometric to micrometric scale particles, solving several problems in their administration by offering the possibility of reducing the dose, frequency of administration and favoring the treatment, i.e. improving the absorption of drugs that are poorly soluble in water [13]. Therefore, the use of DDSs is necessary to overcome limitations of current antiretroviral therapy, without reaching non-target cells, organs, or tissues, reduce the risk of toxicity and improve the quality of HIV therapy [14,15].

Scientists often develop DDSs in a formulation-driven approach, considering the physicochemical properties of drugs and their limitations [16]. Despite reports of the use of DDSs for HIV management [6,17–19], many studies have been published each year in a growing to improve HIV treatment in the last 10 years (Fig. 1). Because there is no effective HIV cure, new DDSs and strategies need to be developed for a functional cure and lead to HIV eradication. Achieving effective drug concentrations in HIV reservoirs using solubility and permeability enhancement approaches, increasing their uptake to drug concentrations in target cells are some of the therapy challenges that DDS need to address [20].

Although the number of studies related to the use of DDSs for the management of HIV has grown over the years an and that the use of antiretroviral drugs presents a series of challenges for HAART, not only the already known risks of toxicity and low adherence, but also the physicochemical problems that compromise its absorption and bioavailability, impacting therapy and combating the virus. Therefore, it is necessary to analyze the use of DDSs that can improve the bioavailability of these drugs in target locations and bring better quality to antiretroviral therapy.

Several review articles were found in the literature that focus on the analysis of research on drug delivery systems for the treatment of AIDS. However, the focus of these articles is not the analysis of DDS used in pre-exposure and HIV patients. Some focus on transdermal delivery systems and devices [21], the use of DDS to deliver to the brain reservoir [22–26], or focus on a specific system [27–29] or a specific drug used in therapy [30]. Also, to identify possible emerging research trends that may guide future research to explore new, as yet unexplored horizons.

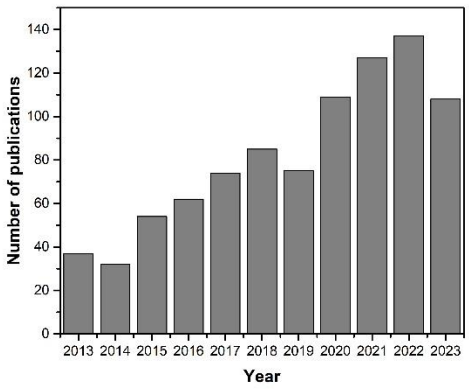

Figure 1. Number of publications in the last 10 years that have the terms “antiretroviral” and “drug delivery systems” (ISI: ScienceDirect, accessed in January 2024)

This literature review analyzes trends and perspectives in the use of DDS for antiretroviral therapy, synthesizing the vast production of knowledge, through reflections on the

topics studied and knowledge gaps that need to be filled. Bibliographical searches were carried out in important databases in the area of pharmaceutical technology, such as ScienceDirect, U.S. National Library of Medicine (PubMed) and Scientific Electronic Library Online (SciELO). Inclusion criteria consisted of original research articles as primary bibliographic sources related to drug delivery systems used for antiretroviral therapy published between 2013 and 2023 written in English. Articles published outside the time range, which are not related to the topic, bibliographic sources that are not research articles and duplicate papers were not considered in this review (Fig. 2).

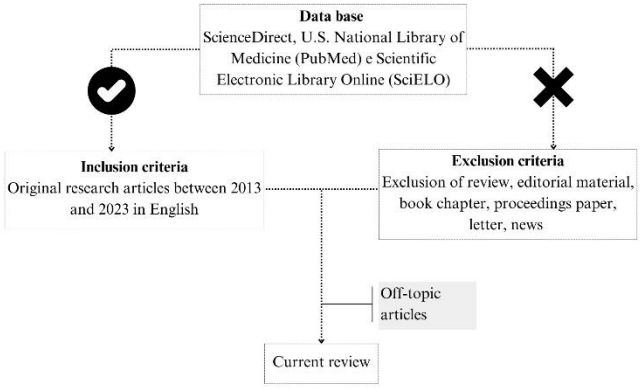

Figure 2. Search methodology flowchart

We have divided this review into three parts. First, we describe the current HAART therapy, through the physicochemical and pharmacological properties of the drugs used and the challenges that the therapy faces. Second, we reviewed each type of DDS used to treat HIV infection, with the aim of discussing their ability to control *in vitro* and *in vivo* drug release. The third and final part focuses on the challenges, perspectives, and opportunities for the use of DDSs in the treatment of HIV.

2. ANTIRETROVIRAL THERAPY AND CHALLENGES

Until 1996, the clinical management of HIV consisted of prophylaxis against opportunistic pathogens and the management of AIDS-related diseases, until the development of reverse transcriptase and protease inhibitors [12]. Several challenges arose in the first therapeutic regimens, such as the considerable number of tablets, inconvenient dosage, treatment-limiting toxicity, and incomplete virulent suppression, leading to several resistance mutations, with long-term treatment consequences [31].

Since then, several classes of antiretroviral (ARV) drugs have been developed and divided into subclasses according to their mechanism of action at the different stages of the HIV viral replication cycle as illustrated in Fig. 3: nucleotide reverse transcriptase inhibitors (NRTIs), non-nucleotide-reverse transcriptase inhibitors (NNRTIs), protease inhibitors, CCR5 inhibitors, and integrase inhibitors (INSTIs) [32,33].

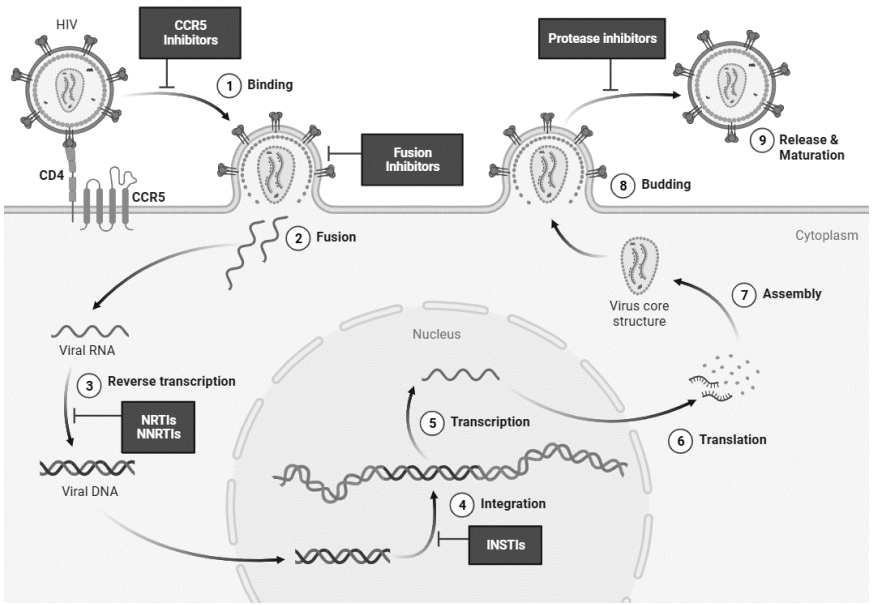

Figure 3. Site of action of ARVs during the HIV viral replication cycle

Since its introduction in the late 90s, HAART has proven to be extremely effective, being the most successful therapeutic strategy by combining at least three drugs of different pharmacological ARV classes in a single-dose one-tablet regimen for the treatment of HIV infection [33–35]. In a treatment whose adherence is essential for the success of the therapy, the combined use of drugs reduces the risks of viral resistance, improves the efficacy of the drugs, or prolongs

their effects, helping to eradicate the circulating virus without the need for several dosage forms to be administered during the day [36,37].

Therapeutic guidelines [38–40] recommend the use of first-line therapy such as the use of two nucleoside/nucleotide reverse transcriptase inhibitors associated to a third drug from the following classes: integrase inhibitors, non-nucleoside reverse transcriptase inhibitors, or protease inhibitors [11,41,42]. After the introduction of the use of Pre-Exposure Prophylaxis (PrEP) and Post-Exposure Prophylaxis (PEP) to individuals not infected before and after exposure to the virus, respectively, the number of newly infected individuals decreases each year by providing an important tool for preventing the establishment of HIV infection after transmission, with results of clinical trials pointing to safety in daily administrations and with a reduction in the risk of infection to the virus through sexual contact [20,43–45].

Despite the advantages of oral administration, such as minimal invasiveness, painlessness and ease of administration, there are limitations in oral HAART that go beyond pharmacological efficacy or toxicity and depend on patient adherence and the low bioavailability of the drug caused by its low aqueous solubility [46,47]. The unpleasant taste of many ARVs leads to poor adherence by the patient, favoring the interruption of treatment, especially in children who use liquid formulations, damaging therapy [18,48,49]. In addition, most ARVs are absorbed in the small intestine and with variable effects from food, requiring dosage forms that protect the drugs from the gastric environment, preventing drug degradation [18].

The low aqueous solubility compromises the dissolution of the drug in the gastrointestinal tract, compromising its absorption and, so, its bioavailability when administered by conventional oral dosage forms [50,51]. This problem also occurs with drugs with a low ability to permeate membranes, which also have difficulties in being absorbed by the body. To reverse this problem, increasing doses becomes a way out, but it can lead to increased adverse effects and toxicity.

The solubility and permeability of the drug are two parameters that classify the molecules in the Biopharmaceutical Classification System (BCS) proposed by Amidon et al (1995), being useful in the prediction of drugs with low aqueous solubility, classifying them in Class II and Class IV (Table 1). Thus, the disintegration rate of solid formulations and the dissolution rate are important criteria evaluated in the development of solid oral formulations of poorly soluble drugs, since the dissolution of the drug is a prerequisite for its absorption [52,53]. The main drugs and their physicochemical properties are described in Table 1.

Table 1. Physicochemical properties of the main drugs used in HIV antiretroviral therapy. Physicochemical data from the Drug Bank website (http://go.drugbank.com).

Antiretroviral		BCS class	Water solubility (mg/mL)	Log P	pKa	Problems	Reference
Pharmacological class	**Drug**						
Nucleotide reverse transcriptase inhibitors (NRTI)	Zidovudine	I	16.3	0.05	9.96	Virulent resistance and hematological toxicity	[54,55]
	Lamivudine	III	70	-1.4	14.29	Low permeability	[56]
	Emtricitabine	I	119	-0.43	2.65	Lactic acidosis and liver problems	[57]
	Tenofovir	III	13.4	-1.6	1.35	Low permeability	[58]
Non-nucleotide reverse transcriptase inhibitors (NNRTI)	Nevirapine	II	0.105	2.5	14.98	Low solubility	[59]
	Efavirenz	II	0.00855	3.89	12.52	Low solubility	[60]
	Etravirine	IV	0.0169	3.67	10.99	Low permeability	[61]
Protease inhibitors	Ritonavir	IV	0.00126	3.9	13.68	Low solubility and low permeability	[62]
	Lopinavir	IV	0.00192	3.91	13.39	Low solubility and low permeability	[62]
	Darunavir	II	0.0668	1.76	13.59	Low solubility	[63]
	Indinavir	IV	0.0482	3.26	13.01	Low solubility and low permeability	[64]
CCR5 inhibitors	Maraviroc	III	0.0106	4.3	13.98	Low permeability	[65]
Integrase inhibitors (INSTI)	Raltegravir	II	0.0976	1.3	7.02	Low solubility	[66]
	Dolutegravir	II	0.0922	0.98	10.1	Low solubility	[67]
	Cabotegravir	II	0,0062	1.04	10.04	Low solubility	[68,69]

BCS: biopharmaceutical classification system (I – high solubility and high permeability; II – low solubility and high permeability; III – high solubility and low permeability; IV – low solubility and low permeability).

LogP: octanol-water partition coefficient

3. DELIVERY SYSTEMS FOR ANTIRETROVIRAL THERAPY

DDSs are an innovative and vast field of research for pharmaceutical administration of compounds that affect the therapy of humans or animals, by developing new materials or carriers for effective therapeutic delivery of drugs for different purposes [70–72]. Although most of the current drugs are administered by conventional dosage forms, such as solutions, suspensions, tablets, and immediate-release capsules, they cannot always facilitate an excellent therapeutic response, with adverse effects, low bioavailability caused by low solubility and/or low permeability of drugs, and poor patient adherence.

Thus, to overcome these limitations, many drugs need to make dose adjustments, which can cause aggravated side effects and increase cases of toxicity [72]. DDSs offer an effective way out against the limitations of conventional forms, since they have their own size, surface area, biodistribution, toxicity, pharmacokinetics, and excretion profiles, and can incorporate and transport water-soluble and hydrophobic drugs [73].

The advantages of DDSs are many, such as the high bioavailability of low solubility drugs, the reduction of dose-associated toxicity, modification of pharmacokinetic parameters favoring the improvement of bioavailability, greater availability of the drug at specific target sites, increased drug stability, fewer adverse effects, masking of unpleasant tastes and modulation of drug release [15].

The use of DDSs for the treatment of HIV offers viable alternatives to the problems associated with treatment, such as poor adherence, solubility problems, and toxicity. These systems include amorphous solid dispersions (ASDs) [74], co-amorphous (CAMs) [75,76], co-crystals (CCs) [77], cyclodextrin (CDs) [78], and different nanoparticulate systems, like nanoparticles (NPs) [79,80], liposomes (LPs) [81,82], dendrimers and nanoemulsions (NEs) [83,84] are used to improve HIV treatment using drugs used in current therapy. Table 2 show studies on the application of DDS in the management of HIV, with emphasis on the main results obtained by authors.

Table 2. DDs used in HIV prevention and treatment in the last 10 years.

DDS	ARV DRUG	OBJECTIVES	MAIN PHYSICOCHEMICAL RESULTS	IN-VITRO ANALYSIS	IN-VIVO ANALYSIS	REF.
Cyclodextrins	Lopinavir and ritonavir	Improve drug palatability, solubility, and dissolution	Significant interaction occurs between components. Thermic events were not seen for the ternary complexes. Complex formulations are amorphous.	The spray-dried ternary complex showed improved dissolution, with a dissolution of 11% after 2 h and 9.5% after the pH adjustment.	-	[85]
Cyclodextrins	Lopinavir	Increase bioavailability and biodistribution without the need for a second drug	Complexes prepared by spray drying showed a higher reduction in the carbonyl band intensities compared to those prepared by solvent evaporation. The degree of crystallinity or amorphization was affected by the type of high degree of substitution used and molar ratio of such mixtures.	Increased drug solubilization with γ-CyD, HP-γ-CyD and HP17-γ-CyD resulting in an 87-, 114- and 129-fold increase, respectively	-	[86]
Cyclodextrins	Cabotegravir	Evaluate the use of cyclodextrin to Increase the solubility of Cabotegravir Sodium and the effect on Intradermal Release via Hydrogel-forming Microarray Patches	The conversion of the crystalline structure of drug to one that was amorphous, most likely due to successful inclusion complex formation. It was reveling total drug inclusion into the CD cavity. Hydrogen bond interaction between components is suggested. The drug content of the formulated CAB-Na/HP-β-CD tablets was approximately 10,325 ± 35.82 μg per tablet.	The “Super swelling” formulation based on Gantrez® S-97 had a swelling capacity that was approximately 9-fold greater than the polymer hydrogel.	Skin deposition 141 ± 40 μg of cabotegravir; Cmax of 53.4 ± 10.16 μg/mL after 24h patch application. Cmax observed was 58.98 ± 9.95 μg/mL. $AUC_{0–28}$ values for the were 644.76 ± 55.43 μg/mL/day.	[87]
Cyclodextrins	Saquinavir and ritonavir	To compare the pharmacokinetics and improved bioavailability of CDs following oral administration in rats	-	-	The CD complexes of both saquinavir (3860.93±138.50 ng.h/ml) and ritonavir (2300.19±118.21 ng.h/ml) had shown higher $AUC_{0-\infty}$ values compared to pure drugs.	[88]
Cyclodextrins	Efavirenz	Prepare CDs based on polymeric nanosuspensions	Diameter: 143.8nm - 284.4nm; Polydispersity index: <0.3; Zeta potential (mV): -38,3 to -27,5 mV; Layered morphology	Dissolution efficiency > 60%	-	[88]

		for solubility increase				
Cyclodextrins	Efavirenz	Increase the aqueous solubility and bioavailability of efavirenz	Physical mixtures had an overlap of the components pattern profiles. Possible complexation with the components is suggested with hydrogen bonding. Presence of CD and polymer hinder the drug melting process, leading to both its shift to a higher temperature and enlargement of the peak.	The complex with 1% polymer promoted the best increase in the solubility and delivery of drug. In 30 min, more than 80% of the total drug was delivered, against less than 25% compared with drug alone	-	[89]
Cyclodextrins	Rilpivirine	Increase solubility and dissolution rate using CD-based nanosponges	Spectral characterization confirmed inclusion complexation. It was inferred that electronic interactions, hydrogen bonding, and van der Waals forces are involved in the supramolecular interactions.	Saturation solubility was 10-13 folds higher in distilled water and 12-14 in HCl 0.1 N. Bioavailability increased by almost 2 folds	-	[90]
Co-amorphous	Nevirapine	Cause a rapid dissolution of nevirapine solid dispersion	The solid dispersion thermograms show no change in the drug's melting peak. There was no interaction between the components. Amorphous nature of the systems was confirmed	The highest solubility was obtained in a solution of lactose and citric acid at the best ratio of 15:25.	-	[91]
Co-amorphous	Ritonavir	Improve solubility and permeability with the aid of Quercetin as a vitreous former	Crystalline peaks were not detected. Physical stability at 40°C supported for 90 days.	Significant improvement (on an average 5-fold) in saturation solubility was seen for all three binary amorphous systems, the highest being 8.74 ± 0.27 µg/ml	Cmax value of ritonavir:quercetin 1:2 was found 1.26-fold higher than pure ritonavir. The difference is statistically significant.	[76]
Co-amorphous	Ritonavir and darunavir	To investigate the contribution of amorphous state and the composite-rich phase impact of drugs generated by pH change on the supersaturation of coamorphous formulations	Presence of amorphous material. No detection of glass transition event. Indication of intermolecular interactions between drugs.	Generation of liquid liquids phase separation by changing the pH from acidic to neutral, decreasing the concentration of darunavir and ritonavir.	Decreased supersaturation leads to decreased drug flux.	[75]

Co-amorphous	Ritonavir	Stabilize the amorphous form of ritonavir for increased solubility	Amorphous material. Presence of glass transition. No evidence of intermolecular interactions.	3-fold increase in ritonavir solubility	-	[92]
Co-crystal	Etravirine	Forming CCs of Etravirine to raise the solubility of the drug using L-tartaric acid as a coformer	Endotherms of the cocrystals reveal two endothermic peaks relating to the components. Different infrared spectra of the mixture were obtained compared to pure drug. Chemical stability provided for molar ratio 1:1 and 1:2 of Etravirine and L-tartaric acid.	-	-	[61]
Co-crystal	Emtricitabine	Improves drug diffusion by using benzoic acids to form cocristal	In all three cocrystals, heterosynthon was found to be prevalent. Hydroxyl group was hydrogen-bonded to the hydroxyl groups of the coformers as well as to the carbonyl groups of other drug molecules. In the other cocrystal hydrates, the drug-OH group formed hydrogen bonds with water only.	CC decreased the solubility of the native drug. Cocrystals decreased its diffusion rate compared to its native drug due to reduced concentration gradient/solubility and higher hydrophobic interactions	-	[57]
Co-crystal	Lopinavir	Increase the rate of dissolution and intestinal absorption	Solid state characterization shown formation of lopinavir-menthol CCs at best molar ratio of 1:2. Additional menthol underwent phase separation due to possible self-association.	The dissolution efficiency from 24.96% in case of unprocessed lopinavir to 91.43% in optimum formulation. Co-perfusion with menthol increased intestinal permeability	-	[77]
Co-crystal	Lopinavir and ritonavir	To improve solubility, dissolution, and oral bioavailability by cocrystallization	The diffractograms showed intense, sharp, and unique crystalline peaks, which were entirely different from the initial constituents. Hydrogen bond formation confirms the cocrystal formation. Sample showed more prominent, robust, and rectangular shaped crystals	Aqueous solubility of CAM formulation was increased 3.7-fold, while cocrystals had 5.9-fold increase compared to pure drug. CAM and cocrystals formulations showed 86% and 94% drug respectively.	-	[93]
Dendrimer	Tenofovir and maraviroc	To determine the potential use of the dendrimer in combination with	-	100% inhibition were obtained and displayed a synergistic profile against different HIV-1 isolates in TZM.bl cells. A potent	-	[94]

		ARV for topical microbial use		activity was showed and did not activate an inflammatory response.		
Dendrimer	Zidovudine, tenofovir and efavirenz	To evaluate the use of different combinations of dendrimers and antiretrovirals against HIV-1 infection	-	A synergistic activity profile was showed with in the majority of the combinations tested against the tropic HIV-1 in cell lines, as well as in human primary cells	-	[95]
Dendrimer	Tenofovir and maraviroc	To study the synergistic activity of triple combination of dendrimers for topical application	-	Combinations showed a greater broad-spectrum anti-HIV-1 activity than the single-drug and preserved this activity in acid environment or seminal fluid.	No irritation was detected in female BALB/c mice	[96]
Dendrimer	Zidovudine	To explore dual targeting of anti-HIV drug via sialic acid conjugated-mannosylated poly(propyleneimine) (PPI) dendritic nano-constructs	Mannosylation of dendrimers was confirmed by appearance of characteristic peaks of imine. The percentage loading of zidovudine in dendrimers was significantly ($p<0.001$) increased. Thermic analysis clearly demonstrated and confirmed the formation of drug dendrimer complex.	Zidovudine dendrimers have shown reduced hemolytic toxicity, cytotoxicity and *in vitro* drug release at pH 7.4. Extremely significant ($P<0.001$) increase in cellular uptake of zidovudine by macrophage cells was observed in case of SMPPI as compared to PPI and free drug.	The *in vivo* blood level and tissue distribution studies in albino rats demonstrated potential of dual targeted system. The drug concentration in lymph nodes was increased to about 28 times in case of SMPPI (1335 ± 17.6 ng/g) as compared to free drug (48 ± 5.8 ng/g) at 6th hr.	[97]
Dendrimer	´Tenofovir and raltegravir	To develop of topical microbicide formulations for vaginal delivery to prevent HIV-2 sexual transmission	-	Dendrimers inactivated the virus at an early stage of viral replication. Triple combinations increased the anti-HIV-2 activity, consistent with synergistic interactions (CIwt: 0.33-0.66).	No vaginal irritation was detected in BALB/c mice after two consecutive applications for 2 days with 3% G2-S16.	[98]
Dendrimer	Efavirenz	To prepare of novel PEGylated PAMAM (poly-amidoamine)	Entrapment efficiency was found to be 65.71%. Absence of peak in thermic curves indicates drug encapsulation. Surface morphology of particles found	Dendrimers have shown prolonged drug-release property	-	[99]

		dendrimers for delivery of anti-HIV drug Efavirenz	to be having smooth surface and spherical in shape. Efavirenz-loaded PEGylated 5.0 G PAMAM dendrimers at 40±2°C for 3 months it has been found no change either in appearance or in its drug release.			
Solid dispersion	Darunavir	To study the effectiveness of various methods to improve the solubility and bioavailability of darunavir by mesoporous carriers and water-soluble polymers in solid dispersions	An amorphous halo is clearly observed in all the obtained X-ray diffraction patterns. Particle sizes were between 17-257 µm.	Eudragit EPO systems showed the best dissolution result.	The bioavailability test revealed the highest efficacy of the polymer dispersion on the mannitol particles	[100]
Amorphous solid dispersion	Dolutegravir	Improve solubility and increase dolutegravir efficacy	No physicochemical interaction was found between the drug and P407 in the fabricated solid dispersion. Crystalline state of the drug was changed to amorphous.	Release of DTG was observed from the solid dispersion (>95%), which is highly significant ($p<0.05$) as compared to pure drug (11.40%), physical mixture (20.07%) and marketed preparation of dolutegravir (35.30%), with Cmax (14.56 µg/mL).	An improved drug bioavailability (AUC: 105.99±10.07 µg/h/mL) was showed when compared to the AUC of animals administered with physical mixture (54.45±6.58 µg/h/mL) and pure drug (49.27±6.16 µg/h/mL).	[67]
Amorphous solid dispersion	Efavirenz	Improve solubility using water-soluble polymer	Thermic results indicated a characteristic peak of efavirenz in all physical mixtures, but it was not evident in solid dispersions, indicating loss of crystallinity. Microscopy images revealed the crystalline form of efavirenz with orthorhombic crystals, which were not seen in the solid dispersions. This was corroborated by the diffraction results that confirmed the amorphous nature of the solid dispersions.	The systems obtained by evaporation did not show an increase in solubility, with a negative effect observed when decreasing the polymer proportions. In systems obtained by kneading, increasing the polymer ratio reduced drug release, with the 4:1 ratio showing the highest dissolution of efavirenz (58.83%)	-	[60]

Amorphous solid dispersion	Nevirapine	Develop nevirapine tablets to improve solubility using the solid dispersion technique	Infrared spectra of the physical mixtures reveal no interactions between the components.	Drug release was greater in systems obtained by the fusion method.	-	[101]
Amorphous solid dispersion	Nevirapine	Improve bioavailability by varying gastric pH	Solid dispersions were generated without crystalline residuals.	Solid dispersions made of enteric polymers were independent to gastric pH variability and exhibited superior dissolution performances compared to their respective physical mixtures and neat nevirapine.	-	[102]
Amorphous solid dispersion	Dolutegravir	Prepare effective amorphous dispersions of Dolutegravir	Though quench cooling successfully stabilized the drug into amorphous form, solvent evaporation technique failed to render the drug completely amorphous. Prepared dispersions were found stable at room temperature for 60 days.	The dissolution advantage between prepared dispersions and pure drug in USP phosphate buffer was found bridged in the bio-relevant media. Dispersions prepared by quench cooling method was found endured in FeSSIF. Subsequently, the dissolution advantage was translated into the improved flux.	The overall exposure of Dolutegravir was improved by 1.7 fold, while the maximum plasma concentration demonstrated 2 fold increase after comparing with crystalline Dolutegravir.	[103]
Amorphous solid dispersion	Nevirapine	Increase solubility and dissolution rate	Interactions between nevirapine and the polymer were evidenced	The initial solubility of Nevirapine was found to be 16.13%. Solubility increased in solid dispersion up to 97.14%	-	[74]
Amorphous solid dispersion	Nevirapine	To verify the impact of drug loading on the elevation of drug aqueous solubility and diffusion	There was a good miscibility between components which stabilized the drug in its amorphous state.	All amorphous systems had an increment in aqueous solubility compared to nevirapine alone, although 10% ASD kept drug supersaturation at very high concentrations longer, having the greater drug flux	-	[59]

Amorphous solid dispersion	Ritonavir and atazanir	Evaluation of the thermodynamic properties of solid dispersion	Thermodynamic studies indicated that the components of the mixture are miscible in the molten state, generating amorphous solid dispersions confirmed by X-ray diffraction and calorimetry scanning, with a glass temperature identified in the range of 139-160°C.	Formulation binary achieved 50% of the supersaturation. For ternary dispersion, the Cmax of each drug was only one third of that achieved for the single drug formulations. Occurred a decreased flux across Caco-2 cells for the drug combinations compared to drug alone.	-	[104]
Amorphous solid dispersion	Dolutegravir	Solubility and bioavailability enhancement using ASD of dolutegravir amorphous salt and acid-free dispersions of dolutegravir	Partial crystallinity and amorphity was observed for solid dispersions. No intermolecular interactions were observed between the components from the infrared spectra of solid dispersions.	Solid dispersions improved the solubility of Dolutegravir up to 5.7 folds compared to the pure forms, with drug release 2 folds higher than that in the pure form. Drug permeability was enhanced.	Pharmacokinetic profiles of SD of drug salts and SD free acid, where 4.0 and 5.6 folds, respectively, improved drug Cmax.	[105]
Solid dispersion by mesoporous carriers	Darunavir	To evaluate the main silica-like mesoporous carriers on the market in terms of their possible use for the preparation of ASD	Amorphous material was obtained for all samples obtained, with differences perceived by microscopy images. No traces of crystallinity were detected in thermal analyzes	An 8-fold increase in solubility was shown when compared to the isolated drug.	-	[63]
Liposomes	Tenofovir and emtricitabine	Develop microbicidal hydrogels with the drugs, using liposomal systems	Mean diameter of 134 ± 13 nm, with an encapsulation efficiency of approximately 84%, and a transition temperature of 41 °C. Liposomal hydrogels featured pseudoplastic profiles that were deemed suitable for topical application.	It was show non-cytotoxic to HEC-1-A and CaSki cells and favoring permeation across polysulfone membranes (Jss = 9.9 $\mu g/cm^2/h$). Drug release profile reached around 60% within 3–6 h.	-	[106]
Liposomes	Efavirenz	To evaluate the encapsulation efficiency of efavirenz using different mass	LP exhibited high encapsulation (99%). The average particle size and Zeta Potential were found to be 411.10 ± 7.40 nm and $-53.5.3 \pm 0.06$ mV, respectively.	A relatively controlled release behavior was shown being similar to the dissolution profile of un-encapsulated drug.	-	[107]

		ratios of lecithin and cholesterol				
Liposomes	Lamivudina and dolutegravir	To develop and characterize LP conjugated to anti-CD4 antibody and peptide dendrimer to improve therapeutic efficacy	Particle size of the optimized LP was 133.7 ± 4.04 nm, with spherical morphology of the LP confirmed. The entrapment efficiency was 34 ± 4.9 % and 54 ± 1.8 % for lamivudine and dolutegravir, respectively	Slower in vitro release of drugs was observed when entrapped into LP. Conjugation of anti-CD_4 antibody and PD2 enhanced the uptake of LP into the cells. LP exhibited better HIV inhibition with lower IC50 values (0.0003 ± 0.0002 μg/mL).	-	[81]
Liposomes	Efavirenz	Formulate efavirenz-laden LP in the presence of glutathione to increase the ability to reach target reservoirs.	Formulate efavirenz-laden LP in the presence of glutathione to increase the ability to reach target reservoirs by investigating intracellular liposome uptake with and without glutathione by human monocytic monolithic leukemic cells and examining cell viability and scavenging activity of ROS	Efficiency encapsulation was greater than 90%. Particle size reported was about 120 nm to 205 nm without and with glutathione, respectively, whereas polydispersity index value <0.3 indicated that liposomal vesicles were unimodal. Zeta potential values were greater than −50 mV.	Addition of glutathione demonstrated an almost 2-fold increase in the intracellular concentration of drug. Drug uptake was increased in 1.2-fold by LP at the end of 24 h. LP formulated increased the cell viability up to 78% of untreated cells in comparison to only 5% with pure drug.	[82]
Eutectic mixture	Efavirenz and tenofovir	To evaluate the impact of tenofovir on the solubility and dissolution of efavirenz	Thermic results indicate the formation of a eutectic mixture, the molar ratio of 65/35 being the eutectic point.	Efavirenz solubility in water was increased in the presence of tenofovir and was decreased in phosphate buffer pH 6.8. Tenofovir solubility was not significantly influenced by the presence of efavirenz.	-	[108]
Nanoemulsion	Efavirenz	To develop a dose adjustable nanotechnology based liquid formulation of efavirenz with improved	Percentage transmittance was closer to 100%, with a very low viscosity. The value of refractive index for the optimized formulations was found to be close to 1.42. Some formulations showed the small particle size and least polydispersity index of 28.833 ± 2.084 on average.	More than 80% was released within 6 h	Cmax and $AUC_{0\text{-}24h}$ was extremely significant ($p < 0.0001$) in comparison to that of drug suspension. Bioavailability compared demonstrated significantly ($p < 0.001$)	[109]

		bioavailability for HIV therapy			greater extent of absorption than that from drug suspension. Absorption of efavirenz from nanoemulsion was 2.6-fold higher.	
Nanoemulsion	Efavirenz	To develop a self-nanoemulsifying drug delivery system to improve the oral bioavailability of efavirenz	Particle size was below 50 nm. Infrared studies showed the retention of the characteristic peaks of drug in the preconcentrate.	In vitro dissolution profile released more than 80% drug within 30 min.	A 2.63 fold increase in $AUC_{0-\infty}$ was showed in comparison to plain efavirenz suspension.	[110]
Nanoemulsion	Darunavir	To investigate the potential of solid self-nanoemulsifying drug delivery system in improving the dissolution and oral bioavailability of darunavir	Analysis revealed the formation of nanoemulsion (144 ± 2.3 nm). Solid state studies concluded the presence of drug in non-crystalline amorphous state without any significant interaction of drug with the other components.	An initial rapid release of about 13.3 ± 1.4% within 30 min and reached a maximum of 62.6 ± 3.5% release at the end of 24 h. A faster dissolution from the developed formulation was 3-folds greater.	Enhanced values of peak drug concentration was showed for liquid NE (2.98 ± 0.19 µg/mL) and solid NE (3.7 ± 0.28 µg/mL) compared to pure darunavir (1.57 ± 0.17 µg/mL).	[111]
Nanoemulsion	Darunavir	To formulate darunavir loaded lipid nanoemulsion to increase its oral bioavailability and enhance brain uptake	The optimized batch had globule size of 109.5 nm, zeta potential of -41.1 mV, entrapment efficiency 93% and creaming volume 98%. The batch remained stable at 4 °C for 1 month with an insignificant change in globule size and zeta potential ($p > 0.05$).	There was 76% drug release in 8 h and 95% by the end of 12 h.	An increase of 223% bioavailability of Darunavir was shown. Cmax was 2-fold higher in nanoemulsion. The organ biodistribution study indicated 2.65 fold higher brain uptake for nanoemulsion than that for suspension	[112]
Nanoemulsion	Indinavir	To develop an oil/water lipid nanoemulsion of indinavir using Tween 80 as co-emulsifier to	The total drug content of formulations was greater than 9.80±0.11 mg/mL and encapsulation efficiency values above 98.9±0.2.	There was no significant difference in cumulative drug release	Brain uptake was improved for a 1% Tween 80 containing formulation (F5). Brain level of indinavir subsequent to administration of F5 was	[113]

		improve its brain specific delivery			significantly ($p<0.05$) higher than produced by administration of a drug solution (2.44-fold) or a control nanoemulsion (1.48-fold).	
Nanoparticles	Lopinavir	To formulate nano systems of antiretroviral drug for brain targeting to reduce HIV associated neurocognitive disorder	Particle size of 196.6 nm, entrapment efficiency of 83.6%, zeta potential of 21.2 mV. The evaluation of zeta potential of the optimized uncoated and coated nanoformulation yielded values of 21.2 mV and 29.6 mV, with uniform shape of the particles with size less than 200 nm	Significant improvement in the cytotoxicity and uptake performance was shown on Caco-2 cells and macrophages.	A 4.8-fold and 16.5-fold increase in peak plasma concentration and area under curve from lopinavir nanostructured lipidic carriers vis-à-vis plain lopinavir, along with 2.8-fold improvement in the brain biodistribution potential.	[114]
Nanoparticles	Indinavir	Use polymeric NPs as a vehicle for oral release of indinavir	The weight and number-based average molecular weights of the mPEG-PCL copolymer were 13.313 and 8.507 Kda respectively. Infrared spectra indicate the formation of the copolymer. The prepared NPs had an average particle size of 211 + 10.12 nm with a polydispersity index of 0.220 + 0.15. The morphology of the NPs is spherical.	Up to 90% of free indinavir was released in the initial hours, with a maximum concentration achievable after 96 hours in PBS pH 1.2, 6.8 and 7.4 of 60%m 40% and 15% respectively, while the NPs had a release close to 60% in simulated gastric fluid and 15% in PBS.	The plasma AUC_{0-t}, $t_{1/2}$ and Cmax were increased by 5.30, 5.57 and 1.37 fold compared to the control solution, respectively	[64]
Nanoparticles	Darunavir	Investigation of the use of coaxial electrospraying in the preparation of NPs made of nanocrystals encapsulated within a polymer.	Plate shaped crystals with sharp edges were observed in the original darunavir, but the electrosprayed particles were more spherically shaped with wrinkled surfaces. The average particle size ranged from 3 to 5 µm. Darunavir encapsulation efficiency of approximately 90%.	The enteric coating layer reduced the percentage of Darunavir release in acidic medium to ca. 20%.	-	[115]

Nanoparticles	Lopinavir and ritonavir	Develop a nanotechnology to formulate fixed-dose combination of pediatric low-solubility drugs in a children-friendly, flexible solid dosage form	Particle size was less than 158 nm with mono-dispersed distribution, over 95% entrapment efficiency and stability over 8 h in simulated physiological conditions. The granules with were palatable and stable at room temperature over 6 months.	There was no significant difference on release from 0 to 8 h based on group comparison ($p > 0.05$) for both granules, with same release profile ($p > 0.05$) at each time point	The nanogranules displayed a 2.56-fold increase in bioavailability and significantly increased drug concentrations in tested tissues, especially in HIV sanctuary sites	[79]
Nanoparticles	Rilpivirina and cabotegravir	Releasing antiretrovirals into the brain for the treatment of HIV-associated neurocognitive disorder by forming microcrystals	Drug content of lyophilized formulations were found to be 53.89 ± 2.89% w/w for rilpivirine and 53.88 ± 2.9% w/w for cabotegravir. The characteristic peaks in the raw drugs spectra are still seen in the spectra for their respective physical mixtures and final formulations, indicating that there have been no chemical interactions occurring.	-	A Cmax was seen at 21 days of 619.17 ± 73.32 ng/g for rilpivirine, with potentially therapeutically relevant levels were maintained for 28 days. For cabotegravir, a Cmax was seen at 28 days of 478.31 ± 320.86 ng/g.	[80]
Nanoparticles	Ritonavir	Preparing ritonavir nanosuspensions for increased solubility	NPs had particle size about 200 nm and zeta potential -25 mV. The drug loading of the NPs was approximately 7% (w/w).	NPs were nontoxic to TZM-bl cells and ectocervical explants, showing potent protection against HIV-1 BaL infection in vitro	The HIV inhibitory effect showed up to a 50-fold reduction in the 50% inhibitory concentration (IC50) compared to free drug. NP-EFV combined with free TFV demonstrated strong synergistic effects (CI50=0.07) at a 1:50 ratio of IC50 values and additive effects (CI50=1.05) at a 1:1 ratio of IC50 values.	[116]
Nanoparticles	Darunavir and ritonavir	To develop high drug loading nano formulations for the treatment of HIV	All formulations had encapsulation efficiencies of ≥92.5% were all spherical in shape with smooth surfaces. The mean diameter were up	There was not a burst drug release, only ~2% of darunavir was released after 0.5 h (the first time point). All formulations showed	-	[117]

			to 224 nm ± 74. DLS analysis provided Z-average diameters ~250 nm.	controlled drug release over 24 h period, where ~60% occurred over 24 h.		
Nanoparticles	Etravirine	Development of nanostructured etravirine lipid carriers to improve anti-HIV therapy and reduce oxidative stress associated with long-term treatment	Spherical core-shell type of a system and the presence of selenium at the core-shell of the nanocarrier was confirmed. Confocal microscopy and flow cytometry results exhibited enhanced uptake in TZM-bl cells compared to plain drug.	Infected TZM-bl cells exhibited higher efficacy for the dual-loaded nanocarrier system than the plain drug.	A significant increase of antioxidant activity factors was observed in animals administered with the dual-loaded nanocarrier system containing nano-selenium. Improvement in the *in vivo* pharmacokinetic parameters was also observed, along with a higher accumulation of the dual-loaded nanocarrier in remote HIV reservoir organs like the brain, ovary, and lymph node.	[118]

3.1.Cyclodextrin

CDs are a group of cyclic oligosaccharides produced from starch or its derivatives by the bacterial enzyme glycosyltransferase CD, containing six or more monomers attached to each other, forming the different families: α-CD (six units), β-CD (seven units) and γ-CD (eight units) (Fig. 4)[119]. CD form a truncated cone with a central cavity into which the active molecules insert. The outer surface is characterized by several hydroxyl groups, while the central cavity is filled with oxygen atoms and carbon-hydrogen atoms [120]. Due to the arrangement formed, CDs can form complexes with host molecules by internalizing them within, promoting the increase of solubility of host drugs with low aqueous solubility, with improved stability and bioavailability, preventing drug:drug interactions, reducing gastric irritation promoted by drugs and masking unpleasant flavors and odors [121–123].

Ivone *et al*. developed pediatric CD-based formulations of two drugs used as fixed-dose combination, lopinavir and ritonavir. CDs from each drug were prepared by spray-drying and the release studies were performed with a change of pH from 1.2 to 6.8, to verify the impact of the change on the solubility of the drugs. The authors found that the complexes obtained exhibited improved dissolution profiles at pH 1.2 compared to pure drugs and physical mixtures, especially the complexes obtained with ritonavir β-CD, reaching a cumulative ritonavir released near to 100% [85].

As a weakly basic drug with pH-dependent solubility, ritonavir (RTV) increases solubility with decreasing pH through protonation of thiazole groups, resulting in greater dissolution of ritonavir compared to lopinavir. Crude RTV promotes a cumulative release of 70% after 2 hours. In contrast, formulations containing only the complex between the drug and Soluphus show a reduction in this dissolution, which is consistent with the formation of salts between the drug and the polymer in an acidic medium. . Thus, by introducing this drug-polymer complex into the CD inclusions, it protects the thiazole groups from the formation of salts with the polymers. This induces a release of 96% of the RTV [85].

Adeyoe *et al.* have formulated lopinavir complexes to increase its bioavailability and biodistribution without the need for a second drug, since it is used in a fixed-dose combination due to its limited oral bioavailability. Therefore, the authors applied an in-silico method to select the best CD for the inclusion of lopinavir. Thus, they predicted a high-substitution-grade derived γ-CD (HP17-γ-CD) which was compared with a non-derived γ-CD and a commercial HP-γ-CD. The complexes were obtained by supercritical assisted spray drying (SASD) and co-evaporation (CoEva) and were able to amorphize and solubilize lopinavir in phosphate buffer pH 7.4, especially through the SASD method which showed greater release of lopinavir from HP17-γ-CD complexes and solubility consequently [86]. In the HPLC-MS/MS analyses used to quantify the solubility of LPV and the in vitro release of the drug, CyD derivatization increased the solubilization of LPV with γ-CyD, HP-γ-CyD and HP17-γ-CyD, resulting in an increase of 87, 114 and 129 times, respectively. Evidence that HP17-γ-CyD size increase is complementary to LPV complex formation [86].

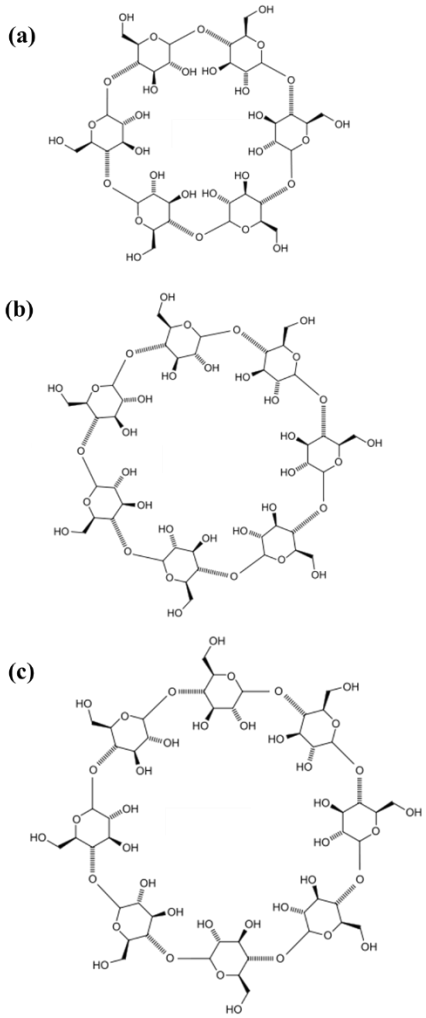

Figure 4. Structures of the three CD families. (a) α-CD, (b) β-CD and (c) γ-CD

Chemically modified CDs are created by etherifying or introducing functional groups into the 2-, 3-, and 6-hydroxyl groups of glucose residues. These modifications improve solubility through two mechanisms: the breaking of hydrogen bonds and the prevention of crystallization as a result of the creation of a material which gives rise to a loving product [124].

Microneedles patches (MAPs) are a series of micrometer-sized needles capable of perforating the stratum corneum and absorbing interstitial fluid (Fig 5). Swelling of the polymeric matrix promotes the release of drugs. The drugs can be contained within the matrix or underneath it through a drug reservoir, where after swelling the drug reservoir dissolves and releases the drug intradermally in a controlled manner[125]. Volpe-Zanutto *et al.* used CD technology to increase the solubility of cabotegravir sodium by evaluating its intradermal release through hydrogel-forming MAPs, a prolonged painless and minimally invasive system capable of delivering drugs intradermally [87].

Initially, the authors formulated reservoir tablets of the drug and hydroxypropyl-β-CD (HP-β-CD), which were combined with two different HF-MAP formulations (MAP1 and MAP2) and tested *ex vivo* and *in vivo*. They obtained interesting results, showing an approximate amount of 141 μg and 142 μg of drug being disposed in the skin *ex vivo* for MAP1 and MAP2 respectively after 24 hours. The *in vivo* pharmacokinetics of MAP2 was investigated for 28 days, demonstrating an extended release after 24 hours of patch application and a maximum concentration (Cmax) of approximately 53.4 μg/ml, while the formulation approved by Food and Drug Administration reached a Cmax near of 43,6 μg/ml [87]. MAP2 was shown to be capable of delivering 456±90.51 μg/mL in 24 h, a total drug 2.23 times greater than that observed with MAP1. In which the total distribution was 324 ± 38.04 μg/0.5 cm2, of which 132.60 ± 52.47 μg/0.5 cm2 penetrated through the skin. The formulations with matrices containing the reservoir with the CDs and the drug were able to release the hydrophobic drug due to the encapsulation in the CDs, which promoted an increase in the solubility of the drug [87].

Sogai *et al.* aimed to compare the pharmacokinetics and bioavailability of saquinavir and ritonavir and their optimized complexes following oral administration in rats. CDs were made with a 1:1 molar ratio β-CD with the drugs. A dose equivalent to 10mg/kg was administered orally to rats and blood samples were collected to evaluate the half-life, apparent volume of distribution, total body clearance and bioavailability for the pure drugs and their complexes obtained. The authors reported that the values of the area under the curve (AUC) were higher for the drug complexes compared to the pure drugs, revealing higher bioavailability and plasma concentrations for the CDs obtained [78].

Kommavarapu *et al.* aimed to improve the solubility and dissolution rate of efavirenz using β-CD based on polymeric nanosuspensions. The combined use of DDS takes advantage of the nanometer scale to lower the cost of CD preparation. They prepare four formulations varying the drug:polymer ratios by precipitating the physical drug:polymer mixtures that have been dissolved in the organic phase of an aqueous phase mixture. They showed that the maximum diameter of the NPs was 281.4 nm, with the polydispersity index indicating monodisperse uniformity with zeta potential ranging from -38 ζ to -27 ζ. The solubility and dissolution profile of the drug was increased compared to its pure version, with dissolution efficiency greater than 60% for each formulation obtained [88]. The results showed that the complexes promoted a twofold increase in the maximum concentration value (Cmax) and a relative percentage of bioavailability of 168% [88].

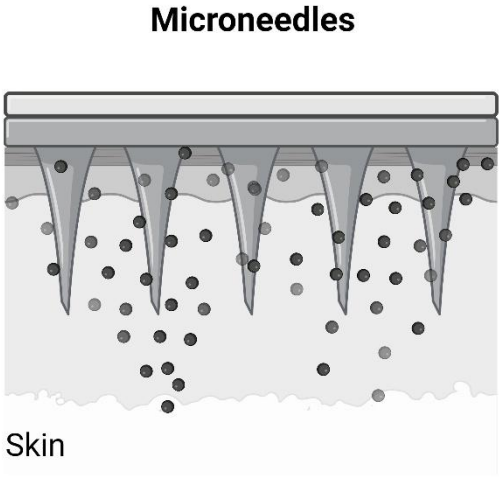

Figure 5. The mechanism through which drug release occurs via microneedles, as a transdermal delivery device.

Vieira *et al.* also associated the use of efavirenz CD with polymers, developing ternary drug systems with β-CD and the hydrophilic polymer Polyvinylpyrrolidone (PVP) K-30 to increase the solubility of the drug for better pharmacological therapy. Initially, the authors chose the best CD through a solubility-phase diagram, proving that methyl-B-CD was the most efficient. The interaction between PVP K-30 and β-CD takes place through electrostatic interactions, that is, through van der Waals and hydrogen bonds, which can be favored by the reactive groups of efavirenz and β-CD, thus promoting the stability of the complex. [89].

Rao *et al.* investigated the use of CD-based nanosponges to increase the solubility and bioavailability of rilpivirine. Nanosponges are biocompatible nanoporous particles that can form inclusion complexes with low aqueous solubility drugs and were prepared by the authors using β-CD to form the complexes with rilpivirine by the solvent evaporation method. They confirmed the stable complexation of the systems,

whose saturation solubility results indicated a 10-13-fold increase with the ternary systems in distilled water and 12-14 folds higher in acidic medium. Oral bioavailability was also investigated, with an almost 2-fold increase. The authors attribute the success of the system's stability to electronic interactions, hydrogen bonds, and van der Waals forces between the drug and CD [90].

The articles under review demonstrate the potential of combining CDs with other therapeutic innovations. The resulting combination can yield improvements in drug performance, including enhanced solubility and bioavailability—dependent upon the physicochemical characteristics of the drugs involved.

3.2.Solid Dispersions

Solid dispersion (SD) is characterized by the dispersion of one or more active substances in an inert carrier, generating supersaturated solutions capable of maintaining elevated levels of the drug in gastrointestinal fluids by increasing the rate of dissolution, increasing the rate of absorption and bioavailability (Fig. 6) [126–128]. According to their solid phase and physical state, they can be classified into eutectic mixtures, solid solutions, and glass solutions, in addition to the subdivision into polymeric or non-polymeric glass solutions according to the stabilizer used [128]. Eutectic mixtures (EM) are dispersed systems that have a lower melting point when compared to individual components, where the heterogeneous microcrystalline composition maintained by weak interphase bonds, lead to high thermodynamic functions and the anticipated melting point, ensuring greater solubility [129].

The most conventional SDs are polymeric ones, also known as amorphous solid dispersions (ASDs), where the drug with low aqueous solubility is molecularly dispersed in a polymeric matrix, which stabilizes the amorphous molecules of the drug generated by the production process, reducing molecular mobility, inhibiting the recrystallization process, and generating high concentrations of the drug [59,130]. Co-amorphous dispersions (CAMs) are alternative strategies to amorphous polymer, which combine low molecular weight excipients with low aqueous solubility drugs in a single homogeneous amorphous phase, overcoming the difficulties and problems that ASDs present [131–133]. Dispersions based on mesoporous silica are obtained by trapping amorphous drug molecules in nanoscale mesopores, suppressing recrystallization, and improving the dissolution rate, generating drug supersaturation in the aqueous medium [134].

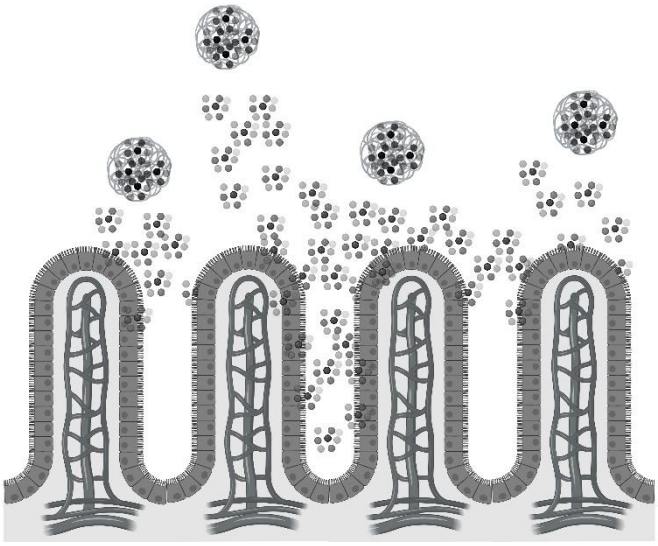

Figure 6. The mechanism by which enteric release and drug dissolution occurs in solid dispersions encapsulating pharmaceutical agents is of great interest to the pharmaceutical industry.

In particular, solid dispersions represent an optimal approach for neglected diseases. This is due to the fact that they are a cost-effective solution [67]. Poloxamer 407 is a water-soluble triblock copolymer comprising a hydrophobic polyoxypropylene residue sandwiched between two hydrophilic polyoxyethylene units. The use of a hydrophilic carrier in the matrix can facilitate the solubility of numerous hydrophobic drugs. However, the solubilization capacity of these polymers may be constrained, potentially leading to the supersaturation of the drug [135].

Chaudhary *et al.* intended to improve the solubility of dolutegravir, to increase its efficacy using the solid dispersion technique. Thus, they conducted a drug miscibility study, where they found that Poloxamer 407 was the best polymer to conduct the study. The SDs were obtained by the solvent evaporation technique, but no physicochemical interactions were found, despite the confirmation of the amorphous solid state, which led to the rapid release of the drug (>95%) and Cmax (14.56 µg/ml) higher than that of the physical mixture and the isolated drug. This is reflected in the improved bioavailability in the *in vivo* studies [67].

Alves *et al.* aspired to improve HIV antiretroviral therapy by solving the problem of efavirenz solubility and absorption. They tested different polymers but chose PVP-K30 through the study of phase solubility diagram and prepared formulations obtained by the solvent evaporation and kneading method with different drug:polymer ratios. They found that SD prepared by solvent evaporation did not show

satisfactory results, with a decrease in the dissolution rate despite the amorphous state. However, the SD obtained by kneading in a 4:1 ratio (drug:polymer) has a high dissolution rate, with good stability [60].

Mamatha *et al.* intended to develop nevirapine tablets with solubility improved by ASD technology. They prepared ASDs with Plasdone S-630 and Soluplus using kneading and melting method, performing in vitro dissolution studies that indicated a significant increase in the dissolution rate of nevirapine ASDs. The pre-formulation studies were carried out indicating a good compatibility between nevirapine and carriers and nevirapine tablets were prepared subsequently by direct compression method, whose post-compression evaluations indicated that the best formulation used Plasdone S-630 in a 1:2 ratio, which showed greater drug release, becoming an excellent carrier for increasing nevirapine solubility [101].

Monschke *et al.* wished to avoid the influence of gastric pH variation on dissolution when preparing nevirapine ASDs with enteric polymers by the hot-melt extrusion technique. They found that the ASDs generated did not have crystalline residues. Due to the basic nature of the drug (pKa = 2.8), drug dissolution studies demonstrated almost complete dissolution at pH 1. However, at pH 5.5 and 6.8 there were supplies of the drug available. The dissolution study was carried out in non-sink conditions applying two pH change experiments to simulate different gastric conditions and observed that the ASDs were independent of pH variation, with dissolution superior to physical mixtures and the pure drug [102].

Lakshman *et al.* prepared dolutegravir ASD for solubility enhancement. They determined the miscibility of the drug in the polymer in theoretical and experimental studies and, after choosing the polymer, obtained ASD by the quench cooling and solvent evaporation method. The first technique amorphized the drug, achieving a good stability of 60 days. They obtained a good dissolution performance in biorelevant medium, which reflected in the improvement of membrane flow. Oral bioavailability *in vivo* proved a higher amount of dolutegravir, with a 1.7 fold higher AUC and 2 fold higher Cmax compared to pure dolutegravir [103].

Bompelwar *et al.* wished to increase the solubility and dissolution rate of nevirapine. Thus, they developed ASDs by the solvent evaporation method, using HPMC E5LV as polymer in different ratios. To choose the best ratio, they used solubility assays, where they noticed that the 1:4 and 1:3 ratios were the ones that showed the best results [74].

Santos *et al.* studied the effect of drug loading of Nevirapine ASDs on drug dissolution and diffusion. Thus, they used the solvent evaporation method to obtain the PVP K-30 as polymeric matrix, using three different drug loadings. Then, they characterized the systems obtained and subjected them to dissolution and permeation tests to verify the influence of drug loading on the performance of the systems. They noticed that the lower the drug loading, the faster and greater the drug release, reaching a higher supersaturation and Cmax, reflecting in the greater flow of nevirapine across the membrane [59].

Alhalaweh *et al.* evaluated the thermodynamic properties of solutions that evolve from the non-sink dissolution of ASDs containing two or more drugs, focusing on the maximum achievable supersaturation and the tendency of the system to undergo liquid-liquid phase separation (LLPS). Thus, they developed ternary ASDs of ritonavir and atazanavir with the PVP polymer at different molar ratios of each drug. In the non-sink dissolution study, the authors studied the phase behavior of supersaturated solutions, comparing them with supersaturated solutions generated by the addition of antisolvents, using Caco-2 cells for complementary transport/diffusion studies. They showed that the formulation containing the 1:1 molar ratio reached only 50% of the supersaturation achieved by the isolated drugs and the Cmax decreased as the amount of atazanavir in the formulation decreased. They attribute this fact to the decrease in the concentration at which the drugs are subjected to LLPS in the presence of other soluble drugs, reducing the maximum achievable supersaturation of each drug and, consequently, the amount of flow through the Caco-2 cells [104].

Yarlagadda *et al.* explored the solubility and bioavailability of sodium salts and their acids and their dolutegravir-free acidic solid dispersions to increase solubility. Thus, they used Soluplus as a polymeric carrier and the quench cooling technique to prepare the ASDs. In characterization, they realized that there was no evidence of intermolecular interactions and that complete amorphization was obtained only in the free acidic solid dispersion. However, both showed improved solubility and rapid dissolution, leading to increased permeability and bioavailability [105].

Zolotov *et al.* developed darunavir SDs using mesoporous carriers based on silica and magnesium aluminosilicate using three different techniques, hot-melt extrusion, solvent wetting, and spray drying. They proved that the properties of the systems are equal to the properties of the corresponding carriers. The dissolution studies showed that silica SD showed better dissolution than darunavir and that it was used to formulate tablets, which showed improved dissolution compared to the original [63].

Zolotov *et al.* studied the effectiveness of various methods in improving the solubility and bioavailability of darunavir by

mesoporous carriers and water-soluble polymers in the form of ASDs. Initially, a screening was performed with several hydrophilic polymers to choose the best one to be the basis of the formulations, which were prepared by the hot-melt extrusion and spray-drying methods and mixed with suitable excipients to form dispersible tablets that were evaluated in *vitro* and *in vivo*. The best systems were obtained with Eudragit EPO, showing the best dissolution compared to the physical mixture in the polymer-free mesoporous carrier. Bioavailability tests also confirmed the success of polymeric dispersion [100].

Madan *et al.* wished to improve the solubility of nevirapine with rapid dissolution using hydrotropic agents, such as urea, lactose, citric acid, and mannitol, to produce CAM solid dispersions. Initially, they studied the solubility of nevirapine in the presence of each agent at different concentrations, where they found that the highest solubility was obtained at the concentration of 40% citric acid in the solution. They mixed the agents in different ratios for ternary formulations, finding that the 15:25 lactose and citric acid solution was the best ratio. SD based on this ratio did not show intermolecular interactions, which can be a long-term stability problem, since the interactions between drug and carrier help with physicochemical stability, by reducing the mobility of the drug, maintaining its amorphous state preserved [91].

Dengale *et al.* prepared, characterized, and evaluated the bioavailability of CAM ritonavir and quercetin, an excellent glass former capable to stabilize amorphous drugs. The preparation of the CAMs was performed by solvent evaporation in molar ratios of 1:1, 1:2 and 2:1. They proved the complete amorphization of the systems obtained by the characterizations performed, although crystalline traces were recorded in the 1:1 ratio after 90 days. The solubility increment was almost 5 times in saturation solubility. Oral bioavailability in *vivo* was conducted with 1:2 CAM alone, where Cmax increased 1.26-fold and the maximum time (Tmax) to reach Cmax decreased 2 hours after administration, but significant increase in oral bioavailability (1.12-fold) was not found [76].

Shete *et al.* studied the implications of phase solubility/miscibility and drug-rich phase formation on darunavir CAM performance with second drugs, such as ritonavir and indomethacin, on pH change. Indomethacin was chosen for the CAM generated from it to act as a comparator, since this drug is a weak acid while ritonavir is a weak base, in addition to being an excellent glass former. Initially, they prepared rich CAM phases of the drugs to see the effect of pH change on them. They found that the decrease in supersaturation was found proportionally to the mole fraction of the respective drug within the CAMs. The change of pH from acid to neutral led to the generation of drug-rich phases and LLPS for the darunavir:ritonavir CAM. The pH-dependent solubility and molecular weight of the individual components were the main reasons for the relative amount of each component within the drug-rich phases [75].

Dengale *et al.* prepared and characterized ritonavir:indomethacin CAMs prepared by solvent evaporation to improve the dissolution and physical stability of drugs. Thus, they prepare CAMs in molar ratios 2:1, 1:1 and 1:2 (ritonavir:indomethacin). Stability studies were performed at 25°C and 40°C for 90 days, in addition to the investigation of solubility by in *vitro* dissolution. They proved that amorphization was achieved for all CAMs, with glass transition temperature above 40°C. No evidence of intermolecular interactions was found between the components. However, a significant increase in the dissolution rate was found for ritonavir [92].

Bazzo *et al.* evaluated the impact of the presence of tenofovir disoproxil fumarate on the solubility of efavirenz in a eutectic mixture of a water-soluble drug and a low-aqueous drug. Different molar ratios were used to prepare the binary mixtures, whose results indicated the formation of a eutectic mixture with the eutectic point identified in the molar ratio 65:35. An increase in the solubility of efavirenz was observed in the acidic and biorelevant medium, despite the decrease in the phosphate buffer pH 6.8 caused by the loss of solubility of tenofovir in this medium, proving that the solubility of efavirenz is dependent on the solubility of tenofovir in the medium [108].

3.3.Co-Crystal

The use of CCs is one of the most famous strategies to increase the solubility, dissolution rate and bioavailability of poorly water-soluble drugs [136]. As CAMs, CCs have two or more components, one of them being the drug, in stoichiometric ratios, forming structurally homogeneous systems (Fig. 7), whose intermolecular interactions occur intimately through hydrogen bonds, π-π or van der Waals forces to maintain the thermodynamic stability of the cocrystals [137].

Rekdal *et al.* formed CCs of etravirine to increase the solubility of the drug using L-tartaric acid as a co-former. Co-crystallization occurred in molar ratios 1:1, 1:2 and 2:1 using slow evaporation and physical mixing to mix the components of the formulation. They showed that the mixture of etravirine and L-tartaric has a different infrared spectrum compared to the pure drug, confirming the presence of intermolecular interactions. Chemical stability has been proven for 1:1 and 1:2 molar ratios, ensuring that these systems can be promising for treatment and, although the authors did not carry out

solubility tests, they point out that their CCs can improve the drug's performance, since they managed to obtain stable systems formed by the interactions between the drug and L-tartaric acid [61].

Shajan *et al.* investigated the effect of emtricitabine CCs with aromatic carboxylic acids on drug solubility and permeability, with the intention of improving drug permeability. Thus, they prepared anhydrous emtricitabine CCs by solvent-assisted grinding in equimolar ratio of the drug with meta-hydroxybenzoic acid (MHB), vanillic acid (VAN) and ferulic acid (FER), in addition to the preparation of hydrated CCs with para-methylbenzoic acid (PMB), para-chlorobenzoic acid (PCB) and para-nitrobenzoic acid (PNB), performing the characterization and performance studies afterwards. Although the authors reported intermolecular interactions between specific functional groups of the drug and the coformers, there was no improvement in the solubility rate of the drug of any CCs obtained in the phosphate buffer pH 6.8, which is reflected in the lower diffusion rate, due to the decrease in the concentration gradient and greater hydrophobic interactions formed between the components [57].

Noha *et al.* developed lopinavir-menthol CCs to improve intestinal dissolution rate and absorption, due to low oral bioavailability, extensive presystemic metabolism and significant intestinal efflux P-glycoprotein. They employed the use of assisted kneading ethanol for the preparation of CC with menthol in different molar ratios, characterizing the formulations thereafter. Dissolution and permeability tests with the optimized ratio of 1:2 were also performed. They found a significant increase in the dissolution rate with an increase in the dissolution efficiency from 24.96% to 91.43% compared to the pure drug. There was an improvement in intestinal permeability by co-perfusion with menthol, making this substance an interesting co-former [77].

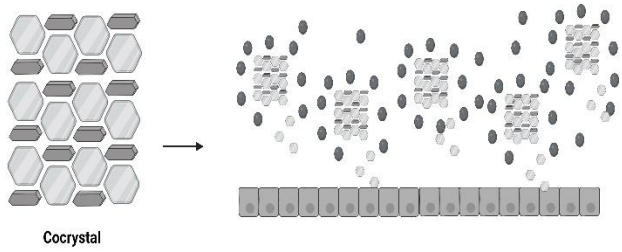

Figure 7. The mechanism of drug dissolution in cocrystals

Chaudhary *et al.* formulated lopinavir-ritonavir CCs to increase the solubility and dissolution of two poorly water-soluble drugs. Co-crystallization was performed by wet grinding and solvent evaporation methods, followed by characterization, dissolution, and stability studies. They found that the CCs developed showed superior solubility and dissolution, with a growth of 3.7 times in the wet grinding method and 5.9 times in the solvent evaporation method after a 48-hour study. They proved that the CCs presented a fast release, with excellent stability and physicochemical characteristics [93].

3.4.Nanoparticulate system delivery

NPs comprise a large field of materials research that employs materials ranging from 1-100 nm at the nanoscale level, widely used for drug delivery, chemical and biological sensing, and gases [138]. They can also be used to treat specific diseases like melanoma and cardiovascular, skin, and liver conditions, whereas drugs associated with nanotechnology can improve drug efficacy and bioavailability [139]. Sophisticated kinds of nanoparticles include nanocarriers including metal NPs, dendrimers, LP, polymer-based NPs, inorganic vectors, lipid-based NPs, and peptide-based NPs, leading to systems with different morphologies, size and chemical properties [15,140]. In the modern day, NPs are finding increasing application in tissue micro-engineering, drug delivery, microfluidics, biosensors, and microarrays for the targeted treatment of illnesses [16]. Its use has potential advantages to HIV treatment, such as the possibility of modifying properties such as solubility, drug release profiles, diffusivity, and bioavailability, leading to the improvement of convenient routes of administration, decreased toxicity, few adverse effects and extended drug life cycle [141].

Kurd *et al.* prepared indinavir NPs using the mPEG-PCL polymer as a drug vehicle to reverse their aqueous solubility problems. For this, the preparation of the polymeric NPs was optimized by experimental design and occurred by the emulsification solvent evaporation technique, whose characterization occurred soon after by different physicochemical techniques. The authors also made use of Caco-2 cells to assess cell uptake and transport. They found an increase in AUC (5.30-fold), $t_{1/2}$ (5.57-fold) and Cmax (1.37-fold) of the NPs compared to pure indinavir solution, generating a promising biodegradable system to aid in the treatment of HIV [64].

Nguyen *et al.* encapsulated darunavir in the Eudragit L100 polymer using a coaxial electrospraying to verify its feasibility in the preparation of polymeric NPs. Thus, they prepared aqueous nanosuspensions of darunavir and solutions of the polymer that were subjected to coaxial electrospraying, producing fine NPs with high encapsulation efficiency (about 90%). They found that using optimized darunavir nanosuspensions, the enteric coating layer reduced the amount of the drug released into the acidic dissolution medium to

approximately 20%, proving that the technique is useful for encapsulating drug nanocrystals in a polymeric matrix [115].

Pham *et al.* developed pediatric lopinavir and ritonavir granules from NPs, to create an antiretroviral combination technology that would improve solubility problems and increase the efficacy of pediatric ARV treatment. To do this, they used an innovative nanotechnology that produces self-assembling NPs in situ when the beads come into contact with water. The prepared NPs had a mean size of less than 158 nm with monodisperse distribution and encapsulation efficiency above 95% for both drugs. The authors were able to obtain palatable and stable NPs at room temperature for six months. An increase in bioavailability was recorded, with a 2.56-fold increase in lopinavir, demonstrating that the NPs obtained by them are an excellent strategy for the fight against pediatric HIV [79].

Abbate *et al.* formulated rilpivirine and cabotegravir nanoparticulate systems for brain delivery of drugs for the treatment of HIV-associated neurocognitive disorder using microneedle microcrystal formulation. The formulation of both drugs and their incorporation into microneedles released levels in the brains of rats above those available on the market, reaching an approximate Cmax of 619 ng/g for rilpivirine in 21 days, with potentially therapeutic levels maintained for 28 days. For cabotegravir, therapeutic levels have not been reached as expected, but they could be when administered to humans according to the authors [80].

Karakucuk *et al.* prepared ritonavir nanosuspensions to resolve its poor water solubility issues by microfluidization method. Two polymers were considered, hydroxypropyl methylcellulose and PVP, for the formulation and experimental design approach was used to choose the best formulation parameters. Type of polymer, drug:polymer ratio, and number of passes were the parameters evaluated. After choosing the best formulation, they lyophilized the nanosuspension making them dry NPs and submitted them to solubility tests. Thus, they realized that the NPs were partially amorphous, with a spherical shape and an average size of 500 nm. The increase in solubility was proven, with a 3.5-fold growth compared to the pure drug and a dissolved amount above 90% in the FeSSIF medium, concluding that the use of experimental design is an excellent tool for the development of formulations for the increase of ritonavir [116].

LP are considered one of the most widely used carriers for several hydrophobic and hydrophilic active molecules due to their high biocompatibility, biodegradability, and low immunogenicity [142]. They are lipid spherical vesicles, with particle diameter size between 50-500 nm and are composed of one or more lipid bilayers formed by emulsification in the aqueous medium [143,144].

Due to their small size at the nanoscale, amphiphilic characteristics and capable of carrying drug molecules inside or on their surface, they are promising DDSs for diagnosis and therapy by various routes of administration, such as ocular, oral, pulmonary, transdermal, and parenteral, and may contain polymers and membrane proteins to improve the effectiveness of the encapsulated drug [142].

Faria *et al.* carried out a rational development of liposomal hydrogels for vaginal delivery of ARVs in the prevention of HIV. To do this, they used tenofovir disoproxil fumarate and emtricitabine as drugs and conducted in silico and *in vitro* studies to evaluate the physicochemical characteristics of the drugs and the biophysical impact on lipid systems. They reported that the LP developed had a mean diameter of 134 nm, a tenofovir encapsulation efficiency close to 84%, and that they were not cytotoxic to HEC-1 and CaSki cells, being favorable to membrane permeation of the drug. The release of the drug in the liposome hydrogels was sustained for about 3-6 hours at 60%, proving the promising use of the system for HIV prophylaxis by vaginal route [106].

Okafor *et al.* encapsulated efavirenz in LP and characterized them to enhance ARV therapy. Thus, they used different ratios of crude soybean lecithin mass and cholesterol, using the thin film hydration preparation method. They proved that there was a 99% encapsulation in a 1:1 ratio of crude, lecithin, and cholesterol. The average particle size was about 411 nm and the zeta potential found was -53.5 mV, showing nanoparticulate characteristics which looks promising for the targeted delivery of efavirenz to the infected lymphocytes. The *in vitro* release studies revealed the potential for sustained release of efavirenz and for specific site delivery, with the possibility for surface modification of the resultant nano-systems for site targeting. This could reduce the adverse effects of the drug caused by its low solubility and expansion of its release to uninfected cells. Although the controlled release of the encapsulated drug have been similar to the non-encapsulated drug, efavirenz LP are still a promising delivery system due to the advantages of nanoscale release, according to the authors [107].

Mutalik *et al.* developed and characterized lamivudine and dolutegravir LP conjugated to anti-CD4 antibody and peptide dendrimer to improve therapeutic efficacy and achieve better treatment for HIV. Initially, they made a factorial design to optimize the preparation of LP, ensured by cytotoxicity and cellular internalization. They observed that the LP had a mean size of 133 nm, spherical morphology, and average encapsulation of 34% and 54% for lamivudine and dolutegravir, respectively. Cytotoxicity was not different between LP and free drugs, but conjugated formulations showed better HIV inhibition, showing that formulated LP have enormous potential for HIV treatment [81].

Kenchappa *et al.* formulated efavirenz LP in combination with glutathione to reduce the amount of reactive oxygen species (ROS) in tissues and improve HIV therapy by strengthening the immune system. They proved that the combined treatment with the two molecules can increase uptake and reduce cytotoxicity and that the encapsulation of the drug increased its level in macrophages, especially when glutathione was present, causing a greater fusion of intracellular ROS, bringing innovation to the treatment of HIV by glutathione supplementation [82].

The highly branched nanomolecules known as dendrimers have uniform, monodisperse, and well-defined structures made up of arms or branches that resemble trees that are created by adding branching units one after the other from an initiator. Most dendrimer-based nanomedicines have diameters between 1 and 16 nm and a molecular weight of 30-200 kDa, placing them in the same range as therapeutic proteins and liposomal or nanoparticulate delivery methods [84]. Due to their ability to bind to their target in a multivalent manner and overcome weak monovalent interactions, dendrimers with various types of functionalized groups at their periphery have demonstrated effective anti-HIV-1 activity as non-specific microbicides [97–99]. This suggests a potential strategy for the development of viral entry inhibitors.

In contrast to other nanoparticulate delivery system, dendrimers exhibit a high degree of structural variety and are well defined. The three primary parts of dendrimer structures - a multivalent surface, an inner shell around the core, and a central core - also set them apart from conventional polymers [145]. The dendrimer's host-guest characteristics are influenced by its interior, its three-dimensional form is determined by its core, and its ionic charge is mostly determined by its surface functional groups, which include a high number of potentially reactive sites [83].

According to Sepúlveda-Crespo *et al*., the G2-STE16 carbosilane dendrimer may be used as a topical microbicide against HIV-1 when combined with other carbosilane dendrimers and ARVs. The researchers demonstrated that in a model of TZM.bl cells, all combinations produced 100% inhibition and showed a synergistic profile against several HIV-1 isolates. In an environment of acidic vaginal or seminal fluid, the results demonstrated a robust action without inducing an inflammatory response. Dendrimer/dendrimer or dendrimer/ARV combinations as topical anti-HIV-1 microbicides were supported by subsequent research, which they saw as the initial step toward investigating the use of other anionic carbosilane dendrimers in combination and toward creating a safe microbicide [94].

Vacas-Córdoba *et al*. assessed the anti-HIV-1 efficacy of several combinations of anionic carbosilane dendrimers with sulfated (G3-S16) and naphthyl sulfonated (G2-NF16) ending groups using distinct ARVs. Most of the combinations evaluated against the X4 and R5 tropic HIV-1 in cell lines and human primary cells had a synergistic or additive activity profile with zidovudine, efavirenz, and tenofovir. Consequently, the antiviral efficacy of polyanionic carbosilane dendrimers and ARVs together is increased, and our results encourage more clinical investigation into combinational strategies as possible microbicides to prevent HIV-1 from being transmitted through sexual activity [95].

Sepúlveda-Crespo et al. investigated the cytotoxicity, anti-HIV-1 activity, vaginal irritation, and histological examination of triple combinations to examine the synergistic activity of carbosilane dendrimers with tenofovir and maraviroc as topical microbicide. When exposed to acidic environments or seminal fluid, the combinations exhibited more robust broad-spectrum anti-HIV-1 action compared to the single drug. G2-STE16/G2-S24P/tenofovir, G2-STE16/ G2-S16/maraviroc, and G2-STE16/tenofovir/maraviroc, with ratios of 2:2:1, 10:10:1, and 10:5:1, were the most potent combinations identified. The weighted average combination indices, which ranged from 0.06 to 0.38, allowed the authors to show a robust synergistic activity profile. There was no sign of irritation in the female BALB/c mice [96].

Gajbhiye *et al*. studied the use of sialic acid conjugated-mannosylated poly(propyleneimine) (PPI) dendritic nano-constructs for the dual targeting of the anti-HIV drug zidovudine. The fourth generation of PPI dendrimers, like sialic acid conjugated PPI dendrimers (SPPI), mannose conjugated PPI dendrimers (MPPI), and dual ligand system sialic acid conjugated-mannosylated PPI dendrimers (SMPPI), were synthesized and characterized. At a pH of 7.4, zidovudine-loaded dendrimers have demonstrated decreased cytotoxicity, hemolytic toxicity, and in vitro drug release. When compared to PPI and free drug, there was a highly substantial ($p<0.001$) increase in the cellular absorption of zidovudine by macrophage cells in the SMPPI condition. Studies *in vivo* also showed the promise of a dual targeted method for sialoadhesin and carbohydrate receptors. In the case of SMPPI, the drug concentration in lymph nodes rose to around 28 times (1335 ± 17.6 ng/g) compared to free drug (48 ± 5.8 ng/g) at the 6-hour mark. According to the findings, the dual ligand dendritic system (SMPPI) has the potential to improve antiretroviral drug biocompatibility and site-specific delivery [97].

Briz et al. used second and third-generation polyanionic carbosilane dendrimers with a silicon atom core and 16 sulfonate (G2-S16), napthylsulfonate (G2-NS16), and sulphate (G3-Sh16) end-groups to create topical microbicide formulations for vaginal distribution to inhibit HIV-2 sexual transmission. They investigated the cytotoxicity, anti-HIV-2,

anti-sperm, and antibacterial properties of dendrimers containing tenofovir and raltegravir, as well as the method of antiviral activity in the inhibition of HIV-2 infection. According to their results, G2-S16, G2-NS16, and G3-Sh16 all have anti-HIV-2 activity early in the course of viral replication by keeping the virus inactive, preventing HIV-2 from spreading from cell to cell, and inhibiting gp120 from binding to CD4 and allowing HIV-2 entry. Triple combinations comprising tenofovir and raltegravir increased anti-HIV-2 effectiveness, indicating synergistic interactions (CIwt: 0.33-0.66). After two consecutive 2-day treatments of 3% G2-S16, no vaginal discomfort was seen in BALB/c mice. The findings clearly suggest that G2-S16, G2-NS16, and G3-Sh16 are highly effective against HIV-2 infection. The mechanisms of action support their multifactorial and non-specific ability, suggesting that these dendrimers warrant more study as prospective candidate microbicides to prevent vaginal/rectal HIV-1/HIV-2 transmission in humans [98].

Pyreddy *et al*. developed innovative PEGylated PAMAM (poly-amidoamine) dendrimers to deliver the anti-HIV drugs Efavirenz. They produced around 5.0 G PAMAM dendrimers utilizing an ethylene diamine core by Michael addition by divergent approach, and PEGylation was performed using polyethylene glycol 600 with epichlorhydrin as a linker. PEGylated 5.0 G PAMAM dendrimers containing Efavirenz were tested for solid state characterization, drug release, and stability. They discovered an entrapment effectiveness of 65.71%. Particles had smooth surfaces and were spherical. After 3 months at 40±2°C, efavirenz-loaded PEGylated 5.0 G PAMAM dendrimers remained unchanged in appearance and drug release. The results show that this procedure is less time consuming, affordable, and repeatable. Drug-release studies indicate that PEGylated 5.0 G PAMAM-EFV dendrimers have shown prolonged drug-release property [99].

Dispersions of oil and water are known as nanoemulsions and are created when the disperse phase droplets, stabilized by a surface active layer, are in the nano size range of 20 to 200 nm, which gave it another name for submicron emulsion . The main components of a such nanosystems are water, oil, co-surfactant, and surfactant [112]. Because of their nanoscale droplets, nanoemulsions have a substantially larger oil-water contact area than traditional emulsions. The qualities of continuous release, drug targeting, and decreased toxicity make nanoemulsions attractive drug delivery systems [146]. BCS class II and IV drugs, whose low solubility frequently limits their systemic absorption, have demonstrated improved dissolution and, consequently, bioavailability when synthesized as nanoemulsions, due the loaded in a solubilized condition in the internal oil phase of an oil/water nanoemulsion and nanosized droplets, which increase contact area with the gastrointestinal mucosa, faciliting drug absorption [109,113,117].

Kotta *et al.* aimed to develop a dose adjustable nanoemulsion formulation of efavirenz with improved bioavailability using ternary phase diagram in phase inversion composition method. The authors studied globule size of the oil/water nanoemulsion and the optimized formulations were subjected for in vitro dissolution studies and *in vivo* studies and compared with drug suspension. The results revealed that the globule size of optimized formulation was less than 30 nm, more than 80% was released within 6 h which was highly significant ($p > 0.05$) and pharmacokinetic studies also proved a promising *in vivo* absorption profile when compared to the efavirenz suspension. The developed nanoemulsion proved to be an effective dose adjustable formulation of efavirenz for pediatric HIV therapy [109].

Senapati *et al.* developed a self-nanoemulsifying drug delivery system based on non-ionic surfactant mixtures to improve the oral bioavailability of efavirenz. Using solubility studies of drug in various excipients, they constructed pseudo ternary phase diagram to delineate the area of monophasic region of the pseudo ternary phase diagram. Different accelerated physical stability studies, self-emulsification assessment, globule size distributions, infrared spectroscopy, and in vitro dissolution were also performed on the formulations. Two optimized post diluted formulations confirm the size in nanometric range for below 50 nm. The infrared spectroscopy showed the retention of the characteristic peaks of EFZ in the preconcentrate and more than 80% drug was released within 30 min in case of optimized formulation while it was approximately 18.3% in the case of plain drug powder. The Pharmacokinetic data reveal a 2.63 fold increase in $AUC_{0-\infty}$ in comparison to plain drug suspension [110].

Inugala *et al.* investigated the potential of solid self-nanoemulsifying drug delivery system (S-SNEDDS) composed of an oil, surfactant and co-surfactant in improving the dissolution and oral bioavailability of darunavir. First, they formulated a liquid self-nanoemulsifying drug delivery systems (L-SNEDDS) . Then, further ternary phase diagram was constructed to determine the self-emulsifying region, in addition to other physicochemical parameters. In vitro drug release studies showed initial rapid release of about 13.3 ± 1.4% within 30 min from L-SNEDD. The globule size analysis revealed the formation of nanoemulsion (144 ± 2.3 nm) from the optimized L-SNEDDS formulation. In vitro dissolution studies indicated faster dissolution of darunavir from the developed S-SNEDDS and the solid state studies concluded the presence of drug in amorphous state without any significant interaction of drug with the components of S-SNEDDS. Furthermore, *in vivo* pharmacokinetic studies

resulted in enhanced values of Cmax for L-SNEDDS (2.98 ± 0.19 μg/mL) and S-SNEDDS (3.7 ± 0.28 μg/mL) compared to pure darunavir (1.57 ± 0.17 μg/mL) [111].

Desai *et al.* formulated lipid nanoemulsion to increase darunavir oral bioavailability and enhance brain uptake. They prepared various batches of lipid nanoemulsion by high pressure homogenization using soya bean oil, egg lecithin and Tween 80. The optimized batch DNE-3 had globule size of 109.5 nm, zeta potential of −41.1 mV, entrapment efficiency 93% and creaming volume 98% with stability at 4 °C of one month. In-vivo pharmacokinetics indicated 223% bioavailability of Darunavir relative to drug suspension. Cmax of DNE-3 was 2-fold higher than suspension form, with the organ biodistribution study 2.65 fold higher brain uptake for DNE-3 [112].

Due to the poor efficiency of indinavir in eliminating the virus in the brain, Prabhakar et al. created an oil/water lipid nanoemulsion (LNE) of indinavir utilizing Tween 80 as a co-emulsifier to increase its brain specific delivery. Following preparation of LNEs with various compositions, drug content, stability, and entrapment efficiency of five formulations (F1–F5) were assessed. Fluorescently tagged LNEs were then used in brain uptake tests. Following intravenous injection in mice, pharmacokinetic and tissue distribution tests were carried out. When comparing a formulation (F5) containing 1% Tween 80 to one containing 0.3% cholesterol (F2), it was shown that the former had better brain absorption of indinavir. The brain level of indinavir subsequent to administration of F5 was significantly ($P<0.05$) higher than produced by administration of a drug solution (2.44-fold) or a control nanoemulsion (F1) (1.48-fold) or formulation F2 (1.6-fold). These results suggest Tween 80 containing LNEs could provide a simple but effective means of delivering indinavir to brain [113].

Elkateb *et al.* investigated the factors that influence the comparative production of solid lipid nanoparticles (SLNs), nanostructured lipid carriers (NLCs) and nanoemulsions (NEs) in order to develop high drug loading nanoformulations for the treatment of HIV with a therapeutically relevant drug mixture of darunavir and ritonavir and two different surfactants. They used a simple nanoprecipitation method and screened three key formulation factors (lipid concentration, surfactant selection and drug loading) in order to determine their effect on the particle properties and stability of the formulations. NPs had mean diameters ∼200–300 nm. Drug loadings of 10% w/w darunavir/total lipid was achieved for SLNs, with loadings of 20% w/w was possible for NLCs and NEs, these values are amongst the highest reported for lipid nanoformulations. All formulations had encapsulation efficiencies of ≥92.5%. Overall, this study shows the versatility of the nanoprecipitation method for producing SLNs, NLCs and NEs. The ability to produce all three formulations with identical compositions (other than the lipids) may allow direct comparison of the biological properties in the future [117].

Rojekar et al. created modified nanostructured lipid carriers for etravirine using the double emulsion solvent evaporation process, which were then tested and optimized using the design of experiments approach. The spherical core-shell type of a system was validated using an electron microscope and small-angle neutron scattering. *In vitro* tests against HIV-1-infected TZM-bl cells revealed that the nanocarrier technology outperformed the standard drug. Confocal microscopy and flow cytometry studies showed that TZM-bl cells absorbed the drug more efficiently than plain cells. Animals supplied with the dual-loaded nanocarrier system containing nano-selenium showed a considerable increase in antioxidant genes, indicating the protective potential of the lipidic NP containing nano-selenium. A higher accumulation of the nanocarrier in remote HIV reservoir organs like the brain, ovary, and lymph node was noted. The results suggest the potential of a dual-loaded formulation for synergistically targeting the HIV1 infection improving a prolonged anti-HIV therapy [118].

4. FUTURE PROSPECTS, CHALLENGES AND OPPORTUNITIES

The main objectives of the fight against HIV are the prevention of new infections, achieving a functional cure and complete eradication of the circulating virus. Therefore, antiretroviral therapy has reached new levels of management and care, such as the emergence of the combined use of medications. Despite this, problems persist in current therapy, such as low adherence to the daily use of high pharmacological doses, resistance, toxicity, and low bioavailability of several ARV molecules. Therefore, formulations that include the use of delivery systems have been developed in recent years to overcome these problems in current therapy.

The development of DDSs with the intention of improving the solubility problems presented by the most commonly used drugs in therapy has been widely worked, with satisfactory results obtained for the systems developed compared to pure drugs or those found in commercial dosage forms. The reported studies incorporate the most diverse drugs used in ARV therapy in different DDSs, with varying particle sizes and carriers to improve the efficacy of these drugs. DDSs showed excellent responses in solubility, dissolution rate, absorption, and bioavailability to overcome the problems of the current conventional HAART.

Several *in vitro* and *in vivo* studies have been carried out in order to verify the performance of the formulation and pharmacokinetic parameters in preclinical animal studies. However, little is known about the effect of these systems on humans, and it is necessary to deepen and better understand these formulations for humans. Abbate *et al.* reported an unexpected performance for cabotegravir NPs, but the authors

suggest that in humans the performance could be better, making the value of the preclinical results obtained questionable. It is important that the systems not only have superior efficacy to the existing drug, but also need to be safe, with toxicity data well evaluated and discussed.

In addition, the challenge of industrial scaling persists for most of these formulations since current research work is more focused on preparation and characterization. The large-scale production of DDSs is still problematic for industries, whether due to the lack of adequate equipment, production process yield, product increase in price or formulation stability. Factors such as temperature, humidity, mechanical and thermal stress during processing can contribute to the quality and final performance of the product [147].

Therefore, more in-depth stability studies need to be carried out, in addition to the exploration of the final dosage form in the face of different conditions to which it is subjected. Development of technologies for simple, scalable, efficient, and cost-effective production is welcome for large-scale industrial scale-up, especially for developing or underdeveloped countries where access to ARV treatment is still scarce. Technology transfer and distribution by generic companies could be encouraged at earlier stages of development to facilitate production and distribution in countries most in need [148].

CONCLUSION

In this review, we evaluate the latest innovations in ARV drug delivery using DDS as an interesting alternative for HIV treatment. Excellent results were found *in vitro* and *in vivo* for the different systems, such as high drug encapsulation, aqueous solubility and dissolution rate, reflecting the high permeation rate in cells and membranes and greater bioavailability. Despite the numerous benefits presented by DDS to optimize HIV pharmacological therapy, industrial expansion and the lack of clinical trials present challenges that still need to be overcome for these formulations to reach patients.

From the articles presented, it is clear that many DDS appear together as a strategy to improve the bioavailability and solubility of drugs. This is initially seen in cyclodextrins, where polymers can be used concomitantly with CDs to prevent recrystallization of the drug, and CDs are used to improve its solubility and protected salt formation at acidic pH that contributes to bioavailability. Solid dispersions also appear as an alternative to promote greater oral availability of antiretroviral drugs, mainly due to the low production cost.

The use of microneedles has been considered an alternative for the transdermal delivery of antiretroviral drugs. Through the use of these devices and as DDS there is the possibility of improving the solubility of the drug and promoting intradermal release, avoiding first-pass effects, improving bioavailability of the medication and management of side effects. The search for other routes of drug administration has been expanded, as explored in the article, which also includes discussion of vaginal delivery as an alternative for HIV prevention.

NPs are also being explored for their potential to enhance the efficacy and availability of ARV medications. Formulations containing drugs such as indinavir, darunavir, and lopinavir/ritonavir have yielded promising results in improving drug solubility, promoting sustained release, and increasing bioavailability. The efficacy of liposomal formulations has been demonstrated by increasing drug permeation, sustaining release, and improving the therapeutic outcomes of antiretroviral drugs such as tenofovir and efavirenz. Moreover, dendritic polymers have emerged as a promising strategy for preventing viral entry and inhibiting viral replication, thereby offering a valuable avenue for HIV prevention.

Despite notable advances in the delivery of NP-based medicines for HIV treatment, several challenges and promising opportunities remain ahead. These include the necessity for further optimization of formulations, comprehensive assessment of their safety and efficacy in human trials, and overcoming challenges related to industrial-scale production and distribution. Moreover, there is a pressing need for technology transfer and collaboration to facilitate the widespread availability of NP-based ARV therapies, particularly in resource-limited settings where access to HIV treatment remains a challenge.

AUTHORS CONTRIBUTION

It is hereby acknowledged that all authors have accepted responsibility for the manuscript's content and consented to its submission. They have meticulously reviewed all results and unanimously approved the final version of the manuscript.

LIST OF ABBREVIATIONS

AIDS	=	Acquired immunodeficiency syndrome
HIV	=	Human immunodeficiency virus
SIV	=	Simian immunodeficiency viruses
HAART	=	Highly active antiretroviral therapy
DDS	=	Drug delivery system
ARV	=	Antiretroviral
NRTI	=	Nucleotide reverse transcriptase inhibitors
NNRTI	=	Non-nucleotide reverse transcriptase inhibitors

INSTI	=	Integrase inhibitors
PrEP	=	Pre-exposure prophylaxis
PEP	=	Post-exposure prophylaxis
BCS	=	Biopharmaceutical classification system
CD	=	Cyclodextrin
CC	=	Co-crystal
NP	=	Nanoparticle
Cmax	=	Maximum concentration
SASD	=	Supercritical assisted spray drying
HP17-γ-CD	=	High-substitution-grade derived γ-CD
MAPs	=	Microneedle patches
AUC	=	Area under curve
SD	=	Solid dispersion
ASD	=	Amorphous solid dispersion
CAM	=	Co-amorphous dispersions
LLPS	=	Liquid-liquid phase separation
Tmax	=	Maximum time
ROS	=	Reactive oxygen species

CONSENT FOR PUBLICATION

Not applicable

FUNDING

This work was funded by FINEP-FADE-UFPE project 0120-21.

CONFLICT OF INTEREST

The authors declare no conflict of interest, financial or otherwise.

ACKNOWLEDGEMENTS

The authors thanks the Coordination of Improvement of Higher Education Personnel (CAPES) for the PhD fellowship.

REFERENCES

[1] Pedro, K. D.; Henderson, A. J.; Agosto, L. M. Mechanisms of HIV-1 Cell-to-Cell Transmission and the Establishment of the Latent Reservoir. *Virus Res* **2019**, *265*, 115–121. https://doi.org/10.1016/j.virusres.2019.03.014

[2] Touw, M. Update on Human Immunodeficiency Virus. *Physician Assist Clin* **2017**, *2* (2), 327–343. https://doi.org/10.1016/j.cpha.2016.12.013

[3] Shaw, G. M.; Hunter, E. HIV Transmission. *Cold Spring Harb Perspect Med* **2012**, *2* (11), a006965–a006965. https://doi.org/10.1101/cshperspect.a006965

[4] Melhuish, A.; Lewthwaite, P. Natural History of HIV and AIDS. *Medicine* **2018**, *46* (6), 356–361. https://doi.org/10.1016/j.mpmed.2018.03.010

[5] Sharp, P. M.; Hahn, B. H. Origins of HIV and the AIDS Pandemic. *Cold Spring Harb Perspect Med* **2011**, *1* (1), a006841–a006841. https://doi.org/10.1101/cshperspect.a006841

[6] Ramana, L. N.; Anand, A. R.; Sethuraman, S.; Krishnan, U. M. Targeting Strategies for Delivery of Anti-HIV Drugs. *Journal of Controlled Release* **2014**, *192*, 271–283. https://doi.org/10.1016/j.jconrel.2014.08.003

[7] World Health Organization. *HIV and AIDS*. https://www.who.int/news-room/fact-sheets/detail/hiv-aids (accessed 2023-09-18)

[8] UNAIDS. *Global HIV & AIDS statistics — Fact sheet*. https://www.unaids.org/en/resources/fact-sheet?_gl=1*1gq9cc4*_ga*NTYyNjc5NjYxLjE2OTYyODgzODQ.*_ga_T7FBEZEXNC*MTY5NjI4ODM4My4xLjEuMTY5NjI4ODYwMi40My4wLjA.&_ga=2.91300504.322923887.1696288384-562679661.1696288384 (accessed 2023-10-01)

[9] Joint United Nations Programme on HIV/AIDS (UNAIDS). *Fact Sheet 2022*. https://unaids.org.br/wp-content/uploads/2022/07/2022_07_27_Factsheet_PT.pdf (accessed 2023-05-15)

[10] Ghosn, J.; Taiwo, B.; Seedat, S.; Autran, B.; Katlama, C. HIV. *The Lancet* **2018**, *392*, 685–697. https://doi.org/10.1016/S0140-6736(18)31311-4

[11] Gandhi, R. T.; Bedimo, R.; Hoy, J. F.; Landovitz, R. J.; Smith, D. M.; Eaton, E. F.; Lehmann, C.; Springer, S. A.; Sax, P. E.; Thompson, M. A.; Benson, C. A.; Buchbinder, S. P.; Del Rio, C.; Eron, J. J.; Günthard, H. F.; Molina, J. M.; Jacobsen, D. M.; Saag, M. S. Antiretroviral Drugs for Treatment and Prevention of HIV Infection in Adults: 2022 Recommendations of the International Antiviral Society-USA Panel. *JAMA* **2023**, *329* (1), 63–84. https://doi.org/10.1001/JAMA.2022.22246

[12] Arts, E. J.; Hazuda, D. J. HIV-1 Antiretroviral Drug Therapy. *Cold Spring Harb Perspect Med* **2012**, *2* (4), a007161–a007161. https://doi.org/10.1101/cshperspect.a007161

[13] Silvestre, A. L. P.; Oshiro-Júnior, J. A.; Garcia, C.; Turco, B. O.; da Silva Leite, J. M.; de Lima Damasceno, B. P. G.; Soares, J. C. M.; Chorilli, M. Monoclonal Antibodies Carried

in Drug Delivery Nanosystems as a Strategy for Cancer Treatment. *Curr Med Chem* **2020**, *28* (2), 401–418. https://doi.org/10.2174/0929867327666200121121409

[14] Rojo, J.; Sousa-Herves, A.; Mascaraque, A. Perspectives of Carbohydrates in Drug Discovery. *Comprehensive Medicinal Chemistry III* **2017**, *1–8*, 577–610. https://doi.org/10.1016/B978-0-12-409547-2.12311-X

[15] Leite, J. M. S.; Patriota, Y. B. G.; de La Roca, M. F.; Soares-Sobrinho, J. L. New Perspectives in Drug Delivery Systems for the Treatment Of. *Curr Med Chem* **2021**, *29* (11), 1936–1958. https://doi.org/10.2174/0929867328666210629154908

[16] Vo, C. L. N.; Park, C.; Lee, B. J. Current Trends and Future Perspectives of Solid Dispersions Containing Poorly Water-Soluble Drugs. *European Journal of Pharmaceutics and Biopharmaceutics* **2013**, *85* (3 PART B), 799–813. https://doi.org/10.1016/j.ejpb.2013.09.007

[17] Hari, B. V.; Devendharan, K.; Narayanan, N. Approaches of Novel Drug Delivery Systems for Anti-HIV Agents. *International Journal of Drug Development and Research* **2013**, *5* (4), 1–9

[18] Sosnik, A.; Augustine, R. Challenges in Oral Drug Delivery of Antiretrovirals and the Innovative Strategies to Overcome Them. *Adv Drug Deliv Rev* **2015**, *103* (2016), 105–120. https://doi.org/http://dx.doi.org/10.1016/j.addr.2015.12.022

[19] Cunha, R. F.; Simões, S.; Carvalheiro, M.; Pereira, J. M. A.; Costa, Q.; Ascenso, A. Novel Antiretroviral Therapeutic Strategies for HIV. *Molecules* **2021**, *26* (17), 5305. https://doi.org/10.3390/molecules26175305

[20] Nelson, A. G.; Zhang, X.; Ganapathi, U.; Szekely, Z.; Flexner, C. W.; Owen, A.; Sinko, P. J. Drug Delivery Strategies and Systems for HIV/AIDS Pre-Exposure Prophylaxis (PrEP) and Treatment. *J Control Release* **2015**, *219*, 669. https://doi.org/10.1016/J.JCONREL.2015.08.042

[21] Limenh, L. W. Advances in the Transdermal Delivery of Antiretroviral Drugs. *SAGE Open Med* **2024**, *12*. https://doi.org/10.1177/20503121231223600

[22] Sarma, A.; Das, M. K. Nose to Brain Delivery of Antiretroviral Drugs in the Treatment of NeuroAIDS. *Molecular Biomedicine* **2020**, *1* (1), 15. https://doi.org/10.1186/s43556-020-00019-8

[23] Mehrotra, S.; Salwa; BG, P. K.; Bhaskaran, N. A.; Srinivas Reddy, J.; Kumar, L. Nose-to-Brain Delivery of Antiretroviral Drug Loaded Lipidic Nanocarriers to Purge HIV Reservoirs in CNS: A Safer Approach. *J Drug Deliv Sci Technol* **2023**, *87*, 104833. https://doi.org/10.1016/j.jddst.2023.104833

[24] Nabi, B.; Rehman, S.; Pottoo, F. H.; Baboota, S.; Ali, J. Directing the Antiretroviral Drugs to the Brain Reservoir: A Nanoformulation Approach for NeuroAIDS. *Curr Drug Metab* **2021**, *22* (4), 280–286. https://doi.org/10.2174/1389200221666200923151036

[25] Kakad, S. P.; Kshirsagar, S. J. Neuro-AIDS: Current Status and Challenges to Antiretroviral Drug Therapy (ART) for Its Treatment. *Curr Drug ther* **2020**, *15* (5), 469–481. https://doi.org/10.2174/1574885515666200604123046

[26] Mhambi, S.; Fisher, D.; Tchokonte, M. B. T.; Dube, A. Permeation Challenges of Drugs for Treatment of Neurological Tuberculosis and HIV and the Application of Magneto-Electric Nanoparticle Drug Delivery Systems. *Pharmaceutics* **2021**, *13* (9), 1479. https://doi.org/10.3390/pharmaceutics13091479

[27] Kharwade, R.; More, S.; Mahajan, N.; Agrawal, P. Functionalised Dendrimers: Potential Tool for Antiretroviral Therapy. *Curr Nanosci* **2020**, *16* (5), 708–722. https://doi.org/10.2174/1573413716666200213114836

[28] Asl, F. D.; Mousazadeh, M.; Taji, S.; Bahmani, A.; Khashayar, P.; Azimzadeh, M.; Mostafavi, E. Nano Drug-Delivery Systems for Management of AIDS: Liposomes, Dendrimers, Gold and Silver Nanoparticles. *Nanomedicine* **2023**, *18* (3), 279–302. https://doi.org/10.2217/nnm-2022-0248

[29] Nayan, M. U.; Panja, S.; Sultana, A.; Zaman, L. A.; Vora, L. K.; Sillman, B.; Gendelman, H. E.; Edagwa, B. Polymer Delivery Systems for Long-Acting Antiretroviral Drugs. *Pharmaceutics* **2024**, *16* (2), 183. https://doi.org/10.3390/pharmaceutics16020183

[30] Sarode, I. M.; Jindal, A. B. Current Status of Dolutegravir Delivery Systems for the Treatment of HIV-1 Infection. *J Drug Deliv Sci Technol* **2022**, *76*, 103802. https://doi.org/10.1016/j.jddst.2022.103802

[31] Tseng, A.; Seet, J.; Phillips, E. J. The Evolution of Three Decades of Antiretroviral Therapy: Challenges, Triumphs and the Promise of the Future. *Br J Clin Pharmacol* **2015**, *79* (2), 182–194. https://doi.org/10.1111/bcp.12403

[32] Moss, J. A. HIV/AIDS Review. *Radiol Technol* **2013**, *84* (3), 247–270

[33] Berg, A. Insights of Antiretrovirals: A New Drug Delivery Systems. *J Antivir Antiretrovir* **2020**, *0* (0), 1–1. https://doi.org/10.35248/1948-5964.21.S12.E001

[34] Eron, J. J.; Lelievre, J.-D.; Kalayjian, R.; Slim, J.; Wurapa, A. K.; Stephens, J. L.; McDonald, C.; Cua, E.; Wilkin, A.; Schmied, B.; McKellar, M.; Cox, S.; Majeed, S. R.; Jiang, S.;

Cheng, A.; Das, M.; SenGupta, D. Safety of Elvitegravir, Cobicistat, Emtricitabine, and Tenofovir Alafenamide in HIV-1-Infected Adults with End-Stage Renal Disease on Chronic Haemodialysis: An Open-Label, Single-Arm, Multicentre, Phase 3b Trial. *Lancet HIV* **2019**, *6* (1), e15–e24. https://doi.org/10.1016/S2352-3018(18)30296-0

[35] Venter, W. D. F.; Moorhouse, M.; Sokhela, S.; Fairlie, L.; Mashabane, N.; Masenya, M.; Serenata, C.; Akpomiemie, G.; Qavi, A.; Chandiwana, N.; Norris, S.; Chersich, M.; Clayden, P.; Abrams, E.; Arulappan, N.; Vos, A.; McCann, K.; Simmons, B.; Hill, A. Dolutegravir plus Two Different Prodrugs of Tenofovir to Treat HIV. *New England Journal of Medicine* **2019**, *381* (9), 803–815. https://doi.org/10.1056/NEJMoa1902824

[36] O'Cofaigh, E.; Lewthwaite, P. Natural History of HIV and AIDS. *Medicine* **2013**, *41* (8), 411–416. https://doi.org/10.1016/j.mpmed.2013.05.009

[37] Zhang, J.; Vernon, K.; Li, Q.; Benko, Z.; Amoroso, A.; Nash, M.; Zhao, R. Y. Single-Agent and Fixed-Dose Combination HIV-1 Protease Inhibitor Drugs in Fission Yeast (Schizosaccharomyces Pombe). *Pathogens 2021, Vol. 10, Page 804* **2021**, *10* (7), 804. https://doi.org/10.3390/PATHOGENS10070804

[38] Department of Health and Human Services. Panel on Antiretroviral Guidelines for Adults and Adolescents. Guidelines for the Use of Antiretroviral Agents in Adults and Adolescents with HIV. https://clinicalinfo.hiv.gov/en/guidelines/adult-and-adolescent-arv (accessed 2024-01-19)

[39] Brasil. Ministério da Saúde. Secretaria de Vigilância em Saúde. Departamento de Vigilância, P. e C. das I. S. T. do H. e das H. Virais. Protocolo Clínico e Diretrizes Terapêuticas Para Manejo Da Infecção Pelo HIV Em Crianças e Adolescentes. Secretaria de Vigilância em Saúde, Programa Nacional de DST e AIDS, Brasília: Brasília 2018, p 218

[40] Brasil. Ministério da Saúde. Secretaria de Vigilância em Saúde. Departamento de Vigilância, P. e C. das I. S. T. do H. e das H. Virais. Protocolo Clínico e Diretrizes Terapêuticas Para Manejo Da Infecção Pelo HIV Em Adultos. *Protocolo Clínico e Diretrizes Terapêuticas para o Manejo da Infecção pelo HIV em adultos*. 1st ed. Secretaria de Vigilância em Saúde, Programa Nacional de DST e AIDS, Brasília: Brasília 2017, p 416

[41] Orkin, C.; Arasteh, K.; Górgolas Hernández-Mora, M.; Pokrovsky, V.; Overton, E. T.; Girard, P.-M.; Oka, S.; Walmsley, S.; Bettacchi, C.; Brinson, C.; Philibert, P.; Lombaard, J.; St. Clair, M.; Crauwels, H.; Ford, S. L.; Patel, P.; Chounta, V.; D'Amico, R.; Vanveggel, S.; Dorey, D.; Cutrell, A.; Griffith, S.; Margolis, D. A.; Williams, P. E.; Parys, W.; Smith, K. Y.; Spreen, W. R. Long-Acting Cabotegravir and Rilpivirine after Oral Induction for HIV-1 Infection. *New England Journal of Medicine* **2020**, *382* (12), 1124–1135. https://doi.org/10.1056/NEJMoa1909512

[42] Sax, P. E.; Arribas, J. R.; Orkin, C.; Lazzarin, A.; Pozniak, A.; DeJesus, E.; Maggiolo, F.; Stellbrink, H.-J.; Yazdanpanah, Y.; Acosta, R.; Huang, H.; Hindman, J. T.; Martin, H.; Baeten, J. M.; Wohl, D. Bictegravir/Emtricitabine/Tenofovir Alafenamide as Initial Treatment for HIV-1: Five-Year Follow-up from Two Randomized Trials. *EClinicalMedicine* **2023**, *59*, 101991. https://doi.org/10.1016/j.eclinm.2023.101991

[43] Garg, A. B.; Nuttall, J.; Romano, J. The Future of HIV Microbicides: Challenges and Opportunities. *Antivir Chem Chemother* **2009**, *19* (4), 143–150. https://doi.org/10.1177/095632020901900401

[44] Buckheit, R. W.; Watson, K. M.; Morrow, K. M.; Ham, A. S. Development of Topical Microbicides to Prevent the Sexual Transmission of HIV. *Antiviral Res* **2010**, *85* (1), 142–158. https://doi.org/10.1016/j.antiviral.2009.10.013

[45] Valera, P.; Ali, Z. S.; Cunningham, D.; McLaughlin, C.; Acevedo, S. Exploring Pre-Exposure Prophylaxis (PrEP) and Post-Exposure Prophylaxis (PEP) Knowledge in Incarcerated Men. *Am J Mens Health* **2022**, *16* (4), 15579832211071. https://doi.org/10.1177/15579883221107192

[46] Ensign, L. M.; Cone, R.; Hanes, J. Oral Drug Delivery with Polymeric Nanoparticles: The Gastrointestinal Mucus Barriers. *Adv Drug Deliv Rev* **2012**, *64* (6), 557–570. https://doi.org/10.1016/j.addr.2011.12.009

[47] Davis, M. T.; Egan, D. P.; Kuhs, M.; Albadarin, A. B.; Griffin, C. S.; Collins, J. A.; Walker, G. M. Amorphous Solid Dispersions of BCS Class II Drugs: A Rational Approach to Solvent and Polymer Selection. *Chemical Engineering Research and Design* **2016**, *110*, 192–199. https://doi.org/10.1016/j.cherd.2016.04.008

[48] Choudhary, N.; Avari, J. Formulation and Evaluation of Taste Mask Pellets of Granisetron Hydrochloride as Oro Dispersible Tablet. *Brazilian Journal of Pharmaceutical Sciences* **2015**, *51* (3), 569–578. https://doi.org/10.1590/S1984-82502015000300009

[49] Jjumba, I.; Kanyesigye, M.; Ndagijimana, G.; Wattira, J.; Olong, C.; Akumu Olok, R.; Beebwa, E.; Muzoora, C. Perceived Barriers and Facilitators to Antiretroviral Therapy Adherence among Youth Aged 15-24 Years at a Regional HIV Clinic in South-Western Uganda: A Qualitative Study.

Afr Health Sci **2022**, *22* (2), 54–63. https://doi.org/10.4314/ahs.v22i2.7

[50] Sridhar, I.; Doshi, A.; Joshi, B.; Wankhede, V.; Doshi, J. Solid Dispersions: An Approach to Enhance Solubility of Poorly Water Soluble Drug. *Journal of Scientific and Innovative Research* **2013**, *2* (3), 685–694

[51] Pandi, P.; Bulusu, R.; Kommineni, N.; Khan, W.; Singh, M. Amorphous Solid Dispersions: An Update for Preparation, Characterization, Mechanism on Bioavailability, Stability, Regulatory Considerations and Marketed Products. *International Journal of Pharmaceutics*. Elsevier B.V. August 30, 2020, p 119560. https://doi.org/10.1016/j.ijpharm.2020.119560

[52] Amidon, G. L. ; Lennernäs, H.; Shah, V. P. ;; R., C. J. A Theoretical Basis for a Biopharmaceutic Drug Classification: The Correlation of in Vitro Drug Product Dissolution and in Vivo Bioavailability. *Pharm Res* **1995**, *12* (3), 413–420

[53] Golfar, Y.; Shayanfar, A. Prediction of Biopharmaceutical Drug Disposition Classification System (BDDCS) by Structural Parameters. *Journal of Pharmacy & Pharmaceutical Sciences* **2019**, *22*, 247–269. https://doi.org/10.18433/jpps30271

[54] Soares, K. C. C.; Rediguieri, C. F.; Souza, J.; Serra, C. H. R.; Abrahamsson, B.; Groot, D. W.; Kopp, S.; Langguth, P.; Polli, J. E.; Shah, V. P.; Dressman, J. Biowaiver Monographs for Immediate-Release Solid Oral Dosage Forms: Zidovudine (Azidothymidine). *J Pharm Sci* **2013**, *102* (8), 2409–2423. https://doi.org/10.1002/jps.23624

[55] Mohsin, N. U. A.; Ahmed, M.; Irfan, M. Zidovudine: Structural Modifications and Their Impact on Biological Activities and Pharmacokinectic Properties. *Journal of the Chilean Chemical Society* **2019**, *64* (3), 4523–4530. https://doi.org/10.4067/S0717-97072019000304523

[56] Metry, M.; Polli, J. E. Evaluation of Excipient Risk in BCS Class I and III Biowaivers. *AAPS J* **2022**, *24* (1), 20. https://doi.org/10.1208/s12248-021-00670-1

[57] Shajan, D. K.; Pandey, N.; Ghosh, A.; Chanduluru, H. K.; Sanphui, P. Investigating the Effect of Emtricitabine Cocrystals with Aromatic Carboxylic Acids on Solubility and Diffusion Permeability. *Cryst Growth Des* **2023**, *23* (7), 5289–5300. https://doi.org/10.1021/acs.cgd.3c00485

[58] Patil, S.; Kadam, C.; Pokharkar, V. QbD Based Approach for Optimization of Tenofovir Disoproxil Fumarate Loaded Liquid Crystal Precursor with Improved Permeability. *J Adv Res* **2017**, *8* (6), 607–616. https://doi.org/10.1016/j.jare.2017.07.005

[59] Santos, K. A. dos; Danda, L. J. de A.; Oliveira, T. C. de; Soares-Sobrinho, J. L.; Soares, M. F. de L. R. The Drug Loading Impact on Dissolution and Diffusion: A Case-Study with Amorphous Solid Dispersions of Nevirapine. *Research, Society and Development* **2022**, *11* (14), e168111436117–e168111436117. https://doi.org/10.33448/RSD-V11I14.36117

[60] Alves, L. D. S.; de La Roca Soares, M. F.; de Albuquerque, C. T.; da Silva, É. R.; Vieira, A. C. C.; Fontes, D. A. F.; Figueirêdo, C. B. M.; Soares Sobrinho, J. L.; Rolim Neto, P. J. Solid Dispersion of Efavirenz in PVP K-30 by Conventional Solvent and Kneading Methods. *Carbohydr Polym* **2014**, *104*, 166–174. https://doi.org/10.1016/j.carbpol.2014.01.027

[61] Rekdal, M.; pai, A.; BS, M. Experimental Data of Co-Crystals of Etravirine and L-Tartaric Acid. *Data Brief* **2018**, *16*, 135–140. https://doi.org/10.1016/j.dib.2017.11.019

[62] Saeed, A. M.; Schmidt, J. M.; Munasinghe, W. P.; Vallabh, B. K.; Jarvis, M. F.; Morris, J. B.; Mostafa, N. M. Comparative Bioavailability of Two Formulations of Biopharmaceutical Classification System (BCS) Class IV Drugs: A Case Study of Lopinavir/Ritonavir. *J Pharm Sci* **2021**, *110* (12), 3963–3968. https://doi.org/10.1016/j.xphs.2021.08.037

[63] Zolotov, S. A.; Demina, N. B.; Zolotova, A. S.; Shevlyagina, N. V.; Buzanov, G. A.; Retivov, V. M.; Kozhukhova, E. I.; Zakhoda, O. Y.; Dain, I. A.; Filatov, A. R.; Cheremisin, A. M. Development of Novel Darunavir Amorphous Solid Dispersions with Mesoporous Carriers. *European Journal of Pharmaceutical Sciences* **2021**, *159*, 105700. https://doi.org/10.1016/j.ejps.2021.105700

[64] Kurd, M.; Sadegh Malvajerd, S.; Rezaee, S.; Hamidi, M.; Derakhshandeh, K. Oral Delivery of Indinavir Using MPEG-PCL Nanoparticles: Preparation, Optimization, Cellular Uptake, Transport and Pharmacokinetic Evaluation. *Artif Cells Nanomed Biotechnol* **2019**, *47* (1), 2123–2133. https://doi.org/10.1080/21691401.2019.1616553

[65] Srinivas, N.; Rosen, E. P.; Gilliland Jr, W. M.; Kovarova, M.; Remling-Mulder, L.; De La Cruz, G.; White, N.; Adamson, L.; Schauer, A. P.; Sykes, C.; Luciw, P.; Garcia, J. V.; Akkina, R.; Kashuba, A. D. M. Antiretroviral Concentrations and Surrogate Measures of Efficacy in the Brain Tissue and CSF of Preclinical Species. *Xenobiotica* **2019**, *49* (10), 1192–1201. https://doi.org/10.1080/00498254.2018.1539278

[66] Krishna, R.; Rizk, M. L.; Larson, P. J.; Schulz, V.; Friedman, E.; Gupta, P.; Kesisoglou, F.; Connor, A.; McDermott, J.; Smith, R.; Evans, P. Novel Gastroretentive Controlled Release Formulations for Once-Daily Administration: Assessment of Clinical Feasibility and Formulation Concept

for Raltegravir. *Ther Innov Regul Sci* **2016**, *50* (6), 777–790. https://doi.org/10.1177/2168479016657130

[67] Chaudhary, S.; Nair, A. B.; Shah, J.; Gorain, B.; Jacob, S.; Shah, H.; Patel, V. Enhanced Solubility and Bioavailability of Dolutegravir by Solid Dispersion Method: In Vitro and In Vivo Evaluation—a Potential Approach for HIV Therapy. *AAPS PharmSciTech* **2021**, *22* (3), 127. https://doi.org/10.1208/s12249-021-01995-y

[68] Karunakaran, D.; Simpson, S. M.; Su, J. T.; Bryndza-Tfaily, E.; Hope, T. J.; Veazey, R.; Dobek, G.; Qiu, J.; Watrous, D.; Sung, S.; Chacon, J. E.; Kiser, P. F. Design and Testing of a Cabotegravir Implant for HIV Prevention. *Journal of Controlled Release* **2021**, *330*, 658–668. https://doi.org/10.1016/j.jconrel.2020.12.024

[69] Kovač, L.; Časar, Z.; Trdan Lušin, T.; Roškar, R. Development of an Analytical Method for Determination of Related Substances and Degradation Products of Cabotegravir Using Analytical Quality by Design Principles. *ACS Omega* **2022**, *7* (10), 8896–8905. https://doi.org/10.1021/acsomega.1c07260

[70] Pal, D.; Nayak, A. K. Alginates, Blends and Microspheres: Controlled Drug Delivery. In *Encyclopedia of Biomedical Polymers and Polymeric Biomaterials*; Taylor & Francis, 2015; pp 89–98. https://doi.org/10.1081/E-EBPP-120049967

[71] Tiwari, G.; Tiwari, R.; Bannerjee, S.; Bhati, L.; Pandey, S.; Pandey, P.; Sriwastawa, B. Drug Delivery Systems: An Updated Review. *Int J Pharm Investig* **2012**, *2* (1), 2–11. https://doi.org/10.4103/2230-973X.96920

[72] Nayak, A. K.; Ahmad, S. A.; Beg, S.; Ara, T. J.; Hasnain, M. S. Drug Delivery: Present, Past, and Future of Medicine. In *Applications of Nanocomposite Materials in Drug Delivery*; Elsevier, 2018; pp 255–282. https://doi.org/10.1016/B978-0-12-813741-3.00012-1

[73] Carvalho, S. G.; Araujo, V. H. S.; dos Santos, A. M.; Duarte, J. L.; Silvestre, A. L. P.; Fonseca-Santos, B.; Villanova, J. C. O.; Gremião, M. P. D.; Chorilli, M. Advances and Challenges in Nanocarriers and Nanomedicines for Veterinary Application. *Int J Pharm* **2020**, *580*, 119214. https://doi.org/10.1016/j.ijpharm.2020.119214

[74] Bompelwar, S. S.; Bakde, B. V; Raut, B. M. Enhancement of Solubility of Nevirapine by Using HPMC by Solid Dispersion Method. *ASIO Journal of Pharmaceutical & Herbal Medicines Research* **2019**, *5* (1), 55–63

[75] Shete, S.; Reddy, S. C.; Lakshman, Y. D.; Vullendula, S. K. A.; Mehta, C. H.; Nayak, U. Y.; Dengale, S. Implications of Phase Solubility/Miscibility and Drug-Rich Phase Formation on the Performance of Co-Amorphous Materials: The Case of Darunavir Co-Amorphous Materials with Ritonavir and Indomethacin as Co-Formers. *Int J Pharm* **2021**, *608*, 121119. https://doi.org/10.1016/j.ijpharm.2021.121119

[76] Dengale, S. J.; Hussen, S. S.; Krishna, B. S. M.; Musmade, P. B.; Gautham Shenoy, G.; Bhat, K. Fabrication, Solid State Characterization and Bioavailability Assessment of Stable Binary Amorphous Phases of Ritonavir with Quercetin. *Eur J Pharm Biopharm* **2015**, *89*, 329–338. https://doi.org/10.1016/J.EJPB.2014.12.025

[77] Fayed, N. D.; Arafa, M. F.; Essa, E. A.; El Maghraby, G. M. Lopinavir-Menthol Co-Crystals for Enhanced Dissolution Rate and Intestinal Absorption. *J Drug Deliv Sci Technol* **2022**, *74*, 103587. https://doi.org/10.1016/j.jddst.2022.103587

[78] Sogai, B. S.; Narayansetty, V. B.; Kolapalli, R. M. V. Comparative Single Dose Pharmacokinetics and Bioavailability Studies of Saquinavir, Ritonavir and Their Optimized Cyclodextrin Complexes after Oral Administration into Rats Using LC-MS/MS. *Indian Journal of Pharmaceutical Education and Research* **2018**, *52* (4), 587–593. https://doi.org/10.5530/ijper.52.4.68

[79] Pham, K.; Li, D.; Guo, S.; Penzak, S.; Dong, X. Development and in Vivo Evaluation of Child-Friendly Lopinavir/Ritonavir Pediatric Granules Utilizing Novel in Situ Self-Assembly Nanoparticles. *Journal of Controlled Release* **2016**, *226*, 88–97. https://doi.org/10.1016/j.jconrel.2016.02.001

[80] Abbate, M. T. A.; Ramöller, I. K.; Sabri, A. H.; Paredes, A. J.; Hutton, A. J.; McKenna, P. E.; Peng, K.; Hollett, J. A.; McCarthy, H. O.; Donnelly, R. F. Formulation of Antiretroviral Nanocrystals and Development into a Microneedle Delivery System for Potential Treatment of HIV-Associated Neurocognitive Disorder (HAND). *Int J Pharm* **2023**, *640*, 123005. https://doi.org/10.1016/j.ijpharm.2023.123005

[81] Mutalik, S. P.; Gaikwad, S. Y.; Fernandes, G.; More, A.; Kulkarni, S.; Fayaz, S. M. A.; Tupally, K.; Parekh, H. S.; Kulkarni, S.; Mukherjee, A.; Mutalik, S. Anti-CD4 Antibody and Dendrimeric Peptide Based Targeted Nano-Liposomal Dual Drug Formulation for the Treatment of HIV Infection. *Life Sci* **2023**, *334*, 122226. https://doi.org/10.1016/j.lfs.2023.122226

[82] Kenchappa, V.; Cao, R.; Venketaraman, V.; Betageri, G. V. Liposomes as Carriers for the Delivery of Efavirenz in Combination with Glutathione—An Approach to Combat Opportunistic Infections. *Applied Sciences* **2022**, *12* (3), 1468. https://doi.org/10.3390/app12031468

[83] Kannan, R. M.; Nance, E.; Kannan, S.; Tomalia, D. [91] Emerging Concepts in Dendrimer-based Nanomedicine: From Design Principles to Clinical Applications. *J Intern Med* **2014**, *276* (6), 579–617. https://doi.org/10.1111/joim.12280

[84] Sepúlveda-Crespo, D.; Gómez, R.; De La Mata, F. J.; Jiménez, J. L.; Muñoz-Fernández, M. Á. Polyanionic [92] Carbosilane Dendrimer-Conjugated Antiviral Drugs as Efficient Microbicides: Recent Trends and Developments in HIV Treatment/Therapy. *Nanomedicine* **2015**, *11* (6), 1481–1498. https://doi.org/10.1016/j.nano.2015.03.008

[85] Ivone, R.; Fernando, A.; DeBoef, B.; Meenach, S. A.; Shen, J. Development of Spray-Dried Cyclodextrin-Based Pediatric Anti-HIV Formulations. *AAPS PharmSciTech* **2021**, *22* (5), 193. https://doi.org/10.1208/s12249-021-02068-w [93]

[86] Adeoye, O.; Conceição, J.; Serra, P. A.; Bento da Silva, A.; Duarte, N.; Guedes, R. C.; Corvo, M. C.; Aguiar-Ricardo, A.; Jicsinszky, L.; Casimiro, T.; Cabral-Marques, H. Cyclodextrin Solubilization and Complexation of Antiretroviral Drug Lopinavir: In Silico Prediction; Effects of [94] Derivatization, Molar Ratio and Preparation Method. *Carbohydr Polym* **2020**, *227*, 115287. https://doi.org/10.1016/j.carbpol.2019.115287

[87] Volpe-Zanutto, F.; Vora, L. K.; Tekko, I. A.; McKenna, P. E.; Permana, A. D.; Sabri, A. H.; Anjani, Q. K.; McCarthy, H. O.; Paredes, A. J.; Donnelly, R. F. Hydrogel-Forming Microarray [95] Patches with Cyclodextrin Drug Reservoirs for Long-Acting Delivery of Poorly Soluble Cabotegravir Sodium for HIV Pre-Exposure Prophylaxis. *Journal of Controlled Release* **2022**, *348*, 771–785. https://doi.org/10.1016/j.jconrel.2022.06.028

[88] Kommavarapu, P.; Maruthapillai, A.; Palanisamy, K. Preparation and Characterization of Efavirenz [96] Nanosuspension with the Application of Enhanced Solubility and Dissolution Rate. *HIV & AIDS Review* **2016**, *15* (4), 170–176. https://doi.org/10.1016/j.hivar.2016.11.007

[89] Vieira, A. C. C.; Ferreira Fontes, D. A.; Chaves, L. L.; Alves, L. D. S.; de Freitas Neto, J. L.; de La Roca Soares, M. F.; Soares-Sobrinho, J. L.; Rolim, L. A.; Rolim-Neto, P. J. Multicomponent Systems with Cyclodextrins and Hydrophilic Polymers for the Delivery of Efavirenz [97] *Carbohydr Polym* **2015**, *130*, 133–140. https://doi.org/10.1016/j.carbpol.2015.04.050

[90] Rao, M. R. P.; Chaudhari, J.; Trotta, F.; Caldera, F. Investigation of Cyclodextrin-Based Nanosponges for Solubility and Bioavailability Enhancement of Rilpivirine. *AAPS PharmSciTech* **2018**, *19* (5), 2358–2369. [98] https://doi.org/10.1208/s12249-018-1064-6

Madan, J.; Kamate, V.; Dua, K.; Awasthi, R. Improving the Solubility of Nevirapine Using A Hydrotropy and Mixed Hydrotropy Based Solid Dispersion Approach. *Polymers in medicine* **2017**, *47* (2), 83–90. https://doi.org/10.17219/PIM/77093

Dengale, S. J.; Ranjan, O. P.; Hussen, S. S.; Krishna, B. S. M.; Musmade, P. B.; Gautham Shenoy, G.; Bhat, K. Preparation and Characterization of Co-Amorphous Ritonavir-Indomethacin Systems by Solvent Evaporation Technique: Improved Dissolution Behavior and Physical Stability without Evidence of Intermolecular Interactions. *European Journal of Pharmaceutical Sciences* **2014**, *62*, 57–64. https://doi.org/10.1016/j.ejps.2014.05.015

Chaudhari, K. R.; Savjani, J. K.; Savjani, K. T.; Dahiya, S.; Bhangale, J. O. Enhanced Solubility and Dissolution of Drug-Drug Cocrystals of Lopinavir-Ritonavir. *Indian Journal of Pharmaceutical Education and Research* **2023**, *57* (2s), s292–s300. https://doi.org/10.5530/ijper.57.2s.33

Sepúlveda-Crespo, D.; Lorente, R.; Leal, M.; Gómez, R.; De la Mata, F. J.; Jiménez, J. L.; Muñoz-Fernández, M. Á. Synergistic Activity Profile of Carbosilane Dendrimer G2-STE16 in Combination with Other Dendrimers and Antiretrovirals as Topical Anti-HIV-1 Microbicide. *Nanomedicine* **2014**, *10* (3), 609–618. https://doi.org/10.1016/j.nano.2013.10.002

Vacas-Cordoba, E.; Galan, M.; de la Mata, F. J.; Gomez, R.; Pion, M.; M Angeles Munoz-Fernandez, M. Enhanced Activity of Carbosilane Dendrimers against HIV When Combined with Reverse Transcriptase Inhibitor Drugs: Searching for More Potent Microbicides. *Int J Nanomedicine* **2014**, 3591. https://doi.org/10.2147/IJN.S62673

Sepúlveda-Crespo, D.; Sánchez-Rodríguez, J.; Serramía, M. J.; Gómez, R.; De La Mata, F. J.; Jiménez, J. L.; Muñoz-Fernández, M. Á. Triple Combination of Carbosilane Dendrimers, Tenofovir and Maraviroc as Potential Microbicide to Prevent HIV-1 Sexual Transmission. *Nanomedicine* **2015**, *10* (6), 899–914. https://doi.org/10.2217/nnm.14.79

Gajbhiye, V.; Ganesh, N.; Barve, J.; Jain, N. K. Synthesis, Characterization and Targeting Potential of Zidovudine Loaded Sialic Acid Conjugated-Mannosylated Poly(Propyleneimine) Dendrimers. *European Journal of Pharmaceutical Sciences* **2013**, *48* (4–5), 668–679. https://doi.org/10.1016/j.ejps.2012.12.027

Briz, V.; Sepúlveda-Crespo, D.; Diniz, A. R.; Borrego, P.; Rodes, B.; de la Mata, F. J.; Gómez, R.; Taveira, N.; Muñoz-Fernández, M. Á. Development of Water-Soluble Polyanionic Carbosilane Dendrimers as Novel and Highly Potent Topical

Anti-HIV-2 Microbicides. *Nanoscale* **2015**, *7* (35), 14669–14683. https://doi.org/10.1039/C5NR03644E

[99] Pyreddy, S.; Kumar, P.; Kumar, P. Polyethylene Glycolated PAMAM Dendrimers-Efavirenz Conjugates. *Int J Pharm Investig* **2014**, *4* (1), 15. https://doi.org/10.4103/2230-973X.127735

[100] Zolotov, S. A.; Demina, N. B.; Dain, I. A.; Zolotova, A. S.; Buzanov, G. A.; Retivov, V. M.; Ponomaryov, Y. S. Comparative Study of Methods for the Pharmaceutical Preparation and Effectiveness of Darunavir Ethanolate Compositions with Mesoporous Carriers and Polymer Solid Dispersions. *J Pharm Innov* **2023**, *18* (2), 629–640. https://doi.org/10.1007/s12247-022-09667-5

[101] Mamatha, T.; Naseha; Anitha, N.; Qureshi, H. K. Development of Nevirapine Tablets by Direct Compression Method Using Solid Dispersion Technique. *Journal of Pharmaceutical Research* **2017**, *16* (1), 72. https://doi.org/10.18579/jpcrkc/2017/16/1/112482

[102] Monschke, M.; Wagner, K. G. Amorphous Solid Dispersions of Weak Bases with PH-Dependent Soluble Polymers to Overcome Limited Bioavailability Due to Gastric PH Variability – An in-Vitro Approach. *Int J Pharm* **2019**, *564*, 162–170. https://doi.org/10.1016/j.ijpharm.2019.04.034

[103] Lakshman, D.; Chegireddy, M.; Hanegave, G. K.; Sree, K. N.; Kumar, N.; Lewis, S. A.; Dengale, S. J. Investigation of Drug-Polymer Miscibility, Biorelevant Dissolution, and Bioavailability Improvement of Dolutegravir-Polyvinyl Caprolactam-Polyvinyl Acetate-Polyethylene Glycol Graft Copolymer Solid Dispersions. *European Journal of Pharmaceutical Sciences* **2020**, *142*, 105–137. https://doi.org/10.1016/j.ejps.2019.105137

[104] Alhalaweh, A.; Bergström, C. A. S.; Taylor, L. S. Compromised in Vitro Dissolution and Membrane Transport of Multidrug Amorphous Formulations. *Journal of Controlled Release* **2016**, *229*, 172–182. https://doi.org/10.1016/j.jconrel.2016.03.028

[105] Yarlagadda, D. L.; Nayak, A. M.; Brahmam, B.; Bhat, K. Exploring the Solubility and Bioavailability of Sodium Salt and Its Free Acid Solid Dispersions of Dolutegravir. *Adv Pharmacol Pharm Sci* **2023**, *2023*, 1–10. https://doi.org/10.1155/2023/7198674

[106] Faria, M. J.; Machado, R.; Ribeiro, A.; Gonçalves, H.; Real Oliveira, M. E. C. D.; Viseu, T.; das Neves, J.; Lúcio, M. Rational Development of Liposomal Hydrogels: A Strategy for Topical Vaginal Antiretroviral Drug Delivery in the Context of HIV Prevention. *Pharmaceutics* **2019**, *11* (9), 485. https://doi.org/10.3390/pharmaceutics11090485

[107] Okafor, N. I.; Nkanga, C. I.; Walker, R. B.; Noundou, X. S.; Krause, R. W. M. Encapsulation and Physicochemical Evaluation of Efavirenz in Liposomes. *J Pharm Investig* **2020**, *50* (2), 201–208. https://doi.org/10.1007/s40005-019-00458-8

[108] Bazzo, G. C.; Mostafa, D.; França, M. T.; Pezzini, B. R.; Stulzer, H. K. How Tenofovir Disoproxil Fumarate Can Impact on Solubility and Dissolution Rate of Efavirenz? *Int J Pharm* **2019**, *570*, 118597. https://doi.org/10.1016/j.ijpharm.2019.118597

[109] Kotta, S.; Khan, A. W.; Ansari, S. H.; Sharma, R. K.; Ali, J. Anti HIV Nanoemulsion Formulation: Optimization and in Vitro–in Vivo Evaluation. *Int J Pharm* **2014**, *462* (1–2), 129–134. https://doi.org/10.1016/j.ijpharm.2013.12.038

[110] Senapati, P. C.; Sahoo, S. K.; Sahu, A. N. Mixed Surfactant Based (SNEDDS) Self-Nanoemulsifying Drug Delivery System Presenting Efavirenz for Enhancement of Oral Bioavailability. *Biomedicine & Pharmacotherapy* **2016**, *80*, 42–51. https://doi.org/10.1016/j.biopha.2016.02.039

[111] Inugala, S.; Eedara, B. B.; Sunkavalli, S.; Dhurke, R.; Kandadi, P.; Jukanti, R.; Bandari, S. Solid Self-Nanoemulsifying Drug Delivery System (S-SNEDDS) of Darunavir for Improved Dissolution and Oral Bioavailability: In Vitro and in Vivo Evaluation. *European Journal of Pharmaceutical Sciences* **2015**, *74*, 1–10. https://doi.org/10.1016/j.ejps.2015.03.024

[112] Desai, J.; Thakkar, H. Enhanced Oral Bioavailability and Brain Uptake of Darunavir Using Lipid Nanoemulsion Formulation. *Colloids Surf B Biointerfaces* **2019**, *175*, 143–149. https://doi.org/10.1016/j.colsurfb.2018.11.057

[113] Prabhakar, K.; Afzal, S. M.; Surender, G.; Kishan, V. Tween 80 Containing Lipid Nanoemulsions for Delivery of Indinavir to Brain. *Acta Pharm Sin B* **2013**, *3* (5), 345–353. https://doi.org/10.1016/j.apsb.2013.08.001

[114] Garg, B.; Beg, S.; Kumar, R.; Katare, O. P.; Singh, B. Nanostructured Lipidic Carriers of Lopinavir for Effective Management of HIV-Associated Neurocognitive Disorder. *J Drug Deliv Sci Technol* **2019**, *53*, 101220. https://doi.org/10.1016/j.jddst.2019.101220

[115] Nguyen, D. N.; Clasen, C.; Van den Mooter, G. Encapsulating Darunavir Nanocrystals within Eudragit L100 Using Coaxial Electrospraying. *European Journal of Pharmaceutics and Biopharmaceutics* **2017**, *113*, 50–59. https://doi.org/10.1016/j.ejpb.2016.12.002

[116] Karakucuk, A.; Celebi, N.; Teksin, Z. S. Preparation of Ritonavir Nanosuspensions by Microfluidization Using Polymeric Stabilizers: I. A Design of Experiment Approach.

European Journal of Pharmaceutical Sciences **2016**, *95*, 111–121. https://doi.org/10.1016/j.ejps.2016.05.010

[117] Elkateb, H.; Cauldbeck, H.; Niezabitowska, E.; Hogarth, C.; Arnold, K.; Rannard, S.; McDonald, T. O. High Drug Loading Solid Lipid Nanoparticles, Nanostructured Lipid Carriers and Nanoemulsions for the Dual Drug Delivery of the HIV Drugs Darunavir and Ritonavir. *JCIS Open* **2023**, *11*, 100087. https://doi.org/10.1016/j.jciso.2023.100087

[118] Rojekar, S.; Pai, R.; Abadi, L. F.; Mahajan, K.; Prajapati, M. K.; Kulkarni, S.; Vavia, P. Dual Loaded Nanostructured Lipid Carrier of Nano-Selenium and Etravirine as a Potential Anti-HIV Therapy. *Int J Pharm* **2021**, *607*, 120986. https://doi.org/10.1016/j.ijpharm.2021.120986

[119] Wüpper, S.; Lüersen, K.; Rimbach, G. Cyclodextrins, Natural Compounds, and Plant Bioactives—A Nutritional Perspective. *Biomolecules* **2021**, *11* (3), 401. https://doi.org/10.3390/biom11030401

[120] Braga, S. S. Cyclodextrins: Emerging Medicines of the New Millennium. *Biomolecules* **2019**, *9* (12), 801. https://doi.org/10.3390/biom9120801

[121] Fenyvesi, É.; Vikmon, M.; Szente, L. Cyclodextrins in Food Technology and Human Nutrition: Benefits and Limitations. *Crit Rev Food Sci Nutr* **2016**, *56* (12), 1981–2004. https://doi.org/10.1080/10408398.2013.809513

[122] Haimhoffer, Á.; Rusznyák, Á.; Réti-Nagy, K.; Vasvári, G.; Váradi, J.; Vecsernyés, M.; Bácskay, I.; Fehér, P.; Ujhelyi, Z.; Fenyvesi, F. Cyclodextrins in Drug Delivery Systems and Their Effects on Biological Barriers. *Sci Pharm* **2019**, *87* (4), 33. https://doi.org/10.3390/scipharm87040033

[123] Jambhekar, S. S.; Breen, P. Cyclodextrins in Pharmaceutical Formulations I: Structure and Physicochemical Properties, Formation of Complexes, and Types of Complex. *Drug Discov Today* **2016**, *21* (2), 356–362. https://doi.org/10.1016/j.drudis.2015.11.017

[124] Liu, Z.; Ye, L.; Xi, J.; Wang, J.; Feng, Z. Cyclodextrin Polymers: Structure, Synthesis, and Use as Drug Carriers. *Prog Polym Sci* **2021**, *118*, 101408. https://doi.org/10.1016/j.progpolymsci.2021.101408

[125] Migdadi, E. M.; Courtenay, A. J.; Tekko, I. A.; McCrudden, M. T. C.; Kearney, M.-C.; McAlister, E.; McCarthy, H. O.; Donnelly, R. F. Hydrogel-Forming Microneedles Enhance Transdermal Delivery of Metformin Hydrochloride. *Journal of Controlled Release* **2018**, *285*, 142–151. https://doi.org/10.1016/j.jconrel.2018.07.009

[126] Vasconcelos, T.; Marques, S.; das Neves, J.; Sarmento, B. Amorphous Solid Dispersions: Rational Selection of a Manufacturing Process. *Adv Drug Deliv Rev* **2016**, *100*, 85–101. https://doi.org/10.1016/j.addr.2016.01.012

[127] Sandhu, H.; Shah, N.; Chokshi, H.; Malick, A. W. Overview of Amorphous Solid Dispersion Technologies. In *Amorphous Solid Dispersions*; Shah, N., Sandhu, H., Choi, D., Chokshi, H., Malick, A., Eds.; Springer: New York, 2014; pp 91–122. https://doi.org/10.1007/978-1-4939-1598-9_3

[128] Karagianni, A.; Kachrimanis, K.; Nikolakakis, I. Co-Amorphous Solid Dispersions for Solubility and Absorption Improvement of Drugs: Composition, Preparation, Characterization and Formulations for Oral Delivery. *Pharmaceutics* **2018**, *10* (98), 1–26. https://doi.org/10.3390/pharmaceutics10030098

[129] Figueirêdo, C. B. M.; Nadvorny, D.; de Medeiros Vieira, A. C. Q.; Soares Sobrinho, J. L.; Rolim Neto, P. J.; Lee, P. I.; de La Roca Soares, M. F. Enhancement of Dissolution Rate through Eutectic Mixture and Solid Solution of Posaconazole and Benznidazole. *Int J Pharm* **2017**, *525* (1), 32–42. https://doi.org/10.1016/j.ijpharm.2017.04.021

[130] Danda, L. J. de A.; Batista, L. de M.; Melo, V. C. S.; Soares Sobrinho, J. L.; Soares, M. F. de L. R. Combining Amorphous Solid Dispersions for Improved Kinetic Solubility of Posaconazole Simultaneously Released from Soluble PVP/VA64 and an Insoluble Ammonio Methacrylate Copolymer. *European Journal of Pharmaceutical Sciences* **2019**, *133*, 79–85. https://doi.org/10.1016/J.EJPS.2019.03.012

[131] Dengale, S. J.; Grohganz, H.; Rades, T.; Löbmann, K. Recent Advances in Co-Amorphous Drug Formulations. *Adv Drug Deliv Rev* **2016**, *100*, 116–125. https://doi.org/10.1016/J.ADDR.2015.12.009

[132] Pinal, H. S.; Sudha, B. S. Co-Amorphous Dispersions of Amlodipine and Atorvastatin: Preparation, Characterization, Stability Evaluation and Formulation. *World Journal of Pharmaceutical and Medical Research* **2020**, *6* (6), 207–220

[133] Jensen, K. T.; Larsen, F. H.; Löbmann, K.; Rades, T.; Grohganz, H. Influence of Variation in Molar Ratio on Co-Amorphous Drug-Amino Acid Systems. *Eur J Pharm Biopharm* **2016**, *107*, 32–39. https://doi.org/10.1016/J.EJPB.2016.06.020

[134] Zhang, H.; Li, M.; Li, J.; Agrawal, A.; Hui, H.-W.; Liu, D. Superiority of Mesoporous Silica-Based Amorphous Formulations over Spray-Dried Solid Dispersions. *Pharmaceutics* **2022**, *14* (2), 428. https://doi.org/10.3390/pharmaceutics14020428

[135] Shukla, A.; Dumpa, N. R.; Thakkar, R.; Shettar, A.; Ashour, E.; Bandari, S.; Repka, M. A. Influence of Poloxamer on the

Dissolution and Stability of Hot-Melt Extrusion–Based Amorphous Solid Dispersions Using Design of Experiments. *AAPS PharmSciTech* **2023**, *24* (5), 107. https://doi.org/10.1208/s12249-023-02562-3

[136] Wu, W.; Wang, Y.; Löbmann, K.; Grohganz, H.; Rades, T. Transformations between Co-Amorphous and Co-Crystal Systems and Their Influence on the Formation and Physical Stability of Co-Amorphous Systems. *Mol Pharm* **2019**, *16* (3), 1294–1304. https://doi.org/10.1021/acs.molpharmaceut.8b01229

[137] Löbmann, K.; Laitinen, R.; Grohganz, H.; Strachan, C.; Rades, T.; Gordon, K. C. A Theoretical and Spectroscopic Study of Co-Amorphous Naproxen and Indomethacin. *Int J Pharm* **2013**, *453* (1), 80–87. https://doi.org/10.1016/j.ijpharm.2012.05.016

[138] Khan, I.; Saeed, K.; Khan, I. Nanoparticles: Properties, Applications and Toxicities. *Arabian Journal of Chemistry* **2019**, *12* (7), 908–931. https://doi.org/10.1016/j.arabjc.2017.05.011

[139] Afzal, O.; Altamimi, A. S. A.; Nadeem, M. S.; Alzarea, S. I.; Almalki, W. H.; Tariq, A.; Mubeen, B.; Murtaza, B. N.; Iftikhar, S.; Riaz, N.; Kazmi, I. Nanoparticles in Drug Delivery: From History to Therapeutic Applications. *Nanomaterials* **2022**, *12* (24), 4494. https://doi.org/10.3390/nano12244494

[140] Peer, D.; Karp, J. M.; Hong, S.; Farokhzad, O. C.; Margalit, R.; Langer, R. Nanocarriers as an Emerging Platform for Cancer Therapy. In *Nano-Enabled Medical Applications*; Jenny Stanford Publishing, 2020; pp 61–91. https://doi.org/10.1201/9780429399039-2

[141] Patra, J. K.; Das, G.; Fraceto, L. F.; Campos, E. V. R.; Rodriguez-Torres, M. del P.; Acosta-Torres, L. S.; Diaz-Torres, L. A.; Grillo, R.; Swamy, M. K.; Sharma, S.; Habtemariam, S.; Shin, H.-S. Nano Based Drug Delivery Systems: Recent Developments and Future Prospects. *J Nanobiotechnology* **2018**, *16* (1), 71. https://doi.org/10.1186/s12951-018-0392-8

[142] Nsairat, H.; Khater, D.; Sayed, U.; Odeh, F.; Al Bawab, A.; Alshaer, W. Liposomes: Structure, Composition, Types, and Clinical Applications. *Heliyon* **2022**, *8* (5), e09394. https://doi.org/10.1016/j.heliyon.2022.e09394

[143] Jha, S.; K. Sharma, P.; Malviya, R. Liposomal Drug Delivery System for Cancer Therapy: Advancement and Patents. *Recent Pat Drug Deliv Formul* **2016**, *10* (3), 177–183. https://doi.org/10.2174/1872211310666161004155757

[144] Sun, T.; Zhang, Y. S.; Pang, B.; Hyun, D. C.; Yang, M.; Xia, Y. Engineered Nanoparticles for Drug Delivery in Cancer Therapy. *Angewandte Chemie International Edition* **2014**, *53* (46), 12320–12364. https://doi.org/10.1002/anie.201403036

[145] Wang, J.; Li, B.; Qiu, L.; Qiao, X.; Yang, H. Dendrimer-Based Drug Delivery Systems: History, Challenges, and Latest Developments. *J Biol Eng* **2022**, *16* (1), 18. https://doi.org/10.1186/s13036-022-00298-5

[146] Patel, M. R.; Patel, R. B.; Thakore, S. D. Nanoemulsion in Drug Delivery. In *Applications of Nanocomposite Materials in Drug Delivery*; Elsevier, 2018; pp 667–700. https://doi.org/10.1016/B978-0-12-813741-3.00030-3

[147] Chavan, R. B.; Thipparaboina, R.; Kumar, D.; Shastri, N. R. Co Amorphous Systems: A Product Development Perspective. *International Journal of Pharmaceutics*. Elsevier B.V. December 30, 2016, pp 403–415. https://doi.org/10.1016/j.ijpharm.2016.10.043

[148] Cobb, D. A.; Smith, N. A.; Edagwa, B. J.; McMillan, J. E. M. Long-Acting Approaches for Delivery of Antiretroviral Drugs for Prevention and Treatment of HIV: A Review of Recent Research. *Expert Opinion Drug Delivery* **2020**, 1227–1238. https://doi.org/10.1080/17425247.2020.1783233

APÊNDICE B – COMBINED USE OF COMPUTATIONAL AND THERMAL TECHNIQUES TO OBTAIN NEVIRAPINE CO-AMORPHOUS

Kayque Almeida dos Santos[1], Luíse Lopes Chaves[1,2], Daniela Nadvorny[2], Mônica Felts de La Roca Soares[1,2], José Lamartine Soares Sobrinho[1*]

[1] Quality Control Core of Medicines and Correlates – NCQMC, Department of Pharmaceutical Sciences, Federal University of Pernambuco, Recife, PE, Brazil.
[2] Postgraduate Program in Pharmaceutical Sciences, Pharmaceutical Sciences Institute, Federal University of Alagoas, Maceió, Alagoas, Brazil.

Abstract

This study aimed to assess the formation of nevirapine (NVP) co-amorphs systems (CAM) with different co-formers (lamivudine - 3TC, citric acid - CAc, and urea) through combined screening techniques as computational and thermal studies, solubility studies; in addition to develop and characterize suitable NVP-CAM. NVP-CAM were obtained using the quench-cooling method, and characterized by differential scanning calorimetry (DSC), X-ray diffractometry (XRD), **FOURIER** Transform Infrared Spectroscopy (FTIR), and polarized light microscopy (PLM), in addition to in vitro dissolution in pH 6.8. The screening results indicated intermolecular interactions occurring between NVP and 3TC; NVP and CAc, where shifts in the melting temperature of NVP were verified. The presence of CAc impacted the NVP equilibrium solubility, due to hydrogen bonds. DSC thermograms evidenced the reduction and shifting of the endothermic peaks of NVP in the presence of its co-formers, suggesting partial miscibility of the compounds. Amorphization was proven by XRD and PLM assays. *In vitro* dissolution study exhibited a significant increase in solubility and dissolution efficiency of NVP-CAM compared to free NVP. Combined use of screening studies was useful for the development of stable and amorphous NVP-CAM, with increased NVP solubility, making CAM promising systems for combined antiretroviral therapy.

Keywords: Solubility; Biopharmaceutical Classification System (BCS); Coamorphous; HIV.

INTRODUCTION

HIV infection still represents a public health problem, having caused more than 40 million deaths around the world to date, with continuous transmission in every country in the world [1]. Although there is no cure for the infection, the use of a combination therapy comprising three or more anti-HIV drugs, called highly active antiretroviral therapy (HAART), was a major advance in controlling HIV infection and preventing the progression of the disease. On the other hand, the daily need for multiple tablets in addition to the potential for significant side effects still constitutes a therapeutic challenge. Additionally, most of the more than 25 FDA-approved anti-HIV drugs

administered orally have poor water solubility, limiting the rate and extent of drug absorption [2].

Among the drugs used in HAART, nevirapine (NVP) is one of the drugs used in pediatric therapeutic regimens, specifically for neonates and infants, to prevent mother-to-child vertical transmission, in association with other anti-HIV drugs, with zidovudine and lamivudine, which chemical name is 2',3'-dideoxy-3'-Thiacytidine (3TC) [3]. Despite its notable importance in HAART, NVP is classified as class II according to the biopharmaceutical classification system (BCS), directly impacting the absorption of the drug, since its molecules need to be dissolved in the fluids of the gastrointestinal tract, which are aqueous solutions [4,5].

Therefore, class II drugs have slow absorption that leads to gastrointestinal mucosal toxicity and inadequate and variable bioavailability, which, to be mitigated, requires higher doses to obtain therapeutic benefits that can lead to adverse effects to the patient and negatively affect patient adherence to treatment [6,7]. As a result, the improvement in drug solubility is focus of continued efforts in the bio/pharmaceutical drug development sector [3]. Therefore, several technologies have been applied with the aim of increasing the solubility of drugs as solid dispersions [3,8], nanoparticles [9], nanosuspensions [10], and self-emulsifying drug delivery systems [11,12], besides the use of chemicals as surfactants [13], cyclodextrins [14].

In this context, supersaturated amorphous systems have proven to be an excellent strategy to improve the absorption of drugs with low aqueous solubility as supersaturation drives rapid and sustained absorption in the gastrointestinal tract after dissolution [15]. This solubility improvement may result in enhanced bioavailability, a reduction in the required dosage, and a potential decrease in adverse effects, thereby increasing the overall efficacy and patient compliance in clinical settings. However, materials in the amorphous form have excess energies, like free Gibbs energy, enthalpy, and entropy, promoting an increase in aqueous solubility and dissolution rates [16,17]. Nevertheless, the elevated energy state results in recrystallization, which converts the amorphous material to its crystalline counterpart. This process entails the loss of the solubility advantage associated with the amorphous form [18].

The use of polymeric carriers as an additional component has been used to stabilize the amorphous molecule in a drug delivery system named amorphous solid dispersions, avoiding drug recrystallization and promoting its supersaturation above their equilibrium solubility when in solution in the gastrointestinal tract, elevating [19]the

other hand, the large quantity of polymers required to maintain supersaturation, associated with the high hygroscopicity of most polymers used for this purpose, makes the use of these systems limited, especially in pharmaceutical forms of drugs with high dosages [20].

Alternatively, the application of small molecules has emerged as an alternative to polymers, forming a homogeneous amorphous phase with the drug through intermolecular interactions, creating a new drug delivery system known as co-amorphous (CAM) [21–23]. This approach has some potential advantages over ASD and simple amorphous materials as the drug load can be increased from 20–30 wt % to approximately 50 wt % or even higher in many cases, increasing the stability of CAM systems compared to the amorphous solids while retaining the dissolution advantage of an amorphous form [22].

The low-molecular weight coformers may be other drug substances or low molecular weight excipients such as amino acids, organic acids, and other small molecules, such as urea (URE) and citric acid (CAc). The coformer physically stabilizes the amorphous form of the drug either by interacting with the drug on a molecular level (e.g., by salt formation, hydrogen bonding, and pi–pi interactions) or simply by molecular mixing [24]. The miscibility of the drug and coformer is one of the main issues for the successful formation of a CAM, and this parameter can be determined by experimental, theoretical and/or computational approaches [22]. The use of a second drug as a coformer presents additional advantages when compared to other small molecules as they can serve as platforms to achieve potential combined therapies, being able to increase efficacy, reducing toxicity and side effects to a large extent, in addition to presenting economic benefits [25,26]. In this context, this study aimed develop CAM systems to increase the aqueous solubility of NVP, performing a screening of possible **coformers** molecules among other drug and excipients.

MATERIAL AND METHODS

Material

NVP was purchased from Farmanguinhos (Rio de Janeiro, Brazil). 3TC was donated by the Pharmaceutical Laboratory of Pernambuco (LAFEPE). CAc and URE were purchased from Neon®. Ultrapure water was obtained using the MilliQ® system (Milipore, Bedford, USA). All other reagents and solvents were of analytical grade or liquid chromatography grade and were purchased and used as soon as received.

Screening of CAM formation

Screening of Coformers

The selection of suitable coformers to stabilize the amorphous form of a drug tends to be conducted on a case-by-case basis. Therefore, the selection of the coformers was based on their chemical information, mainly on the number of H^+ donors and acceptors, since the presence of donor and acceptor groups can generate hydrogen interactions between the molecules [27]. The melting point was verified due to the use of temperature for the development of CAMs. Compounds chemical information has been given in the Supplementary File 1.

Computational Studies

The Software *Gaussview* **(Gaussian, Inc.)** was used to construct the molecular structures of NVP, 3TC, CAc, urea, and hydrogen complexes [28]. The obtained structures were used to generate electrostatic potential maps, which illustrate the three-dimensional charge distributions of the molecules on their surfaces, where red represents the most electronegative region and blue highlights the most electropositive, enabling interpretations regarding the possibilities of formation of sites of interaction between the drug and coformer. Calculations were performed using the Gaussian 09 computational package to perform geometry and harmonic frequency optimization through the HF/3-21G calculation level [29]. Through calculations, the values of the intermolecular hydrogen bond energy were found (the more negative the energy, the more stable the hydrogen interaction).

Thermal Analysis DSC

A DSC equipment (8000 model PerkinElmer; PyrisTM Player software) was used to verify the miscibility between the components and the tendency to generate amorphous systems using controlled heating and cooling rates, and characterizing the product obtained as reported by D'Angelo et al. (2018). Briefly, 3 mg (± 0.5 mg) of crystalline NVP and its physical mixtures samples with the coformers in 1:1 molar ratio were added into a hermetically sealed aluminum pan. The heating and cooling program is described in Table I. Initially, the samples were equilibrated at 0 °C and heated to a temperature that was above the lowest melting point of the component present in each sample, at a heating rate of 20 °C/min, whose balance was maintained for 2 minutes.

They were then cooled to 0 °C at a cooling rate of 20 °C/min and reheated to 300 °C at 10 °C/min, since NVP degrades after this temperature [30]. Indium metal standard with purity of 99.9% was used to calibrate the temperature scale and enthalpy response.

Determination of equilibrium solubility

The crystalline solubility of NVP was determined by the shake flask method in phosphate buffer pH 6.8 methods [31,32]. Erlenmeyer flasks with 10 ml of buffer were saturated with an excess amount of crystalline NVP in the absence and presence of each coformer and maintained at 37 °C and shaken at 150 rpm in an orbital incubator (Ethik Technology, São Paulo, BR) for 3 days with the intention of verifying the influence of coformers on the equilibrium solubility of NVP. The collected samples were centrifuged at 14000 rpm for 5 minutes, the supernatant was removed and diluted for quantification by liquid chromatography (Shimadzu®) according to the methodology described in the section **Analytical Chromatographic conditions**.

Obtention of physical mixtures and CAM

The CAM with NVP were obtained according to the methodology proposed by Skotnicki et al. (2021). Samples of NVP and coformers were carefully weighed in a 1:1 molar ratio, and ground with a mortar and pestle to promote intimate contact and obtain physical mixtures (PM). The CAM were obtained by melting their respective PMs in a steel container on a heating plate at 260 °C. After the phase change, the container was quickly taken to an ice bath for immediate cooling. The resulting powder was crushed, standardized to a size of 150 µm, and stored in a desiccator with silica.

Solid state characterization

Fourier Transform Infrared Spectroscopy (FTIR)

FTIR spectra of the pure samples, PM and CAMs were obtained on a PerkinElmer® equipment (model 400) with a total reflection device attenuated with zinc selenide crystal. The spectra were obtained in transmittance mode by averaging 16 scans per sample, with a variation in the wavenumber region 4000 to 650 cm^{-1}.

Differential Scanning Calorimetry (DSC)

The DSC curves of the pure compounds, PM and CAM were obtained using a Shimadzu® DSC equipment, model DSC-50, connected to the Shimadzu® TA-60WS software with a nitrogen atmosphere (50 ml/min) in the temperature range of 25–300 °C at a rate of 10 °C/min. Sample amounts of 3-4 mg were placed in hermetically sealed aluminum pans. Indium standard with purity of 99.9% was used to calibrate the temperature scale.

*X-Ray **Diffractometry** (XRD)*

X-ray **diffractometry** analyses were carried out using a Shimadzu diffractometer, X-ray - 7000, using X-rays generated by a Cu (Kα) anode, operated at 40 kV voltage, 30 mA current and Ni filter. An angular variation (2θ) of 3- 60° was used, with a continuous scanning speed of 2°/min. For the quantification of the crystalline content in the PMs and CAMs, the integrated areas of the NVP diffraction peaks and **coformers** in the analyzed samples were calculated by curve fitting using software (Origin 2018, OriginLab Co, Northampton, MA, EUA).

Polarized Light Microscopy (PLM)

Microscopic analyzes were performed on a Leica DM750M polarized light microscope, coupled with a digital camera (Leica ICC50W) and processed in the LAS EZ software. Lesser amounts of the powdered samples were placed on semi-permanent glass slides and analyzed using 200x magnification (Olympus Corporation, Tokyo, Japan).

Analytical Chromatographic conditions

Quantification of NVP was carried out in an HPLC equipment composed of Shimadzu's 10AVP series system, equipped with an LC-10AVP quaternary pump, an SPP-M10AVP ultraviolet detector according to an adapted method of Vieira-Sellaï et al. (2022) and Anbazhagan et al. (2005). Data acquisition was performed using LC Solutions software (version 1.25). Chromatographic separation occurred on a C8 Shim-Pack column (150 x 4.6 mm; 5 µm), at a temperature of 25 °C and injection volume of 10 µm. Separation was achieved in low pressure gradient mode using 25mM ammonium acetate buffer pH 3.9 as mobile phase A, and methanol as mobile phase B. The gradient profile (%v/v) consisted of a linear increase in phase B from 25% to 75% within 7 minutes while A decreased linearly from 75% to 25% at the same time. The phase proportion inverted between 7 and 8 minutes and remained isocratic until the end of the analysis, in 15 minutes. The calibration curve demonstrated good

linearity (R>0.99) in the relevant concentration range and a preliminary analysis performed showed that 3TC, CAc and URE do not interfere with the retention time of NVP (10.5 min).

In Vitro dissolution test

The dissolution test was evaluated in sink condition in a Vankel VK-7040 Dissolutor according to the methodology proposed by Santos et al. (2022). Samples of pure NVP (20 mg) and the equivalent in drug of PM and CAM were weighed and placed in 250 mL in phosphate buffer pH 6.8 at 37 ± 0.5 °C stirred by the paddle apparatus at 75 rpm. Samples were collected at predetermined times (5, 10, 15, 20, 30, 45, 60, 90, 120, 180, 240, 300, and 360 min), centrifuged and the supernatant was quantified by HPLC, using the method described before. The dissolution profiles of all samples were evaluated for dissolution efficiency (DE%) at 120 min and 360 min (DE% 120 and 360) and similarity factor (F2) using the DD SolverTM software [36,37].

Statistical Analysis

One-way analysis of variance (ANOVA) and Tukey's multiple comparison tests were performed to verify the statistical significance ($p < 0.05$, 95% confidence interval) of the comparisons between the pure NVP, PMs and CAMs.

RESULTS

Screening of CAM formation

Computational studies

NVP map evidenced an electronegative region with high density in its carbonyl (-C=O) of the central aromatic ring, as well as an electropositive region referring to the amine (Fig. 1), while 3TC has a carbonyl on the aromatic and hydroxyl ring, forming two complexes together (Fig. 2a and 2b). The energy resulting from the formation of hydrogen bonds for complexes NVP-3TC A and B were -8.96 and -14.42 kcal/mol, respectively. The hydroxyl regions of CAc were characterized by electropositive bands located throughout all molecular structure (Fig. 2c). These regions can interact with NVP, forming two complex structures from the simultaneous interaction of its carbonyls and hydroxyls from the central part or molecular end, with the carbonyl and amino group of NVP (Fig. 2c and 2d), which have remarkably close hydrogen bond energies,

-23.74 and -22.83 kcal/mol for structures C and D respectively, resulting in greater stability to the formed system.

A theoretical infrared spectrophotometric analysis was performed (Fig. 3) showing changes in the vibrations of the groups responsible for hydrogen interactions in the molecules of the complexed compounds. NVP has a stretch band of its carbonyl at 1880 cm^{-1} that was shifted to 1840 cm^{-1} and 1854 cm^{-1} in the 3TC complexes 1 and 2, which also showed the emergence of new bands at 3703 cm^{-1} and 3559 cm^{-1} respectively, which may indicate the formation of hydrogen complexes through the -NH an -OH groups present in the two compounds. Furthermore, interactions between -OH and –NH bonds involved in the formation of the CAc complexes also are also suggested by the appearance of high intensity bands in 3532 cm^{-1} and 3010 cm^{-1} in the CAc complex 1 and 3505 cm^{-1} and 3136 cm^{-1} in the CAc complex 2. In the two CAc complexes, the stretch band of the carbonyl =O of NVP was also shifted to 1867 cm^{-1} and 1858 cm^{-1}, suggesting intermolecular interactions in the two complexes between NVP and CAc. No bond formations were observed between NVP and URE molecules.

Thermal analysis by DSC

DSC curves and thermic data are shown in Fig. 4 and Supplementary File SII respectively. Pure NVP presented its characteristic melting point at 248°C, and an exothermic band was also detected around 175°C. DSC curves of NVP-3TC PM and NVP-CAc PM showed the shift of NVP melting point at 235.2°C and 238.7°C respectively, with an endothermic peak in the mixture with 3TC at 175.1°C correspondingly to the 3TC melting point [38]. The NVP-URE mixture presented an endothermic peak that indicates the melting point of NVP at 242.5°C.

Determination of equilibrium solubility

NVP concentration values for each sample analyzed are described in Supplementary File III. They are known as saturation concentration or equilibrium solubility. The maximum concentration achieved by NVP was approximately 104.6 µg/mL, being altered at the presence of 3TC, increasing NVP solubility to **114.9** µg/mL, as well as the CAc, which also raised the NVP concentration to 662.46 µg/mL. URE also was able to increase NVP solubility to 132.98 µg/mL.

Solid State Characterization

*X-ray **Diffractometry** (XRD)*

The diffractogram patterns of NVP, 3TC, and CAc, as well as their PM and CAMs are illustrated in Fig. 5. The diffraction planes indicating the crystalline nature of NVP were detected at 9.04°, 12.91°, 15.46°, 17.09°, 18.91 °, 20.64°, 22.49°, 23.19°, 25.33° and 26.55°, following previous results reported in the literature [39,40]. All PMs obtained showed the presence of NVP and the coformer used by their characteristic diffraction planes, while absence of peaks was observed in the CAMs of 3TC and CAc.

Fourier Transform Infrared Spectroscopy (FTIR)

NVP groups are represented in the infrared spectrum (Fig. 6A) at 3188 cm^{-1} and 1642 cm^{-1} corresponding to the vibrational nodes of the stretching -NH and -C=O respectively of the amide group. The spectrum also shows bands at 3123 cm^{-1} that correspond to the -CH bond of the cyclopropyl substituent and at 1584 cm^{-1} that characterize the scissor vibrations of the -CH3 methyl group. Spectrum of 3TC is characterized by the presence of the carbonyl group (-C=O) vibration of the carbamide function at 1633 cm^{-1}, deformation of the -NH group at 1607 cm^{-1} and broad bands of stretching vibration of the -NH2 group at 3328-3500 cm^{-1} [38,41]. Broadenings in the stretching bands at 3328 cm^{-1} of 3TC and at 3188 cm^{-1} of the -NH group of the NVP amide were evident in the CAM NVP:3TC, especially when compared to PM, with shift to the right of the stretching vibration band of the $-NH_2$ group of 3TC. CAc is identified by a -OH stretching vibration at 3492 cm^{-1} and at 3328 cm^{-1} of the carboxylic group (-COOH) [42,43]. The two peaks at 1692 cm^{-1} and 1743 cm^{-1} in the FTIR spectra of CAc arise from the C=O stretch in the carboxylic groups. Both peaks overlap as they move across the NVP:CAc CAM spectrum, while still being present in the PM. Its hydroxyl stretching bands (-OH) had reduced and broadened intensities in the PM with NVP, in addition to the broadening of the C=O stretching in the CAM.

Differential Scanning Calorimetry (DSC)

DSC were performed with the NVP pure, coformers, their PM and CAM (Fig. 7 and Supplementary File IV). NVP has a characteristic melting point at 244°C and 3TC at 175°C. In the PM 3TC, two endothermic fusion peaks were identified with a maximum peak at 175°C and another at 230°C, while in the CAM 3TC, only one endothermic band was identified at 230°C, with an exothermic band at around 135°C.

In addition, a Tg was identified at 52°C in CAM 3TC, CAc has a melting peak at 154°C that appears shifted in PM CAc at 132°C, where an endothermic peak at 230°C was also revealed for NVP fusion. In CAM CAc, a Tg was detected at 63°C, followed by an exothermic recrystallization event at 133°C and an endothermic fusion peak referring to NVP at 239°C.

Polarized Light Microscopy (PLM)

PLM photographs were taken to observe the presence of microcrystals in the generated systems and are illustrated in Supplementary File V. NVP and 3TC are characterized by small colored dots on the photographs, indicating crystalline material, while CAc is represented by a huge mass with colored regions indicating the crystalline nature of the excipient. Numerous crystalline points were noted on the slides of all PM, showing that the simple mixture between the components is not enough to promote the amorphization of the drug. However, the CAMs showed significant differences in relation to their respective mixtures, where no crystalline points with birefringence were visualized.

In Vitro dissolution

The dissolution profiles of NVP pure, PMs and CAMs are illustrated at Fig. 8 and quantitative data of dissolution are shown in Table II and Supplementary File VI. After *in vitro* dissolution tests, it was observed that pure NVP achieved a dissolution of 64% at 360 min, while all CAMs reached higher levels of NVP dissolved, mainly CAM 3TC which had the highest dissolution rate (97.58%) followed by CAM CAc (93.88%). CAM 3TC had the highest dissolution efficiency, with values of 68.7% in 120 min and 81.7% in 360 min, also showing difference between these samples with a similarity factor (F2) of 20.6 for pure NVP and 37.9 for its PM. CAM CAc showed excellent dissolution performance with 62.6% of NVP in 120 min and 62.9% in 360 min. Although it was not statistically different in relation to its PM at the final time, CAM CAc had an excellent dissolution performance, with a similarity factor (F2) of 23.6 for pure NVP and 55.8 for its PM, showing that there was a difference between the samples during the assay.

DISCUSSION

Suitable coformers are crucial for the development of a stable CAM. To achieve this, screening experiments are important to predict the interaction between the components, and thus, the possible formation of CAM using low molecular weight components, such as URE and CAc [44–48], in addition to 3TC, an antiretroviral drug used in multidrug therapy with NVP to combat HIV. Molecular and thermal analysis studies can provide information regarding the possible intermolecular interactions that can occur between NVP and its coformers, and which regions of the molecule have the greatest potential for these interactions, while solubility studies evaluate the impact that the presence of these substances has on the crystalline saturation solubility of NVP when in solution. Coformers that did not indicate potential interactions and miscibility with NVP were not considered for subsequent tests.

The formation of a stable CAM depends on the resulting interactions between its components, especially hydrogen bonds [49]. Molecular regions of 3TC and CAc can interact with NVP, forming two complex structures from the simultaneous interaction of its carbonyls and hydroxyls present in their molecules, with the carbonyl and amino group of NVP, resulting in greater stability to the formed system. The complexes NVP-3TC are formed through the interaction of NVP with 3TC in equivalent molar amounts. In the formation of hydrogen complexes, due to a redistribution in molecular electron density, the charge transfer involved in the donor-acceptor interaction should undoubtedly be considered [50]. In hydrogen interactions, charge transfer occurs from the lone pair of electrons of the proton acceptor atom to the antibonding orbital of the hydrogen bond, which results in bond stretching [51]. Due to the increase in the length of the hydrogen bond, there is a decrease in the vibration frequency when it establishes contact with the atom of the acceptor group [51,52]. This phenomenon can occur in hydrogen interactions between NVP and its coformers, giving evidence of the formation of a CAM [52]. In fact, this was what occurred in all the hydrogen bonds of the complexes formed between NVP–3TC and NVP–CAc, which underwent an increase in their lengths and shifts to lower frequencies were observed, indicating the possibility of hydrogen interactions between NVP and these compounds, also observed in the theoretical infrared spectrophotometric analysis.

A computational approach has already been used to verify the formation of amorphous formulations. Interactions between carbamazepine and α-Glycosyl rutine were analyzed through molecular dynamics simulation, mimicking the melt-quenching method, in addition to calculations by the orbital molecular fragment method. The

authors realized that the multiple hydrogen interactions were greater than the interaction energy of the type π realized between drug and coformer [53]. Ceritinib CAMs was also obtained by a computational approach that estimated the binding energy and intermolecular interactions between the drug and different coformers to choose the best among them to stabilize the amorphous form of ceritinib [54]. Both works highlight the importance of the computational approach to obtain amorphous systems, especially because it provides information about different interactions that are difficult to detect by experimental approaches.

Although URE presents electronegative atoms in the molecule, such as oxygen and nitrogen in the carboxyl and amine groups which allow a great capacity for forming hydrogen bonds, the formation of NVP complex networks with URE molecules was not possible to occur. The URE crystalline structure is composed of eight hydrogen bonds distributed between six neighboring molecules, forming an infinite planar ribbon, with the carbonyl oxygen, accepting four hydrogen bonds instead of the two usually expected, promoting additional stabilization through forces dipole-dipole [55]. These stable interactions between URE molecules prevent the formation of new hydrogen bonds, and thus, the complex cannot be observed [56]. The crystalline form of the molecule and, consequently, its physical properties, such as conductivity, thermal stability, mechanical strength, and optical properties are influenced by hydrogen bonds, which acts as a vector of structural stability [57]. This characteristic makes the interaction between urea molecules highly stable, which favors the formation of their own networks, reducing the possibility of forming complexes with NVP or other molecules.

DSC is an instrumental technique widely used for rapid compatibility screening of different compounds and producing amorphous samples from crystalline materials [58,59]. The objective of the first heating carried out in the study was the melting of the physical mixtures with NVP and consequently their amorphization, while the DSC curves generated in the second heating characterize the material formed after the first heating, providing information about its homogeneity, miscibility of components, and evidence of crystalline material [60]. The crystalline nature of NVP was confirmed on the second heating, due to the recrystallization phenomenon that the drug underwent during the reheating process. The shift of the NVP melting point at PMs with 3TC and CAc suggests probable miscibility between the components, suggesting the possibility of formation of the amorphous systems, which did not occur with the mixture with URE,

where the crystalline nature of NVP was evidenced and there was not good miscibility between the components [61].

When a material vitrifies when cooled from its melted state, it possesses the glass-forming ability, a method that classifies compounds into up to three classes. The first of these classes is defined when a material crystallizes during cooling, the second class is defined when crystallization occurs during reheating, while in the third class there is no crystallization [62]. Although the physical mixtures of NVP with 3TC and CAc indicate that there was miscibility between the components involved, it is perceived that the crystalline signal referring to NVP may indicate that it is not a complete miscibility and that these systems formed, together with the physical mixture with URE, are class II. Despite this, these results corroborate molecular studies, suggesting a better formation of amorphous systems of NVP with 3TC and CAc, through the possible intermolecular interactions that can be formed between them, while NVP and URE have difficulties in establishing bonds, making the formation of amorphous systems improbable.

The saturation solubility of NVP was investigated in its isolated crystalline form and in the presence of the coformers used in this study to verify their influence on its saturation crystalline solubility (Cs). In a review proposed by Korhonen and colleagues, it is asserted that the miscibility between the components is a significant parameter in the selection of excipients for co-amorphous formulations. It is proposed that the tendency of a stabilized amorphous drug to crystallize can be significantly influenced by the degree of mixing behavior between the drug and the coformer. Therefore, solubility parameters can be employed as a means of estimating the degree of molecular similarity [27].

NVP is a weak base with pKa equal to 2.8 and when present in aqueous media with a pH higher than 3, there are more non-ionized NVP molecules, lowering its solubility, and impairing its dissolution in the medium in question [63]. CAc is a carboxylic acid that contains -COOH and -OH groups that can interact with the drug through intermolecular interactions, such as ionic interactions and hydrogen bonds, with drugs with low aqueous solubility and weak bases such as NVP, forming salts of the drug, solubilizing it in the medium [64,65]. A similar phenomenon could be observed in a study carried out with CAM with the weak base drug posaconazole, which showed increases in drug concentrations due to the acidic environment caused by CAc [66]. URE is a hydrotropic substance with an amphiphilic structure that forms

free aggregates with drug molecules, responsible for increasing the aqueous solubility of low-solubility drugs, especially when they are in non-ionized form [67].

In XRD analysis, PM can present the sum of the peaks of the individual components, a fact that occurred in all PMs obtained, where their diffraction angles showed the presence of crystalline NVP and the coformer used in all PMs. The presence of diffraction halos and the absence of peaks in CAMs confirms the amorphous nature of the material [68]. However, CAM 3TC shows signs of crystallinity that can lead to lower physical stability, but without recrystallization. CAMs of posaconazole obtained similar results for XRD analyses, but they were more stable in relation to solid dispersions of the same drug with the polymer Kollidon VA-64 which, due to the hygroscopicity of the system, absorbed moisture from the environment leading to recrystallization, which is more difficult to occur in CAM systems [66].

FTIR spectra obtained can reveal valuable information about the physical and chemical states of solid materials, especially when there is a change from the crystalline to the amorphous state, which can be related to shifting in bands in specific regions of the spectrum [58]. The NVP crystal is characterized by an amide function in a seven-membered ring, adopting a planar conformation, and there is also a cyclopropyl substituent [69,70]. The changes perceived in the infrared spectra of CAMs corroborate the theoretical infrared studied in the screening. Such changes in the peak position and shape may be due to disruption of the structured crystal lattice into the amorphous state, suggesting that there were intermolecular interactions between NVP and its coformers, as occurred in nifedipine and ketoconazole CAMs, whose band shifts of groups involved in hydrogen bonds indicated interactions between the two compounds [71].

Intermolecular interactions play a key role in the stability of the amorphous drug forms and, consequently, a good CAM formation especially when these substances have at least two hydrogen donor/acceptor points, as is the case of the chosen components to stabilize the amorphous NVP [20]. Moreover, the amorphization of the material can also be suggested by the broadenings observed in the CAM spectra in the region between 3500 and 3000 cm^{-1} related to hydrogen bonds (Fig. 7b). The same phenomenon was observed with Atorvastatin-Irbesartan CAM, in which band shifts and broadenings were identified, suggesting that hydrogen interactions between the two drugs occurred, presenting co-amorphization [33]. The results observed through FTIR

agree with those suggested in the screening tests, attesting that previous DSC and computational studies were relevant for the choice of coformers.

DSC assays indicated the recrystallization of the two drugs in PM 3TC, while a partial miscibility between the components was shown in CAM 3TC. The intimate contact promoted by preparation of the material may have caused interactions between the components since the preparation of the PMs and becoming more intense during the CAM formation process [20]. However, the thermal events found in CAM 3TC indicate that the amorphous material underwent recrystallization during the heating process, due to the NVP recrystallization and fusion processes. This recrystallization may have occurred due to the amount of crystalline material present in the CAM, whose crystalline nuclei may have received energy in the heating of the DSC and recrystallized.

The endothermic melting peaks of NVP in systems with CAc are displaced and at a lower intensity, showing that there may be a certain miscibility between the components, as verified in FTIR [61]. However, the results corroborate with XRD, which show amorphization of the CAM CAc, but the material could have received energy to recrystallize as occurred in the CAM 3TC. Recrystallization events followed by drug fusion are possible to occur in co-amorphous materials, as in the case of indomethacin and tryptophan CAM, where peak exothermic recrystallization was followed by drug fusion [72]. The material was considered amorphous according to the authors' studies, but because they recrystallized at elevated temperatures, they were considered stable in relation to the isolated drug [72]. Besides, the reduction and shifting of the endothermic peaks of NVP in the presence of its coformers suggests partial miscibility of the compounds, through a possible partial dissolution of NVP with its fused coformers, as well as in the CAM formed between simvastatin and glipizide, which did not show intermolecular interactions, despite the formation of the amorphous system through a molecular mixture between the drugs, where glipizide served as a stabilizing agent of the amorphous form of simvastatin (anti-plasticizer) [73]. All The characterization results confirm the successful formation of CAMs, since there are differences between CAMs and PMs obtained, where the PLM photographs indicate numerous crystalline points referring to the starting materials in the PMs and that are not observed in the CAM slides.

It is common to observe improved dissolution rates of CAM obtained with two different drugs, compared to their isolated crystalline counterparts, as occurred with

the CAM system of naproxen and cimetidine [74], whose dissolution rate was twice higher, without any evidence of crystallinity, due to the interactions between the two drugs in the exact proportion. The molecular proportion plays a fundamental role in the stability of CAM. The ratio 1:1 ratio is the most common and recommended, even though it is not mandatory, due to the number of specific intermolecular interactions between the components [74,75]. Through these interactions, the compounds form heterodimers that remain formed when in contact with water, preventing recrystallization, what is possible to happen to pure components when they are in CAM of other molar proportions (Jensen et al. 2016). This indicates how the proportion between substances in a CAM system is important for the dissolution of the drug and its increase in solubility.

The presence of CAc is responsible for the increase in the solubility of NVP, verified in the solubility tests, and the improvement is more evident in CAM in relation to its PM. This phenomenon can be explained by the maintenance of the amorphous structure stabilized by the intermolecular interactions between CAc and NVP generated during the formation of the complex, as observed in the characterizations and molecular dynamics [77]. Such interactions may have avoided the occurrence of nucleation and crystalline growth, preventing NVP recrystallization, as occurred in the CAM of loratadine and citric acid 1:1, whose dissolution revealed a solubility increase 50 times greater in relation to the isolated crystalline drug and up to 30 times greater in relation to it amorphous isolated [78].

CAMs can enhance the apparent final solubility of low-solubility drugs in a manner that is dependent on the specific interactions between the drug and its coformer. These interactions can facilitate an anti-plasticization effect within the system, thereby reducing molecular mobility. Additionally, the high energy inherent to the amorphous state and the absence of the energy required to rearrange the crystal structure during dissolution can be leveraged to further optimize the solubility of low-solubility drugs [23]. Moreover, improved wettability of the drug particles can significantly increase the dissolution rate, as it facilitates better interaction between the drug and the dissolution medium. The combined impact of these factors results in an enhanced solubility profile when compared to their crystalline counterparts and individual amorphous forms [20].

Considering the HIV treatment, the use of technologies that allow the improvement of drug solubility may play an important role in the HAART, as most drugs

used in antiretroviral have first-pass metabolism, degradation in the gastrointestinal tract and low aqueous solubility, which leads to a short half-life, reduced and inconsistent bioavailability and risk of multidrug resistance [79]. In this aspect, the development of CAM to increase NVP solubility would be advantageous, especially when combined with 3TC, since a fixed-dose combination therapy using NVP:3TC CAM could not only overcome issues related to NVP solubility, but also make the therapy more accessible, reducing costs, and thus increasing patient treatment compliance.

CONCLUSION

The combined use of screening studies, namely computational, thermal, and solubility studies, was useful in developing NVP CAM. With these studies, it was possible to predict the formation of stable NVP CAM, by observing possible intermolecular interactions and a certain miscibility between the components. Computational methods were able to predict the formation of hydrogen complexes between NVP, 3TC and CAc. For all bonds involving hydrogen in the formation of complexes, shifts to lower frequencies occur, as well as an increase in these bonds CAM of NVP with 3TC and CAc were obtained through quench-cooling after the prediction of hydrogen interactions between the two components. When obtained, the NVP CAMs corroborated the screening studies, showing miscibility between the components, suggesting the formation of hydrogen interactions between NVP and its coformers, allowing the formation of the amorphous system verified by microscopy and XRD analysis. The maintenance of the amorphous form of NVP in CAM was also responsible for increasing the dissolution rate of NVP, reaching higher levels than the isolated drug and making CAM systems promising for antiretroviral combination therapy to combat HIV.

Acknowledgments

The authors would like to thank the *Coordination of Improvement of Higher Education Personnel* (CAPES) for the PhD fellowship; the authors thank *Pharmaceutical Laboratory in Pernambuco* (LAFEPE), *Drug Technology Laboratory* (LTM) of the Federal University of Pernambuco and *Laboratory of Technology of Nanosystems Carriers of Active Substances - TecNano* for solid state characterizations.

Funding Statement

This work was supported by the FINEP-FADE-UFPE under Grant 0120-21.

Conflict of Interest Statement

The authors declare that they have no known competing financial interests or personal relationships that could have appeared to influence the work reported in this paper.

Author Contributions

KAS: research idea conceptualization, conducted laboratory work, conducted data analysis, manuscript writing; and editing. LLC: data analysis, revised and edited the manuscript. DN: conducted laboratory work, conducted data analysis. MFLR: research idea conceptualization, manuscript revision, and study supervision. JLSS: research idea conceptualization, supervised the study, data analysis, revised and edited the manuscript. All authors read and approved the final manuscript.

References

1. World Health Organization. HIV and AIDS [Internet]. 2023 [cited 2023 Sep 18]. Available from: https://www.who.int/news-room/fact-sheets/detail/hiv-aids

2. Arca HÇ, Mosquera-Giraldo LI, Dahal D, Taylor LS, Edgar KJ. Multidrug, Anti-HIV Amorphous Solid Dispersions: Nature and Mechanisms of Impacts of Drugs on Each Other's Solution Concentrations. Mol Pharm. 2017;14:3617–27.

3. Santos KA dos, Danda LJ de A, Oliveira TC de, Soares-Sobrinho JL, Soares MF de LR. The drug loading impact on dissolution and diffusion: a case-study with amorphous solid dispersions of nevirapine. Research, Society and Development. 2022;11:e168111436117–e168111436117.

4. Panzade P, Somani P, Rathi P. Nevirapine Pharmaceutical Cocrystal: Design, Development and Formulation. Drug Deliv Lett. 2019;9:240–7.

5. Rao MRP, Sonawane AS, Sapate SA, Mehta CH, Nayak UY. Molecular modeling and in vitro studies to assess solubility enhancement of nevirapine by solid dispersion technique. J Mol Struct. 2023;1273:134373.

6. Tambosi G, Coelho PF, Soares L, Lenschow ICS, Zétola M, Stulzer HK, et al. Challenges to improve the biopharmaceutical properties of poorly water-soluble drugs and the application of the solid dispersion technology. Revista Materia. 2018;23.

7. Savjani KT, Gajjar AK, Savjani JK. Drug Solubility: Importance and Enhancement Techniques. ISRN Pharm [Internet]. 2012;2012:1–10. Available from: https://www.hindawi.com/archive/2012/195727/

8. Blaabjerg LI, Bulduk B, Lindenberg E, Löbmann K, Rades T, Grohganz H. Influence of Glass Forming Ability on the Physical Stability of Supersaturated Amorphous Solid Dispersions. J Pharm Sci. 2019;108:2561–9.

9. Cooper ER. Nanoparticles: A personal experience for formulating poorly water soluble drugs. Journal of Controlled Release. 2010;141:300–2.

10. Shegokar R, Singh KK. Surface modified nevirapine nanosuspensions for viral reservoir targeting: In vitro and in vivo evaluation. Int J Pharm. 2011;421:341–52.

11. Zhu Y, Ye J, Zhang Q. Self-emulsifying Drug Delivery System Improve Oral Bioavailability: Role of Excipients and Physico-chemical Characterization. Pharm Nanotechnol. 2020;8:290–301.

12. Tang J, Sun J, He Z-G. Self-Emulsifying Drug Delivery Systems: Strategy for Improving Oral Delivery of Poorly Soluble Drugs. Curr Drug ther. 2008;2:85–93.

13. Singh G, Singh N, Kumar R, Bedi N. Development and characterization of nevirapine loaded amorphous solid dispersions for solubility enhancement. Asian Journal of Pharmaceutical and Clinical Research. 2019;12:176–82.

14. Ivone R, Fernando A, DeBoef B, Meenach SA, Shen J. Development of Spray-Dried Cyclodextrin-Based Pediatric Anti-HIV Formulations. AAPS PharmSciTech. 2021;22:193.

15. Hiew TN, Zemlyanov DY, Taylor LS. Balancing Solid-State Stability and Dissolution Performance of Lumefantrine Amorphous Solid Dispersions: The Role of Polymer Choice and Drug-Polymer Interactions. Mol Pharm. 2022;19:392–413.

16. Fong SYK, Bauer-Brandl A, Brandl M. Oral bioavailability enhancement through supersaturation: an update and meta-analysis. Expert Opin Drug Deliv. 2017;14:403–26.

17. Laitinen R, Löbmann K, Grohganz H, Priemel P, Strachan CJ, Rades T. Supersaturating drug delivery systems: The potential of co-amorphous drug formulations. Int J Pharm. 2017;532:1–12.

18. Sarode AL, Wang P, Obara S, Worthen DR. Supersaturation, nucleation, and crystal growth during single- and biphasic dissolution of amorphous solid dispersions: Polymer effects and implications for oral bioavailability enhancement of poorly water soluble drugs. European Journal of Pharmaceutics and Biopharmaceutics. 2014;86:351–60.

19. Baghel S, Cathcart H, O'Reilly NJ. Polymeric Amorphous Solid Dispersions: A Review of Amorphization, Crystallization, Stabilization, Solid-State Characterization, and Aqueous Solubilization of Biopharmaceutical Classification System Class II Drugs. J Pharm Sci. 2016;105:2527–44.

20. Karagianni A, Kachrimanis K, Nikolakakis I. Co-Amorphous Solid Dispersions for Solubility and Absorption Improvement of Drugs: Composition, Preparation, Characterization and Formulations for Oral Delivery. Pharmaceutics. 2018;10:1–26.

21. Mizoguchi R, Waraya H, Hirakura Y. Application of Co-Amorphous Technology for Improving the Physicochemical Properties of Amorphous Formulations. Mol Pharm. 2019;16:2142–52.

22. Yarlagadda DL, Sai Krishna Anand V, Nair AR, Navya Sree KS, Dengale SJ, Bhat K. Considerations for the selection of co-formers in the preparation of co-amorphous formulations. Int J Pharm. 2021;602:120649.

23. Vullendula SKA, Nair AR, Yarlagadda DL, Navya Sree KS, Bhat K, Dengale SJ. Polymeric solid dispersion Vs co-amorphous technology: A critical comparison. J Drug Deliv Sci Technol. 2022;78:103980.

24. Han J, Wei Y, Lu Y, Wang R, Zhang J, Gao Y, et al. Co-amorphous systems for the delivery of poorly water-soluble drugs: recent advances and an update. Expert Opin Drug Deliv. 2020;17.

25. Liu J, Grohganz H, Löbmann K, Rades T, Hempel NJ. Co-amorphous drug formulations in numbers: Recent advances in co-amorphous drug formulations with focus on co-formability, molar ratio, preparation methods, physical stability, in vitro and in vivo performance, and new formulation strategies. Pharmaceutics. 2021;13.

26. Shi X, Zhou X, Shen S, Chen Q, Song S, Gu C, et al. Improved in vitro and in vivo properties of telmisartan in the co-amorphous system with hydrochlorothiazide: A potential drug-drug interaction mechanism prediction. Eur J Pharm Sci. 2021;161.

27. Korhonen O, Pajula K, Laitinen R. Rational excipient selection for co-amorphous formulations. Expert Opin Drug Deliv. 2016;14:551–69.

28. Dennington R, Keith T, Millam J. Gauss View. Semichem Inc., Shawnee Mission; 2009.

29. Froese Fischer C. General Hartree-Fock program. Comput Phys Commun. 1987;43:355–65.

30. Chadha R, Arora P, Garg M, Bhandari S, Jain DS. Thermoanalytical and spectroscopic studies on different crystal forms of nevirapine. J Therm Anal Calorim. 2013;111:2133–42.

31. Food and Drug Administration. FDA. Waiver of in vivo bioavailability and bioequivalence studies for immediate-release solid dosage forms base on a Biopharmaceutics Classification System. Maryland; 2017. p. 1–19.

32. Baka E, Comer JEA, Takács-Novák K. Study of equilibrium solubility measurement by saturation shake-flask method using hydrochlorothiazide as model compound. J Pharm Biomed Anal. 2008;46:335–41.

33. Skotnicki M, Jadach B, Skotnicka A, Milanowski B, Tajber L, Pyda M, et al. Physicochemical characterization of a co-amorphous atorvastatin-irbesartan system with a potential application in fixed-dose combination therapy. Pharmaceutics. 2021;13:1–20.

34. Vieira-Sellaï L, Quintana M, Diop O, Mercier O, Tarrit S, Raimi N, et al. Green HPLC quantification method of lamivudine, zidovudine and nevirapine with identification of related substances in tablets. Green Chem Lett Rev. 2022;15:695–704.

35. Anbazhagan S, Indumathy N, Shanmugapandiyan P, Sridhar SK. Simultaneous quantification of stavudine, lamivudine and nevirapine by UV spectroscopy, reverse phase HPLC and HPTLC in tablets. J Pharm Biomed Anal. 2005;39:801–4.

36. Lodagekar A, Chavan RB, Mannava MKC, Yadav B, Chella N, Nangia AK, et al. Co amorphous valsartan nifedipine system: Preparation, characterization, in vitro and in vivo evaluation. European Journal of Pharmaceutical Sciences. 2019;139:105048.

37. Zhang Y, Huo M, Zhou J, Zou A, Li W, Yao C, et al. DDSolver: An add-in program for modeling and comparison of drug dissolution profiles. AAPS Journal. 2010;12:263–71.

38. Porfírio LDO, Costa AA, Conceição RR, Matos TDO, Almeida EDP, Sarmento VH V., et al. Compatibility study of hydroxypropylmethylcellulose films containing zidovudine and lamivudine using thermal analysis and infrared spectroscopy. J Therm Anal Calorim. 2015;120:817–28.

39. Reguri BR, Chakka R. Crystalline forms of nevirapine. Estados Unidos; 2006. p. 1–7.

40. Sarkar M, Perumal OP, Panchagnula R. Solid-state characterization of nevirapine. Indian J Pharm Sci. 2008;70:619–30.

41. Palei NN, Mamidi SK, Rajangam J. Formulation and evaluation of lamivudine sustained release tablet using okra mucilage. J Appl Pharm Sci. 2016;6,:069–75.

42. Baruah U, Deka MJ, Chowdhury D. Reversible on/off switching of fluorescence via esterification of carbon dots. RSC Adv. 2014;4:36917–22.

43. Pimpang P, Sumang R, Choopun S. Effect of concentration of citric acid on size and optical properties of fluorescence graphene quantum dots prepared by tuning carbonization degree. Chiang Mai Journal of Science. 2018;45:2005–14.

44. Hirakawa Y, Ueda H, Miyano T, Kamiya N, Goto M. New insight into transdermal drug delivery with supersaturated formulation based on co-amorphous system. Int J Pharm. 2019;569.

45. Chambers LI, Musa OM, Steed JW. Prediction and Preparation of Coamorphous Phases of a Bislactam. Mol Pharm. 2022;19:2651–61.

46. Ahuja N, Katare OP, Singh B. Studies on dissolution enhancement and mathematical modeling of drug release of a poorly water-soluble drug using water-soluble carriers. Eur J Pharm Biopharm. 2007;65:26–38.

47. Hirakawa Y, Ueda H, Takata Y, Minamihata K, Wakabayashi R, Kamiya N, et al. Co-amorphous formation of piroxicam-citric acid to generate supersaturation and improve skin permeation. Eur J Pharm Sci. 2021;158.

48. Ueda H, Wu W, Löbmann K, Grohganz H, Müllertz A, Rades T. Application of a Salt Coformer in a Co-Amorphous Drug System Dramatically Enhances the Glass Transition Temperature: A Case Study of the Ternary System Carbamazepine, Citric Acid, and l -Arginine. Mol Pharm. 2018;15:2036–44.

49. Deng Y, Liu S, Jiang Y, Martins ICB, Rades T. Recent Advances in Co-Former Screening and Formation Prediction of Multicomponent Solid Forms of Low Molecular Weight Drugs. Pharmaceutics. 2023;15:2174.

50. Zhang Z, Li D, Jiang W, Wang Z. The electron density delocalization of hydrogen bond systems. Adv Phys X. 2018;3:1428915.

51. Takahashi M, Okamura N, Ding X, Shirakawa H, Minamide H. Intermolecular hydrogen bond stretching vibrations observed in terahertz spectra of crystalline vitamins. CrystEngComm. 2018;20:1960–9.

52. Kolesov B. Hydrogen Bonds: Raman Spectroscopic Study. Int J Mol Sci. 2021;22:5380.

53. Ma X, Higashi K, Fukuzawa K, Ueda K, Kadota K, Tozuka Y, et al. Computational approach to elucidate the formation and stabilization mechanism of amorphous formulation using molecular dynamics simulation and fragment molecular orbital calculation. Int J Pharm. 2022;615:121477.

54. Yarlagadda DL, Anand VSK, Nair AR, Dengale SJ, Pandiyan S, Mehta CH, et al. A computational-based approach to fabricate Ceritinib co-amorphous system using a

novel co-former Rutin for bioavailability enhancement. European Journal of Pharmaceutics and Biopharmaceutics. 2023;190:220–30.

55. Ferrero M, Civalleri B, Rérat M, Orlando R, Dovesi R. The calculation of the static first and second susceptibilities of crystalline urea: A comparison of Hartree–Fock and density functional theory results obtained with the periodic coupled perturbed Hartree–Fock/Kohn–Sham scheme. J Chem Phys. 2009;131.

56. Civalleri B, Doll K, Zicovich-Wilson CM. Ab initio investigation of structure and cohesive energy of crystalline urea. Journal of Physical Chemistry B. 2007;111:26–33.

57. Perpétuo GJ, Janczak J. Supramolecular hydrogen-bonding networks in the 1-(diaminomethylenene) thiouron-1-ium 4-hydroxybenzoate, 3,4-dihydroxybenzoate and 3,4,5- trihydroxybenzoate monohydrate crystals. J Mol Struct. 2013;1041:127–38.

58. D'Angelo A, Edgar B, Hurt AP, Antonijević MD. Physico-chemical characterisation of three-component co-amorphous systems generated by a melt-quench method. J Therm Anal Calorim. 2018;134:381–90.

59. Maheswaram MP, Mantheni D, Perera I, Venumuddala H, Riga A, Alexander K. Characterization of crystalline and amorphous content in pharmaceutical solids by dielectric thermal analysis. J Therm Anal Calorim. 2013;111:1987–97.

60. Rojek B, Wesolowski M. A combined differential scanning calorimetry and thermogravimetry approach for the effective assessment of drug substance-excipient compatibility. J Therm Anal Calorim. 2023;148:845–58.

61. Datta A, Nolas GS. Composition controlled synthesis of Bi rich Bi1−xSbx alloy nanocrystals by a low temperature polyol process. CrystEngComm. 2011;13:2753.

62. Alhalaweh A, Alzghoul A, Kaialy W, Mahlin D, Bergström CAS. Computational Predictions of Glass-Forming Ability and Crystallization Tendency of Drug Molecules. Mol Pharm [Internet]. 2014 [cited 2022 Feb 15];11:3123–32. Available from: https://pubs.acs.org/doi/full/10.1021/mp500303a

63. Adeola AO, de Lange J, Forbes PBC. Adsorption of antiretroviral drugs, efavirenz and nevirapine from aqueous solution by graphene wool: Kinetic, equilibrium, thermodynamic and computational studies. Applied Surface Science Advances. 2021;6:100157.

64. Nangare S, Vispute Y, Tade R, Dugam S, Patil P. Pharmaceutical applications of citric acid. Future Journal of Pharmaceutical Sciences 2021 7:1. 2021;7:1–23.

65. Wu W, Ueda H, Löbmann K, Rades T, Grohganz H. Organic acids as co-formers for co-amorphous systems – Influence of variation in molar ratio on the physicochemical properties of the co-amorphous systems. European Journal of Pharmaceutics and Biopharmaceutics. 2018;131:25–32.

66. Wu H, Ma J, Qian S, Jiang W, Liu Y, Li J, et al. Co-amorphization of posaconazole using citric acid as an acidifier and a co-former for solubility improvement. J Drug Deliv Sci Technol. 2023;80:104136.

67. Beig A, Lindley D, Miller JM, Agbaria R, Dahan A. Hydrotropic solubilization of lipophilic drugs for oral delivery: The effects of urea and nicotinamide on carbamazepine solubility-permeability interplay. Front Pharmacol. 2016;7:379.

68. Krstić M, Manić L, Martić N, Vasiljević D, Mračević SĐ, Vukmirović S, et al. Binary polymeric amorphous carvedilol solid dispersions: In vitro and in vivo characterization. European Journal of Pharmaceutical Sciences. 2020;150:105343.

69. Mui PW, Jacober SP, Hargrave KD, Adams J. Crystal structure of nevirapine, a non-nucleoside inhibitor of HIV-1 reverse transcriptase, and computational alignment with a structurally diverse inhibitor. J Med Chem. 1992;35:201–2.

70. Ayala AP, Siesler HW, Wardell SMSV, Boechat N, Dabbene V, Cuffini SL. Vibrational spectra and quantum mechanical calculations of antiretroviral drugs: Nevirapine. J Mol Struct. 2007;828:201–10.

71. Hatanaka Y, Uchiyama H, Kadota K, Tozuka Y. Improved solubility and permeability of both nifedipine and ketoconazole based on coamorphous formation with simultaneous dissolution behavior. J Drug Deliv Sci Technol. 2021;65:102715.

72. Jensen KT, Larsen FH, Cornett C, Löbmann K, Grohganz H, Rades T. Formation Mechanism of Coamorphous Drug-Amino Acid Mixtures. Mol Pharm. 2015;12:2484–92.

73. Löbmann K, Strachan C, Grohganz H, Rades T, Korhonen O, Laitinen R. Co-amorphous simvastatin and glipizide combinations show improved physical stability without evidence of intermolecular interactions. European Journal of Pharmaceutics and Biopharmaceutics. 2012;81:159–69.

74. Allesø M, Chieng N, Rehder S, Rantanen J, Rades T, Aaltonen J. Enhanced dissolution rate and synchronized release of drugs in binary systems through formulation: Amorphous naproxen–cimetidine mixtures prepared by mechanical activation. Journal of Controlled Release. 2009;136:45–53.

75. Löbmann K, Laitinen R, Grohganz H, Gordon KC, Strachan C, Rades T. Coamorphous drug systems: enhanced physical stability and dissolution rate of indomethacin and naproxen. Mol Pharm. 2011;8:1919–28.

76. Jensen KT, Larsen FH, Löbmann K, Rades T, Grohganz H. Influence of variation in molar ratio on co-amorphous drug-amino acid systems. Eur J Pharm Biopharm. 2016;107:32–9.

77. Lambros M, Tran T (Henry), Fei Q, Nicolaou M. Citric Acid: A Multifunctional Pharmaceutical Excipient. Pharmaceutics. 2022;14:972.

78. Wang J, Chang R, Zhao Y, Zhang J, Zhang T, Fu Q, et al. Coamorphous Loratadine-Citric Acid System with Enhanced Physical Stability and Bioavailability. AAPS PharmSciTech. 2017;18:2541–50.

79. Hari BV, Devendharan K, Narayanan N. Approaches of Novel drug delivery systems for Anti-HIV agents. International Journal of Drug Development and Research. 2013;5:1–9.

LIST OF TABLES

Table I. Heating/cooling/reheating program in DSC for physical mixtures of NVP and coformers screened to obtain CAM

Sample	Program
NVP	0 °C - 260 °C - 25 °C - 300 °C
NVP-3TC	0 °C - 165 °C - 25 °C - 300 °C
NVP-CAc	0 °C - 160 °C - 25 °C - 300 °C
NVP-URE	0 °C - 260 °C - 25 °C - 300 °C

Table II. Dissolution efficiency of NVP and its PM and CAM with 3TC and CAc at times in 120 minutes and 360 minutes

Samples		Dissolution efficiency (%)	
		120 MIN	*360 MIN*
Pure NVP		**28.2 ± 4.7**	**46.3 ± 6.6**
NVP - 3TC	*PM*	**54.3[*a] ± 1.8**	**68.6[*a] ± 2.8**
	CAM	**68.7[*a,b] ± 2.3**	**81.7[*a,b] ± 2.1**
NVP - CAc	*PM*	**54.2[*a] ± 3.3**	**56.6[*a] ± 2.8**
	CAM	**62.6[*a,c] ± 1.3**	**62.9[*a] ± 0.6**

Mean± SD, n = 3;
** Statistically different p<0.05 vs. [a]NVP, [b]PM 3TC e [c]PM CAc*

LIST OF FIGURES

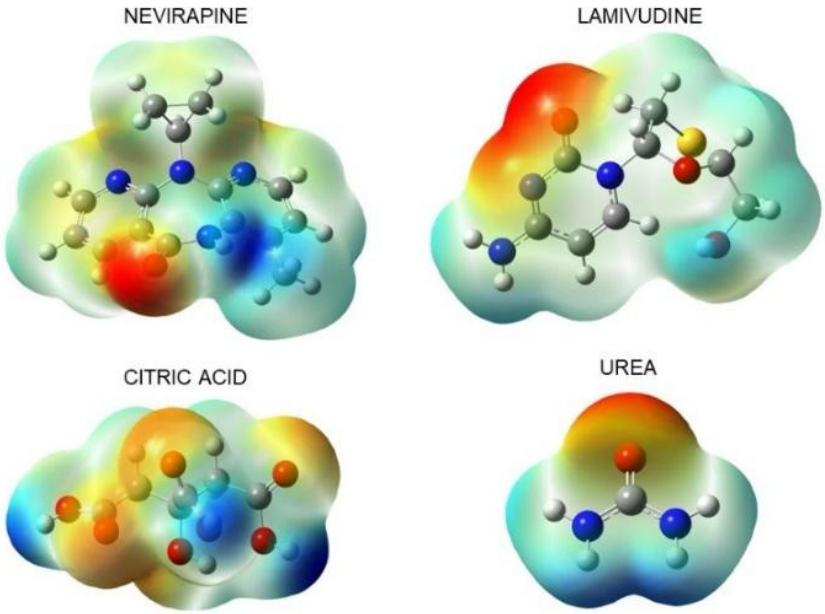

Fig. 1 Electrostatic potential maps of NVP, 3TC, CAc and URE. Regions in red represent electronegative sites and regions in blue represent electropositive sites

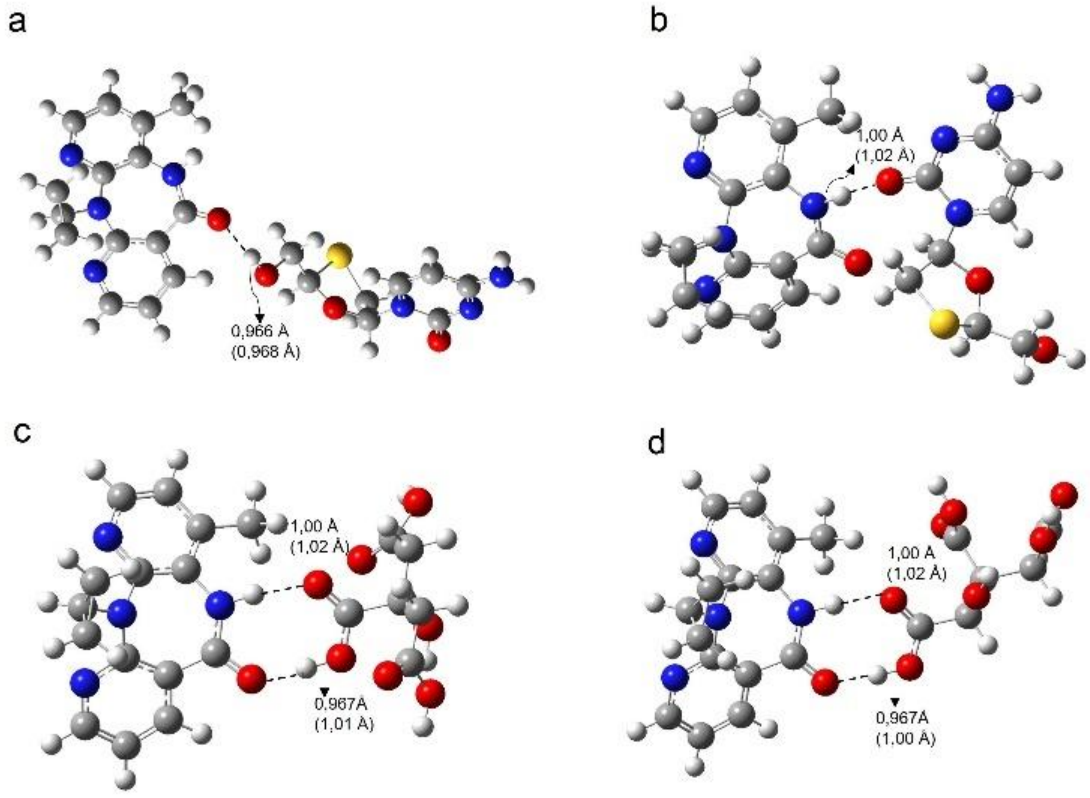

Fig. 2 Complexes formed between NVP, 3TC (A and B) and CAc (C and D) through the Gaussview v.05 program

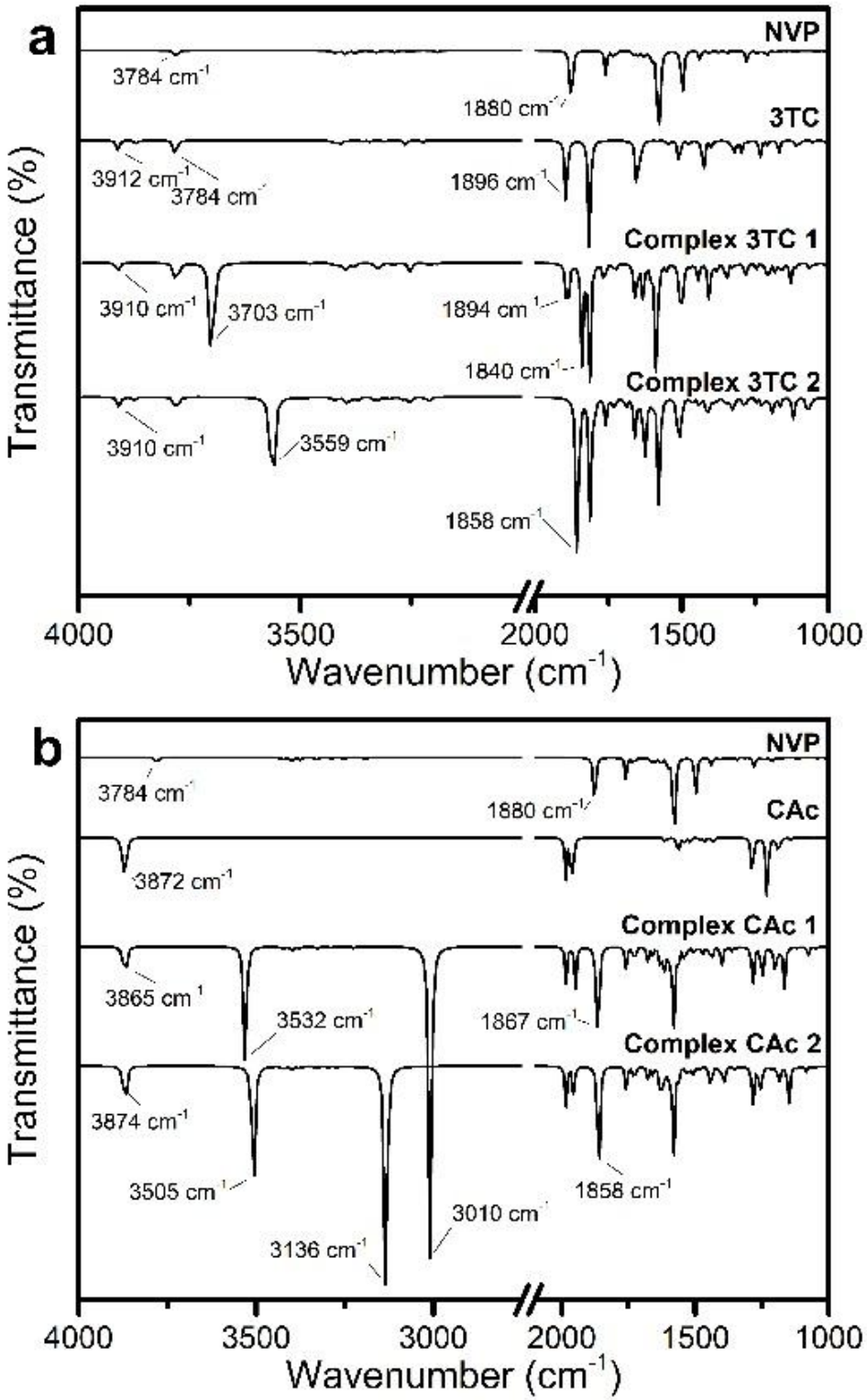

Fig. 3 Theoretical infrared spectrum of complexes formed between NVP with 3TC (a) and CAc (b)

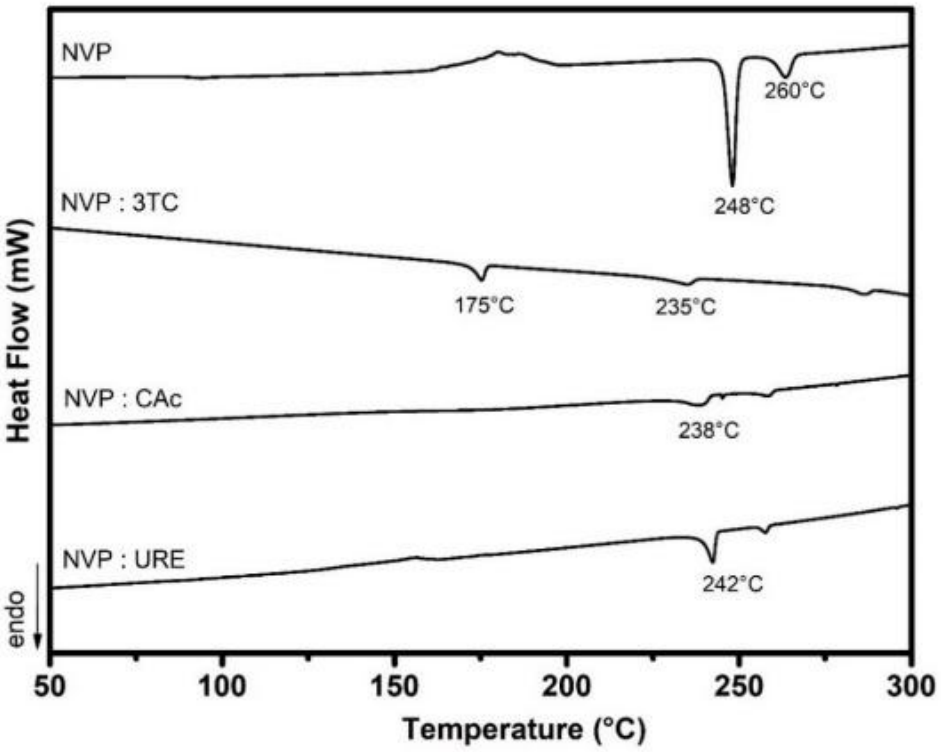

Fig. 4 DSC curves of NVP, NVP - 3TC, NVP - CAc and NVP - URE during the second heating

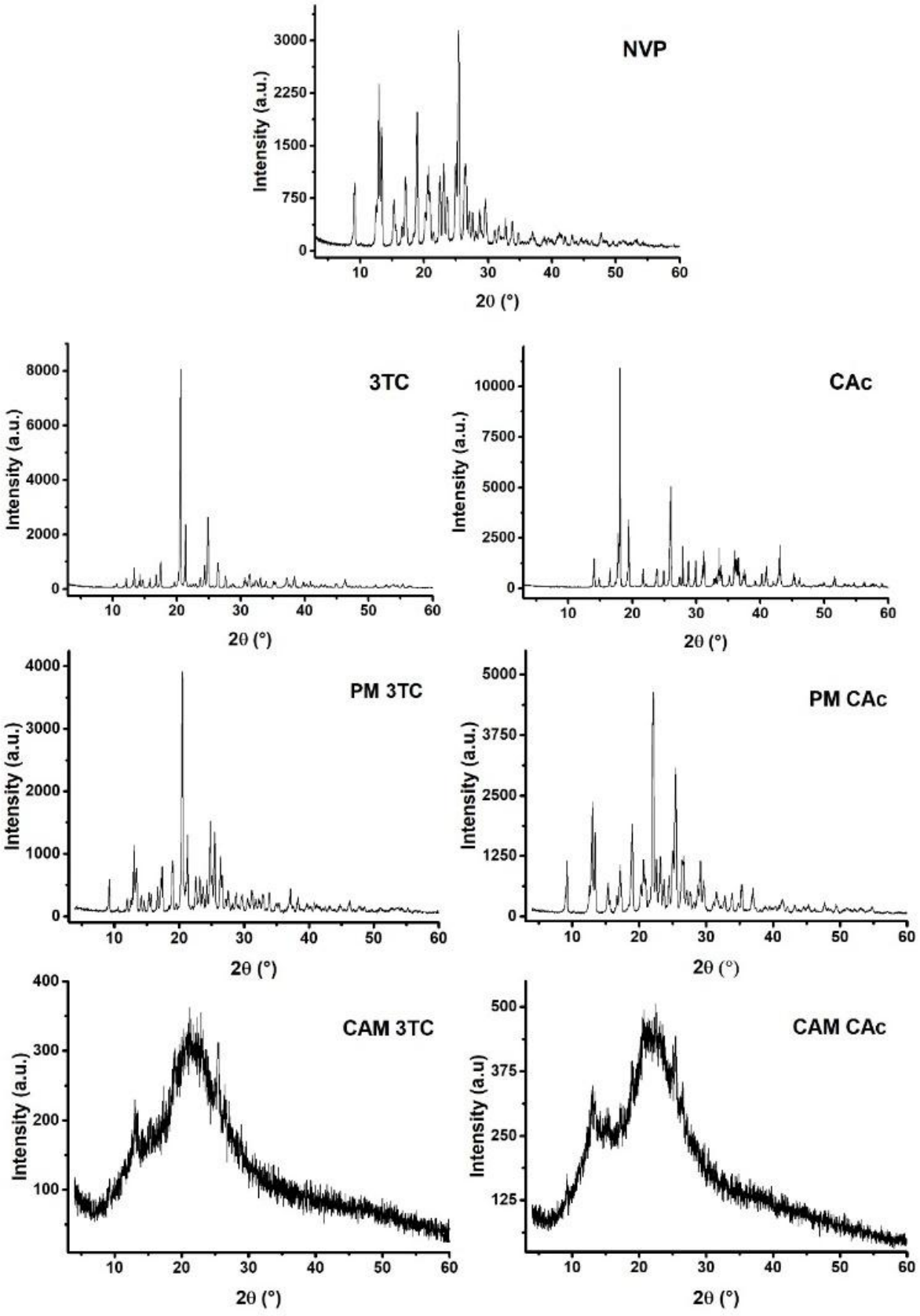

Fig. 5 X-ray diffraction patterns of NVP, 3TC and CAc, their respective PM and CAM

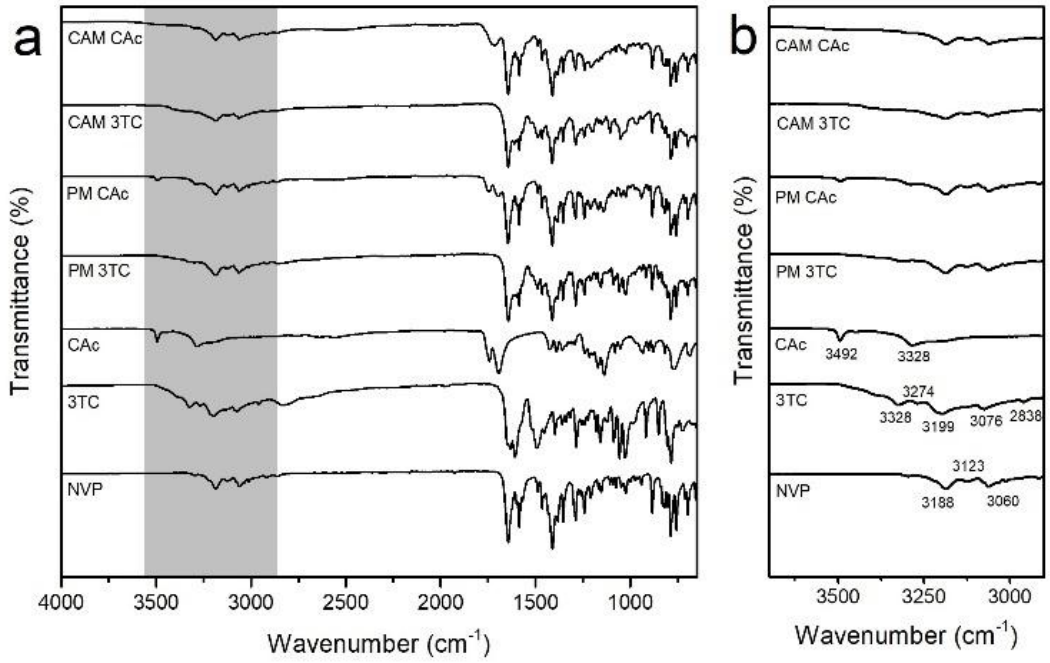

Fig. 6 FTIR spectrum with wavenumber from 4000 to 600 cm^{-1} (a) and with a cutoff in the region from 3560 to 2850 cm^{-1} (b) of NVP, 3TC, CAc, their PM and CAM

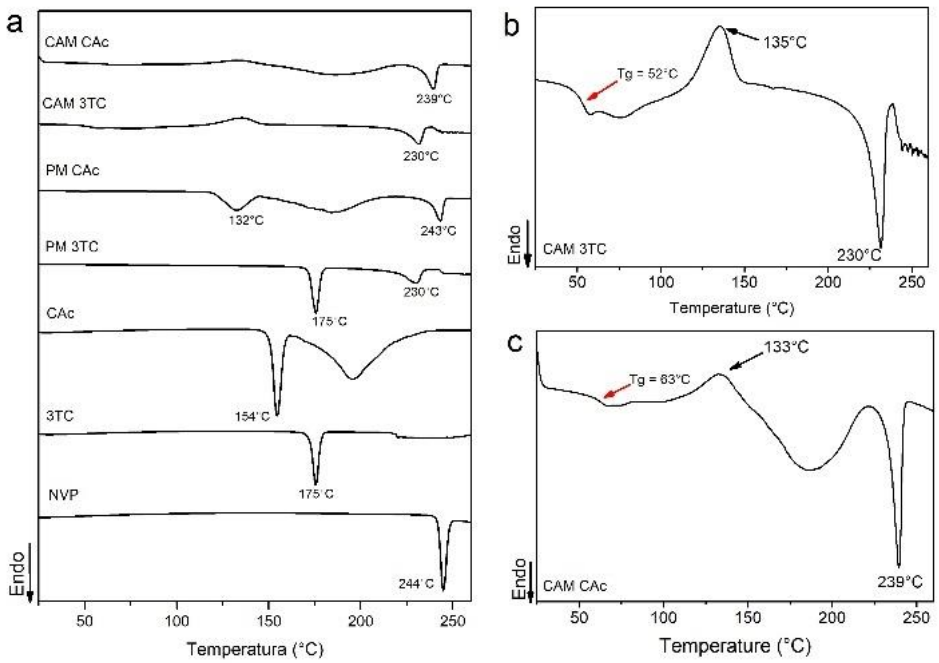

Fig. 7 DSC curves of pure components, PM and CAM (a), with magnification of the DSC curve of the CAM 3TC (b) and the CAM CAc (c)

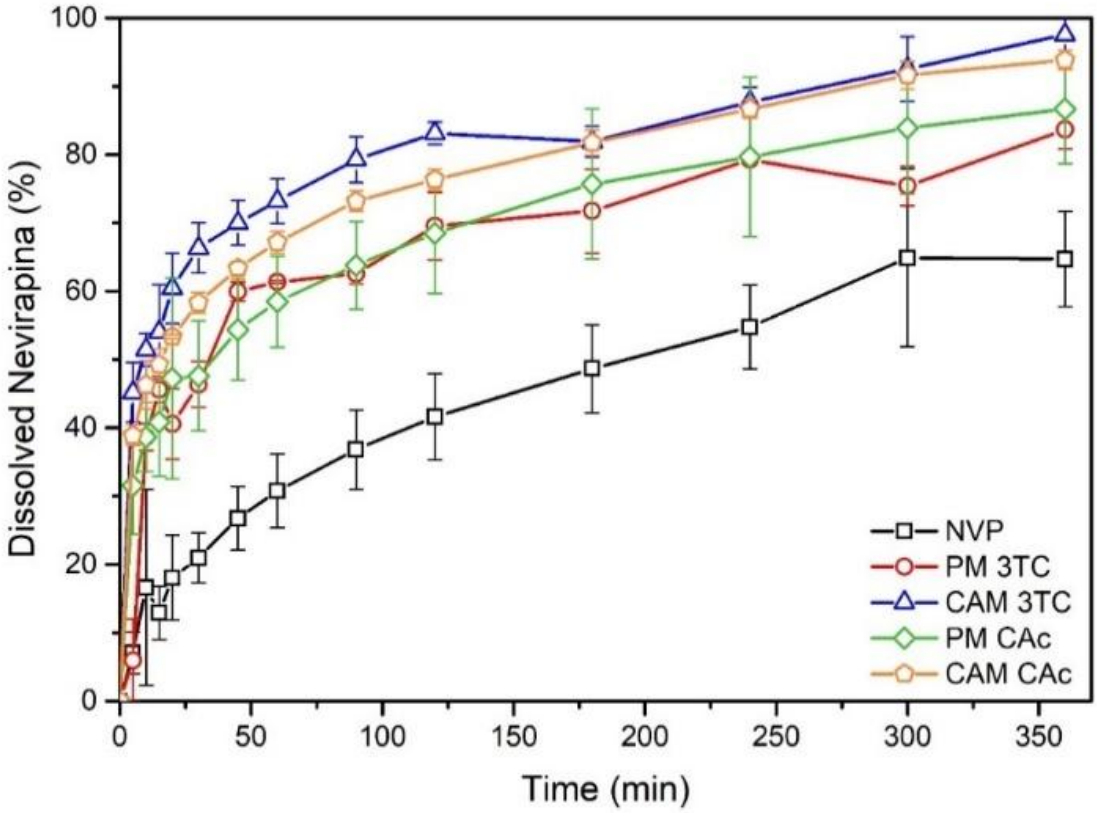

Fig. 8 NVP dissolution profiles with 3TC and its PM and CAM and CAc and its PM and CAM